DESIGN AND DEVELOPMENT OF SIDE UNDERRIDE PROTECTION DEVICES (SUPD) FOR HEAVY VEHICLES

By

Patrick Galipeau-Bélair

A Thesis Submitted In Partial Fulfillment

Of the Requirements for the Degree of

Master of Applied Science

In

The Faculty of Engineering and Applied Science

University of Ontario Institute of Technology

April 2014

CERTIFICATE OF APPROVAL

Submitted by **Patrick Galipeau-Belair**

In partial fulfillment of the requirements for the degree of

Master of Applied Science in **Automotive Engineering**

Date of Defence: **2014/04/01**

Thesis title: Design and Development of Side Underride Protections Devices (SUPD) for Heavy Vehicles

The undersigned certify that the student has presented **his** thesis, that the thesis is acceptable in form and content and that a satisfactory knowledge of the field covered by the thesis was demonstrated by the candidate through an oral examination. They recommend this thesis to the Office of Graduate Studies for acceptance.

Examining Committee

Dr. Hossam Gaber

Chair of Examining Committee

Dr. Marc Rosen
External Examiner

Dr. Moustafa El-Gindy
Research Supervisor

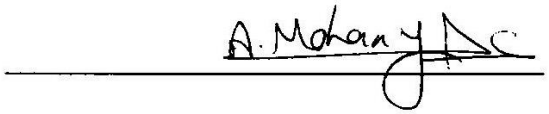

Dr. Atef Mohany
Examining Committee Member

As research supervisor for the above student, I certify that I have read and approved changes required by the final examiners and recommend the thesis for acceptance:

Dr. Moustafa El-Gindy Research Supervisor

ABSTRACT

There exists a large mismatch between the bumper of a passenger vehicle and the ground clearance of heavy vehicles. During collisions between the car and the side of the heavy vehicle, a large amount of intrusion is observed in the passenger compartment due to underride. The results of these collisions often leads to injuries or fatalities. This research aims to develop side underride protection devices (SUPD) to eliminate the incompatibility between the small vehicle's bumper and bottom of the trailer or box of the straight truck. To successfully design these guards, a regulation for testing the effectiveness of the SUPDs during a side crash was created. Guards were then developed utilizing a topology and multi-objective optimization design approach by applying the proposed regulation. These proved feasible when tested dynamically with the Toyota Yaris and Ford Taurus at preventing underride. Additional guards were then created and tested utilizing an aerodynamic shape to reduce drag and improve fuel consumption.

Keywords: Side underride protection device (SUPD), crashworthiness, side collision, underride, vehicle safety, injury and fatality prevention

DEDICATION

I dedicate this thesis to my family and friends. To my parents, Roch and Francine who have always given me their endless support and encouragement and to my sister Janelle, who has always been there for me.

ACKNOWLEDGEMENTS

I would like to express my appreciation to Volvo Group Trucks Technology as well as Auto 21 for supporting and funding this research project. I would like to thank Srikanth Ghantae, David Critchely and Sarathy Ramachandra for their technical support over the course of the research. I would also like to show my appreciation to my supervisor Dr. Moustafa El-Gindy, who through the course of this research has always provided me with his feedback, support and knowledge. Special thanks to all of my friends and family who have always supported me throughout my endeavors and for their encouragement over the course of these past years.

CONTENTS

LIST OF FIGURES

LIST OF TABLES

CHAPTER 1: INTRODUCTION

1.1 MOTIVATION

The basic principle of an underride guard for tractor-trailers or straight trucks is to prevent small passenger cars from going underneath these heavy vehicles. Due to the high ground clearance of the large vehicles and the low height of a small vehicle's bumper, there exists a large incompatibility between them when they collide. During the event of a collision, the bumper of the small car does not make contact with any part of the heavy vehicle, therefore not utilizing the vehicle's crashworthy components which is shown in Figure 1.1. Instead, during the collision, the car completely passes underneath the heavy vehicle which is where the term "underride" originates. The deformation of the passenger compartment is observed when the A-pillars come into contact with the bottom of the trailer or truck. At this point, intrusion is detected and the passenger compartment is completely deformed. In many cases, the collisions often result in severe occupant injury or fatality.

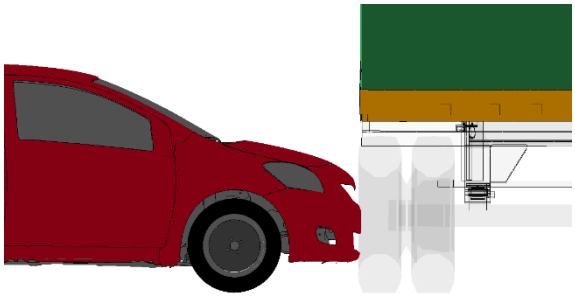

Figure 1.1 - Mismatch between passenger vehicle bumper and trailer

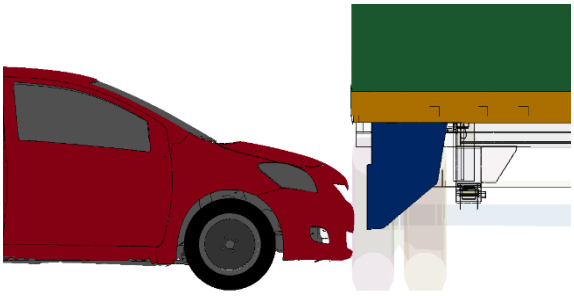

Figure 1.2 - Eliminated mismatch of bumper and trailer with an underride guard

This type of collision can occur from the front, side or rear configuration when investigating the crash from the heavy vehicle's point of view. The car can pass underneath the bumper at the front, the trailer or the box of the straight truck at the side, or the back of the trailer or box at the rear. Guards can be installed in these areas to eliminate the underride effect of the small vehicles and to improve the interaction

between the vehicles. This research investigates and outlines the principles of side underride protection devices to eliminate the incompatibility between the large trucks and small vehicles. An outline of a guard which can be added to a trailer to prevent underride is shown in Figure 1.2.

1.2 OBJECTIVES

The purpose of this research is to investigate the collision statistics for this type of crash to determine the need for the guards. An in depth literature review is conducted explaining the limited current solutions to this problem along with an overview of existing patents. The objective is then to create and design a process for developing the lightest and most feasible side underride guards for heavy vehicles. To first design the guards, a regulation for testing their effectiveness is proposed since no such regulation currently exists for side devices. With the application of the proposed regulation, topology and multi-objective optimization procedures are utilized to create the most feasible guards while reducing their overall mass and increasing their robustness. A number of tests for both tractor-trailers and straight trucks are created to demonstrate the validation of the systems along with their benefits during these collisions.

1.3 COLLISION STATISTICS

There has been a significant amount of statistics and surveys conducted over the years recording the occurrence of passenger vehicle to heavy vehicle collisions. These findings illustrate the injuries, their severity and the amount of fatalities. In Canada, a study conducted between 2001 and 2005 investigated these types of collisions. In total, there was a yearly average of 2500 road accident fatalities. These included all collisions involving passenger cars, vans, light trucks, heavy vehicles and pedestrians. During the same time period, there was a yearly average of 148,828 injuries. Of the 2500 fatalities, 12.4% of them involved tractor-trailers, 6.3% involved straight trucks and 18.3% were with heavy trucks. The other 63.0% was caused by other types of vehicles. Of the 148,828 injuries, 2.7% were caused by tractor-trailers, 3.1% by straight trucks and 5.7% by heavy vehicles [1] [2]. Figure 1.3 shows these statistics in a pie chart arrangement.

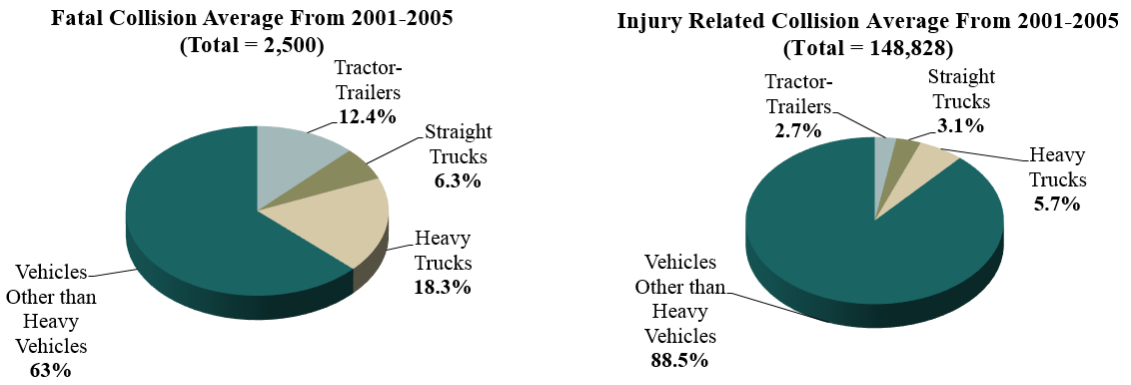

Figure 1.3 - Average of fatal and injury related collisions from 2001 to 2005 [2]

This same research outlines the collisions involving the side of tractor-trailers. Of the total 12.4% shown above, several side configurations can be observed. The "right angle (side crash)" accounts of 13.0% of fatalities, the "side swipe" accounts for 3.9%, the "left turn across traffic" is responsible for 3.0% and the "approaching side swipe" for 2.9%. Other configurations relating to the side of tractor-trailers include the "passing right" and the "right turn". The same can be seen for the injuries in these crashes. The "right angle" is responsible for 8.7% of the injuries, the "right turn" for 2.9%, the "left turn across traffic" for 4.9% and the "side swipe" for 2.9%. The other configurations also play a factor in the injuries [1]. To summarize the research findings, the following charts in Figure 1.4 were made.

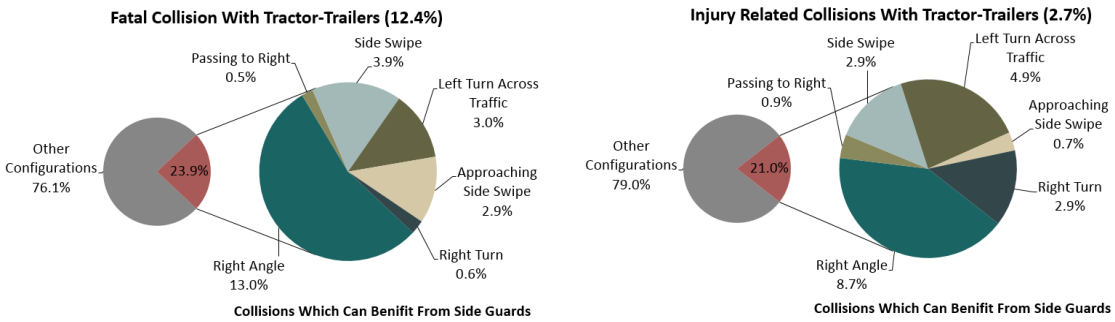

Figure 1.4 - Fatality and injury related collision configuration with tractor-trailers [2]

To get an understanding of how many heavy vehicles are on the roads along with their configurations in Canada in comparison to the amount of light vehicles, the 2009 Canadian Vehicle Survey Summary Report is investigated [3]. The report shows that in

2009, there were 437,997 medium trucks (vehicles between 4.5 and 15 tonnes) and 317,219 heavy trucks (vehicles over 15 tonnes) on the roads. During that year, there was 19,755,954 light vehicles on the road. Figure 1.5 and Figure 1.6 shows the amount of kilometers traveled by each type of vehicle along with the different configurations available in each class.

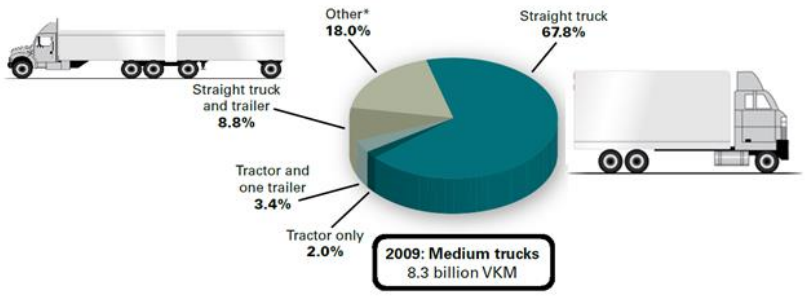

Figure 1.5 - Distance travelled by medium trucks by configuration in 2009 [3]

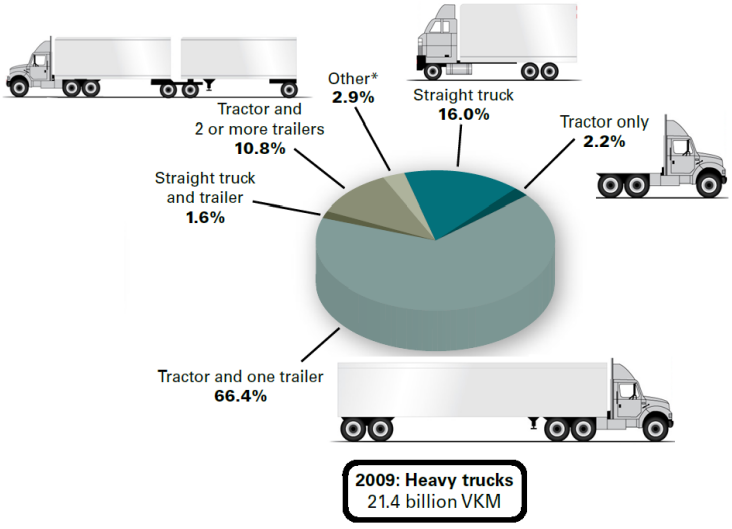

Figure 1.6 - Distance travelled by heavy trucks by configuration in 2009 [3]

In comparison to the Canadian statistics, in 2010, the United States saw 3,675 fatalities related to large truck accidents and approximately 80,000 injuries. The number of fatalities saw a 9% increase compared to 2009 which had 3,380. The statistics show that of all fatalities, 76% were occupants of the small vehicle, 10.0% were non-occupants and

14% were people inside the large trucks. Of these, 18% occurred when the car had an impact point with either the left or right side of the large truck [4].

A paper evaluating light vehicle side underride collisions investigated the data available in the Fatality Analysis Reporting System (FARS) published on the National Highway Traffic Safety Administration (NHTSA) website. They concluded that from 1994 to 2005, there was an annual average of 2,254 fatalities that occurred when light vehicles collided with combination trucks. Of those, 393 occurred when the vehicle crashed into the side of the large vehicle and 78 were considered to be underride. Over the 12 year period of the study, there was 932 light-vehicle fatalities from side underride. The same report estimates that there was a yearly average between 1995 and 2005 of 28,274 injuries related to light vehicle to combination trucks collisions with 5,085 of these being occupants injured during side underride [5] [6]. The NHTSA website published a chart which shows the 2011 statistics of fatal crashes when a motor vehicle would crash into a transport by different initial points of contact. In this chart, the left side of a transport accounted for 266 of fatalities and the right side for 155. It may also be noted that in 2011, there was 3,608 reported deaths involving small car to transport collisions [6]. With the statistics shown above, it is evident that the addition of side guards can prevent and reduce the amount of injuries and fatalities.

CHAPTER 2: LITERATURE REVIEW

2.1 A HISTORY OF UNDERRIDE GUARDS

In the United States, every trailer with a gross vehicle weight rating (GVWR) of 10,000lbs or greater manufactured on or after January 24th 1998 must be equipped with a rear underride guard. These devices must conform to the specifications found in the Federal Motor Safety Standards (FMVSS) No. 223 and 224 [7]. The FMVSS No. 223 describes the load testing, strengths and energy absorbing requirements for the guards and the FMVSS No. 224 describes their size requirements [7] [8] [9]. Previous to this regulation, the Federal Motor Carrier Safety Regulations required rear-impact guards on these vehicles however, they lacked physical strength testing and were of a smaller size. These were effective between January 1st 1952 to January 25th 1998 [7]. In Canada, a regulation resembling the United States regulation is also established. Although the size requirements are the same, an additional strength test is conducted on the guards [10]. These requirements are outline in the next section of this chapter.

In Europe, there exists a regulation for the design and testing of front underride protective devices. The rules and standards are outlined in the Economic Commission for Europe (ECE) Regulation No. 93. This regulation had a date of entry into force of February 27th 1994 [11]. Along with the rear underride regulation, the United Nations also established a Lateral Protection Device (LPD) regulation to govern side guards for the protection of unprotected road users such a cyclists and pedestrians [12]. Much like the rear guards in the United States and Canada, the ECE has their own standards and testing procedures which are outline in the ECE Regulation No. 58 [13].

2.2 STANDARDS AND REGULATIONS

2.2.1 REAR GUARDS

As previously mentioned, FMVSS No. 223 and 224 are the regulations for rear underride protection devices (RUPDs) in the United States. Their purpose is to reduce the amount of fatalities that occur when a light vehicle collides with the rear of trailers and semi-

trailers. As outlined in FMVSS 223, the guard must have a minimum cross section height of at least 100mm at any point on the device itself and must comply with very specific strength tests. At location P1, the guard must resist a force of 50,000N on either the left or right side. At location P2, the guard must hold a force of 50,000N and at location P3, it must resists a force of 100,000N on either the right or left side. During these tests, the maximum allowable deflection of the guard is 125mm. In addition to the load tests, the guard must meet energy absorption guidelines. The guard is required to absorb by plastic deformation at least 5650J of energy within the allowable 125mm of deformation at location P3 [8]. Figure 2.1 from FMVSS No. 223 shows these locations along with basic dimensions of the guards.

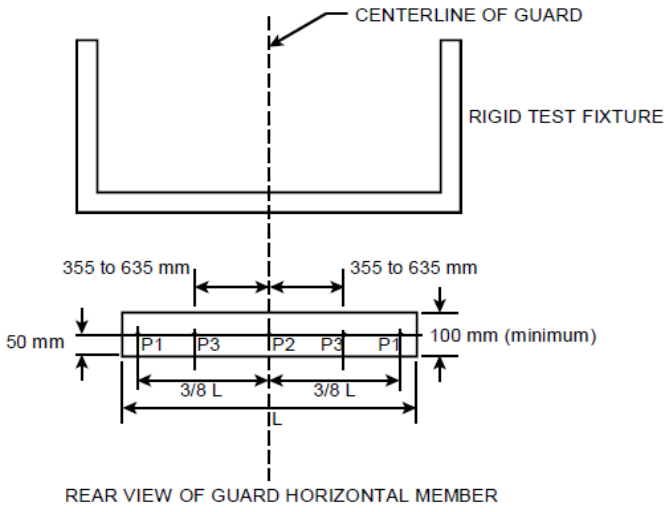

Figure 2.1 - RUPD FMVSS No. 223 test locations [8]

During testing, the guards are mounted on a rigid test fixture and are required to be attached in the same manner as they would be to the vehicle. They use a rigid test fixture to resist the forces that are applied to the guard. To apply these forces, a ram fixed in one direction of motion is utilized. This device consists of a rectangular solid piece of rigid steel which has a height of 203mm, a width of 203mm and a thickness of 25mm. It must have rounded edges with a radius of 5mm +/- 1mm. During testing, it must have a forward displacement of at least 1mm/s and no more than 1.5mm/s. It must be restrained to prevent rotation [8].

In Canada, the relatively same approach is taken in the CMVSS No. 223 report. Figure 2.2 shows the point load test locations from the CMVSS report.

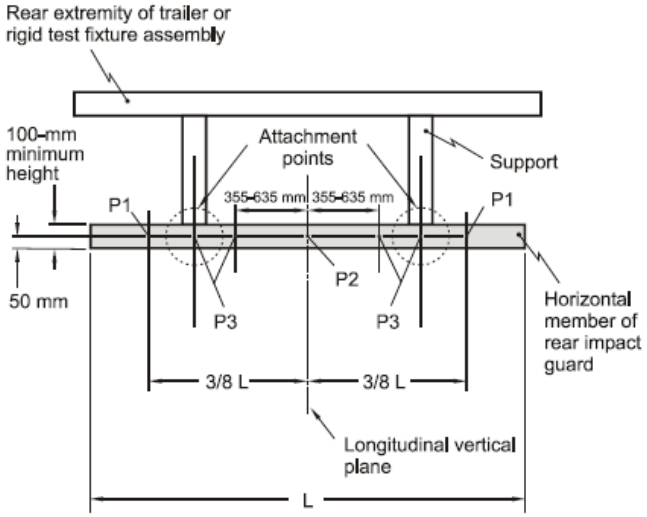

Notes:
1. L means width of the horizontal member.
2. Drawing not to scale

Figure 2.2 - RUPD CMVSS No. 223 test locations [10]

The load tests require that Location P1 and P2 be tested with a force of 50,000N. Location P3 is exempt from the tests. Instead, an additional test is done which consists of a "Uniform Load Test Force Application Device". This device must have a height of 203mm and a width that is larger than the distance between the outside edges of the outer supports of the guards. During testing, the center of the device must be aligned with the center axis of the guard and must be guided to prevent rotation. The displacement rate of the application device is 90mm/min and the guard must hold the force with a maximum deflection of 125mm [10]. The force applied with this device is 350,000N and the guard is required to absorb 20,000J of energy by plastic deformation. If the manufacturer decides to forgo the energy absorption requirement, the guard must be tested with a force of 700,000N. If the guard is symmetrical, it may be tested only on one side, with half of the required force. The ground clearance of the guard must be at maximum of 560mm from the ground and must be measured before and after the tests to pass the regulation [14]. Figure 2.3 shows two additional views of the Canadian

regulation, demonstrating the “Uniform Load Test Force Application Device” and its location.

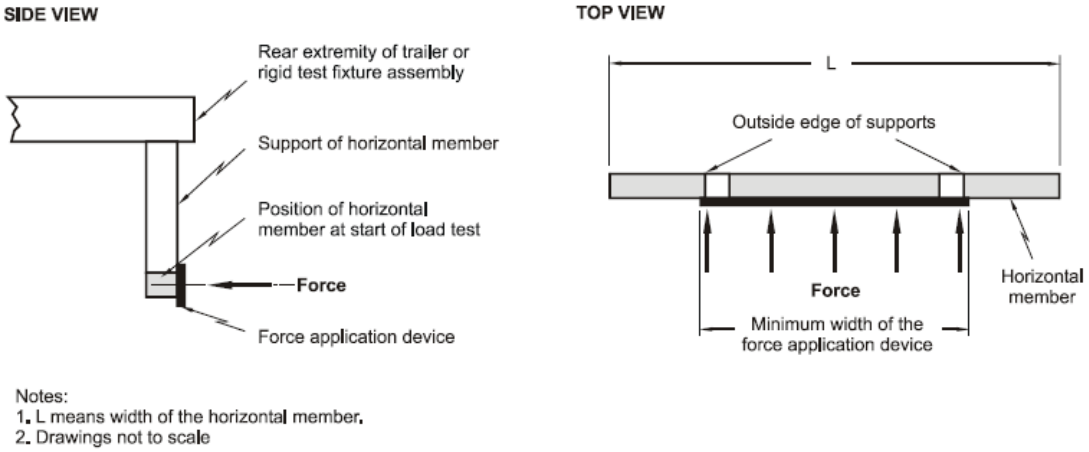

Figure 2.3 - CMVSS Uniform Load Test Force Application Device [10]

2.2.2 FRONT GUARDS

Front underride protection devices regulated by the Economic Commission for Europe utilize the same testing method used in North America for rear guards. They are to be installed on the category N2 and N3 vehicles. An N2 category vehicle has a gross vehicle weight of 3.5 to 12.0 tonnes and an N3 vehicle has a weight of over 12.0 tonnes [15]. For vehicles in the N2 category, the overall height of the device must be 100mm and for the N3 category, the height must be 120mm. The maximum ground clearance of the guard is 400mm and its overall width must not exceed the width of the mudguards nor shall it be more than 100mm shorter than the sides of the foremost axle [11]. During testing, the guard must remain within 400mm of the vehicle’s front end. The force at location P1 and P3 must be at least 50% of the gross vehicle weight with a maximum of 80,000N and location P2 must be 100% of the gross vehicle weight with a maximum of 160,000N [15]. The locations and basic dimensions of the guards are represented in Figure 2.4 from the regulation.

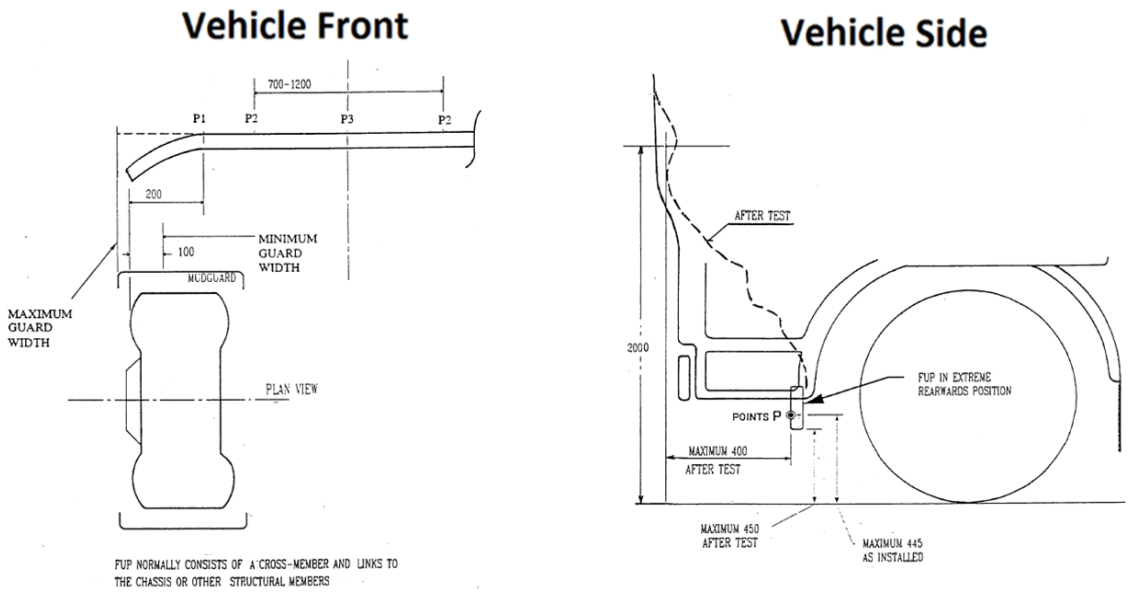

Figure 2.4 - ECE Regulation 93 force locations and dimensions [11]

2.2.3 SIDE GUARDS

The ECE also has a regulation for Lateral Protection Devices (LPDs). The purpose of this device is to prevent unprotected road users classified as pedestrians, cyclists and motor cyclists from falling under the sides of the trucks and trailers and getting caught under the wheels [12]. These guards are required for the N2 and N3 class of vehicles which have previously been explained, along with the O3 and O4 trailer categories. The O2 category represents all trailers with a gross mass of 3.5 to 10 tonnes and the O3 category is any trailer weighing over 10 tonnes [16]. The guard itself can consist of a flat panel or of one or more side rails [15]. The maximum ground clearance of the guard must be 550mm and shall be positioned at a maximum of 30mm away from the outer edge of the vehicle over the rearmost 250mm and 120mm over the rest of the guard. Its testing procedure requires the use of a flat plate with a diameter of 220mm +/- 10mm and the guard must stay rigid with an applied force of 1,000N [15]. Figure 2.5 shows the basic dimensions of the lateral protection device.

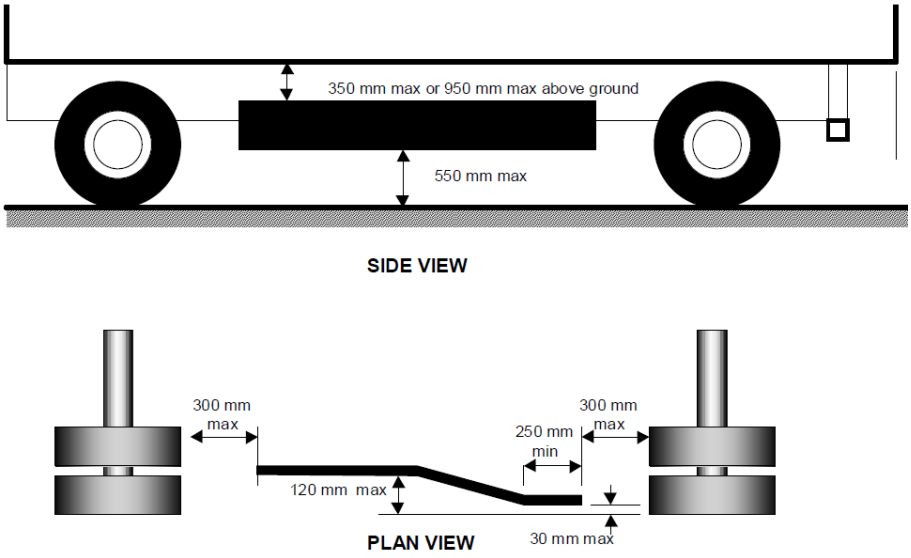

Figure 2.5 - ECE Regulation 73 lateral protection device dimensions [15]

Although these guards proved to be beneficial for stopping unprotected road users from passing under the vehicles and preventing them from getting caught under the wheels, their strength requirements and their dimensions do not prevent light vehicles from underriding. Because of this, it is beneficial to implement a regulation to prevent this type of collision from occurring along with allowing the guards to protect the unprotected road user [17].

Along with the ECE, other countries have either expressed an interest or have implemented their own regulation for side guards. Australia has shown interest in regulating protection on the side of their heavy vehicles. They proposed to implement the ECE Regulation 73 to vehicles with a gross mass of 7.5 tonnes or greater. However, they ruled that the adaptation of side guards would not be beneficial due to the cost and limited amount of injuries and deaths compared to the front and rear statistics. Research showed that out of all underrun accidents that occurred each year, 75% of the fatalities occurred from a front impact, 10% from a rear impact and the other 15% from the side [16] [2]. The Australian Trucking Association has published an Advisory Procedure to assist companies in improving the understanding of side guards. Its requirements are in accordance with the ECE Regulation 73 however, the advisory

procedure is only a guide, and is to be used voluntarily. It is not enforced on manufacturers [18] [2]. Figure 2.6 shows the dimensions outlined in the Advisory Procedure.

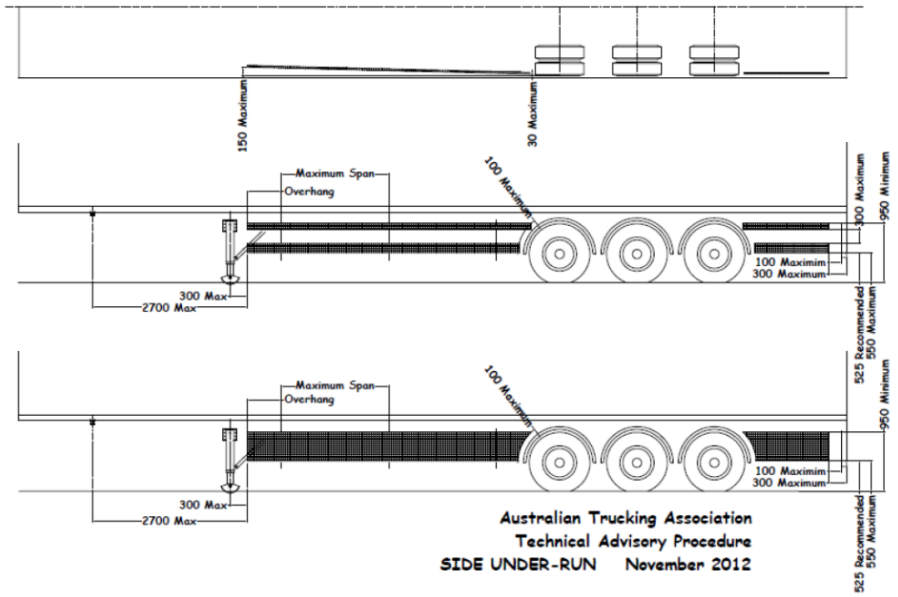

Figure 2.6 - Australian Trucking Association side underrun design and dimensions [18]

The Japanese government has also implemented regulations on pedestrian protection side guards. Their regulation is outlined in two supporting documents: the Safety Regulations for Road Vehicle (Ministerial Ordinance) and its subordinate regulation document (Announcement). The Ministerial Ordinance states that ordinary-sized vehicles used for the transportation of goods or ordinary-sized vehicles with a gross mass of 8 tonnes or greater must be equipped with side guards. An exception to these rules are vehicles that can carry 11 or more passengers. The strength, testing procedures, and dimensions for the regulation are outlined in the Announcement. Their requirements are slightly different compared to Regulation 73. The maximum allowable ground clearance of the bottom of the device is 450mm and the upper edge must be at least 650mm from the ground [16]. As previously mentioned, although beneficial to unprotected road users, these regulations do not prevent vehicle underride or provide any sort of protection to occupants of light vehicles [2].

2.3 DESIGN CONSIDERATIONS FOR SIDE UNDERRIDE GUARDS

There is a limited amount research in the field of side guards for the prevention of vehicle underride. Some institutions and independent companies have conducted projects to develop and test side underride guards to investigate their benefits and reactions during a collision. There was also thesis work conducted on using the principles of rear underride guards to design side guards. Finally, there have been studies examining the effects of side underride collisions without guards on light vehicles.

A thesis from the Graduate School of Wichita State University investigated rear underride guards with a pliers design. The author created a side guard for a straight truck using the same methods as the regulation for rear guards. He conducted experimental collisions with a Ford Taurus at three different speeds: 30, 40 and 50 mph. The Taurus in these cases weighed 1378kg. Each speed consisted of three individual tests: one without a guard installed, one with the new pliers guard design and the other with the pliers guard with added horizontal cables [19]. The guard installed on the 8000kg straight truck is observed in Figure 2.7.

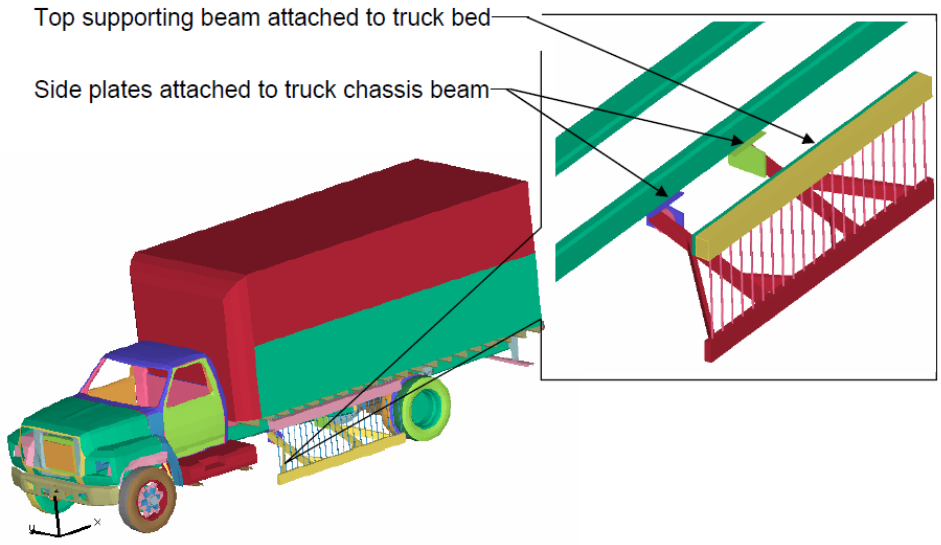

Figure 2.7 - New pliers guard on the side of a straight-truck [19]

For each test case, the passenger compartment intrusion is observed to evaluate the effectiveness of the guards. The displacements, velocities and accelerations are also investigated. The final comparison of all the tests can be seen in Table 2.1.

Table 2.1 - New pliers guard test comparison [19]

	30 mph (13411 mm/s)	40 mph (17881.6 mm/s)	50 mph (22352.0 mm/s)
No Guard			
Displacement of tunnel at the end (mm)	2140	2590	3130
Velocity of tunnel at the end (mm/s)	4730	4920	5260
Maximum tunnel longitudinal acceleration (G)	-34	-39	-39.9
Maximum tunnel transverse acceleration (G)	22.2	25.1	28.9
Maximum tunnel vertical acceleration (G)	-32.8	-40.3	-44.8
New Pliers Guard			
Displacement of tunnel at the end (mm)	1460	1750	2130
Velocity of tunnel at the end (mm/s)	831	1870	2200
Maximum tunnel longitudinal acceleration (G)	-36.2	-42.3	-48.1
Maximum tunnel transverse acceleration (G)	-15.1	-13.8	-23.9
Maximum tunnel vertical acceleration (G)	22.8	24	-35.2
New Pliers Guard with Horizontal Cables			
Displacement of tunnel at the end (mm)	1530	1830	2190
Velocity of tunnel at the end (mm/s)	735	1350	2030
Maximum tunnel longitudinal acceleration (G)	-37.6	-48.3	-44.5
Maximum tunnel transverse acceleration (G)	-15.2	21.3	-23
Maximum tunnel vertical acceleration (G)	26.6	26.1	-34.6

The addition of an underride guard to the F800 straight truck proved to be beneficial when observing the data in Table 2.1. It is evident that adding the guard reduces the distance traveled by the small vehicle under the heavy truck in all three velocity cases when looking at the displacement of the tunnel. In these same cases, the velocity at the end of the runs is also greatly reduced when comparing the collisions with and without a guard. This indicated that at the 0.2s point (the end of the simulation) the vehicle had almost completely stopped. This shows that it is no longer traveling under the heavy vehicle [19].

A project from APROSYS (Advanced Protection Systems) was initiated on April 1st 2004 and had a duration of 60 months. Its purpose was to improve the current state of truck and trailer side protection to reduce the amount of injuries and fatalities that occur from side crashes. Their goal was to utilize an ordinary pallet box to investigate its crash properties then to improve it to be feasible during collisions. When installed under a trailer, the box would add storage space while filling the large unprotected gap between the kingpin and the rear axles. In total, four physical crash tests were conducted. The first two physical tests were conducted using an ordinary pallet box and a reinforced

pallet box mounted on a rigid test rig. Both of these collisions were tested using a 1998 Fiat Punto with an initial velocity of 63km/h. They were then compared to the project's computer simulated models to test their validity [20]. Figure 2.8 shows the difference between the conventional and crashworthy pallet box designs.

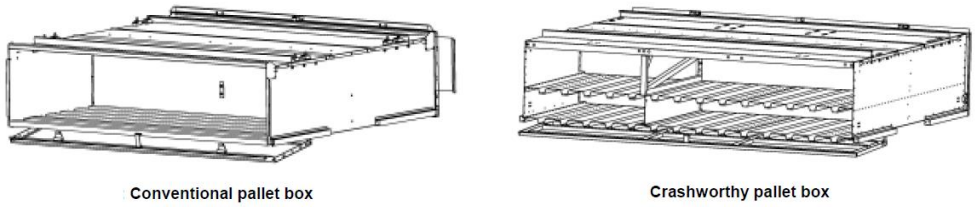

Figure 2.8 - APROSYS conventional and crashworthy pallet box [20]

The conventional pallet box weighed 240kg and the crashworthy pallet box weighed 410kg. These initial tests were conducted to validate the numerical simulations to identify the weak points and to make design changes if necessary. The results showed that with the reinforced pallet box, the system did in fact prevent vehicle underride. The simulated tests also proved to be an accurate representation of the physical crashes. During the initial tests, the author noticed that the door was too heavy and difficult to operate. Because of this, modifications were made before the next tests to reduce the weight while maintaining its crashworthy properties. The second set of tests involved mounting the guard on a physical trailer. The trailer had a triple axle configuration, providing a smaller gap for underride [20]. It must be noted that a larger device would need to be installed on longer or dual axle trailers which would result in more added weight [2]. In the second round of tests, the vehicles used were Fiat Bravos. With the modifications done to the crashworthy box, its mass was now 400kg. The analysis of the tests showed that when the regular pallet box was installed, the car experienced massive deformations of the A-pillars to the point where they were making contact with the B-pillars. This deformation greatly reduced the survival space in the cabin. Most of the deformation was observed in all parts of the vehicle higher than 730mm from the ground. The pallet box in this case was completely deformed. On the other hand, the vehicle that collided with the reinforced pallet box did not have major deformations. Its post-crash properties were that of a normal full frontal crash. The pallet box allowed for

the crashworthy properties of the car to react as they should by simulating a wall like type of collision. In this case, the deformation of the A and B-pillars were negligible and the survival space was still intact. In the end, the deceleration values of the normal pallet box were low and there were large deformations of the vehicles. The reinforced pallet box had high deceleration values but the vehicle deformations were much smaller [20]. The deformation of the post-collision cars are compared in Figure 2.9.

Figure 2.9 - Post crash views of conventional and crashworthy boxes [20]

A paper published by the Society of Automotive Engineers (SAE) examined the scientific approach to tractor-trailer side underride analysis [21]. The authors claimed that a main area of concern when trying to analyse this type of collision resides in the reporting system used by the police. They noted that there is lack of appropriate coding to identify and properly report this type of collision. From their experience, they concluded that side underride crashes occur more often than is reported. The purpose of this paper was to recreate and reconstruct side underride collisions, and analyze the events that lead to and occur during the collisions. Some observations during the side collisions were that passenger cars traveling at speeds approaching 30mph completely passed under the trailers and experienced massive deformations. They noted that very few sedans and larger vehicles colliding at speeds of 35mph involving only the roof structure would not completely pass under the trailers. The authors also noted that at speeds below 40mph, larger vehicles such as vans, SUVs and pickup trucks would most likely not pass under the trailers. There is a lack of tests conducted thus far to establish the upper limit of these tests [21]. The Midwest Institute of Safety has conducted 32 underride tests at speeds between 7 and 37mph. The authors have used this data in their paper to

determine a generic equation to identify the initial speed of an underride crash. Several types of vehicles and crash configurations including multiple approach angles were used. From their analysis, they noted two major observations. The first is that during the crash, the A-pillar would deform rearward and downward since it catches the bottom of the trailer upon contact. This would then cause the roof to collapse and fold rearwards. Their other observation was that during other crashes, they would notice a wedge type effect occurring. In this case, the A-pillars would not catch the bottom of the trailer. Instead, they would travel below the edge of the trailer and wedge the roof under the trailer while compressing it. With the measured parameters after the collisions, the authors were successfully able to establish a general equation to determine the initial velocity of side underride collisions [21].

With the above mentioned, some systems have been designed and proven to be effective at reducing vehicle side underride with the addition of a device to the underside of trailers and trucks. In the case of the pallet box, this design would be difficult to incorporate to a longer trailer with a dual axle due to the large weight of the device. Unlike the typical approach to using the regulations when designing front or rear guards, they do not exist for side guards making it difficult to test the robustness and feasibility of these guards and other possible guard designs [2].

The International Institute for Highway Safety has published some interesting facts on underride guards in one of their Status Reports. They state that during rear impacts, most existing guards do a decent job at stopping the passenger vehicles from sliding under the trailers. But, when the crashes involve only a small portion of the vehicle such as an offset collision, only one out of the 8 tested guards passed the 30% overlap test. This indicates that the established testing regulation for rear guards should be investigated and revised. In this same report, an article is published concerning side guards [22]. The article is an excerpt from a paper explaining the benefits of side guards on large trucks. It states that when fatal underride collisions with tractor-trailers are observed, about one fifth are caused by collisions with the rear, three fifths with the front and the other fifth with the side. When investigating the Large Truck Crash

Causation Study (LTCCS), the authors concluded that there was 206 impacts with sides of large trucks that could be studied. Of these, 143 had injuries or fatalities caused by the accident. Of the 143 collisions, 98 had slight or severe underride of the passenger vehicle. The investigation found that when looking at all 143 crash scenarios, 76 could have benefited from an underride guard to reduce the injuries or could have prevented fatalities. The authors commented on a guard that was designed and tested to prevent underride of small vehicles. The tests were conducted at 56km/h and at a 45 degree angle. The ground clearance of the guard was 510 mm and it had a weight of 435kg [23] [24]. The addition of SUPDs can have some issues when implementation is concerned such as the effect on the payload of the trailers and the effect on aerodynamics. Other issues include the effect on brake cooling, break-over angle, the collection of snow and mud and preventing access to the underbody for inspection and maintenance [22] [16]. The processes and measures taken in this research will address some of these issues by creating lightweight guard designs with aerodynamic benefits.

2.4 PATENT ANALYSIS

Some patents have been filed in the United States regarding the design of possible side underride protection devices. One of these is Patent No. US 7,780,224 B2 filled on June 9th 2008. It incorporates a crash attenuating underride guard as a moulded block placed under the trailer. This block incorporates aerodynamic features to deflect the air away from the non-aerodynamic features of the trailer and wheel assembly. The device itself consists of having an angled front section located at the trailer jack. At the rear, the section is angled allowing for air to travel away from the wheels and the rear of the trailer. Figure 2.10 shows one possibility outlined in the patent document [25].

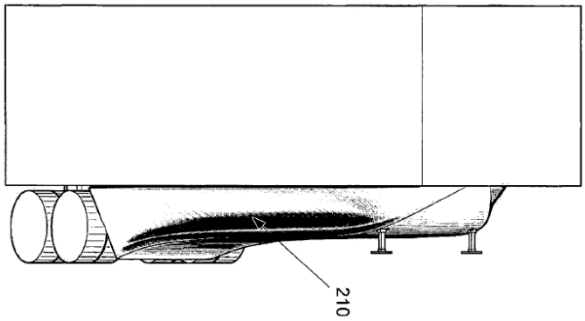

Figure 2.10 - Patent No US 7,780,224 B2 [25]

Patent No. US 2008/0116702 A1 is another patent filed in the United States on November 17th 2006 regarding side underride guards. This particular patent claims the design of an underride guard for large vehicles with trailers that have a high ground clearance. The guard is to be installed under the trailer, in a manner to obstruct a light vehicle from passing underneath. The member must be placed at a sufficient height to prevent underride. The members that hold the guard in place must consist of both upright and angled beams which can be seen in Figure 2.11 [26].

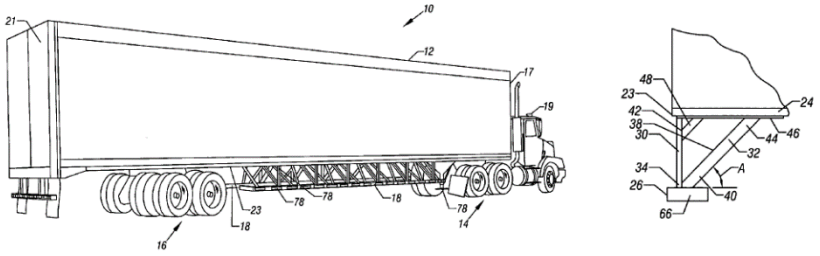

Figure 2.11 - Patent No. US 2008/0116702 A1 [26]

A third patent filled on April 15th 2010 claims the use of a side underride cable system for a trailer. This document has the Patent No. US 8,162,384 B2. It includes front and rear mounted brackets with cables extending the length of the trailer to prevent vehicle intrusion. The brackets are to be positioned at a location separate from one another with a plurality of cables extending from one to the other along the length of the trailer which can be seen in Figure 2.12 [27].

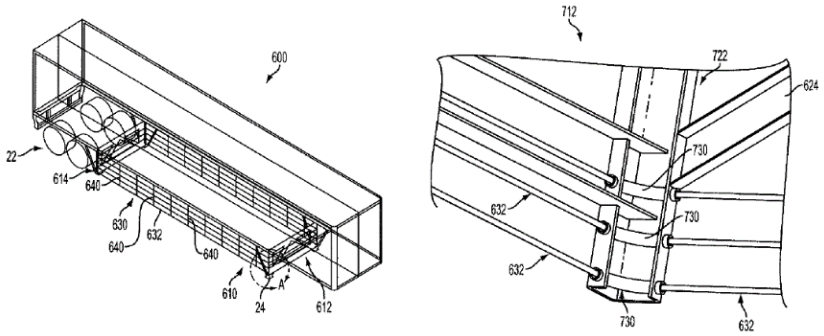

Figure 2.12 - Patent No. US 8,162,384 B2 [27]

These patents show possible designs and configurations for side underride guards to prevent light vehicles from passing under trailers. The patent documents explain the design and principles of the guards with the exclusion of physical testing and results [2]. Further consideration on side underride guards is necessary and will be conducted in this research.

2.5 AERODYNAMIC FAIRINGS

In addition to the safety benefits that side underride guards can bring to trailers and straight trucks, they may also be incorporated with aerodynamic fairings to reduce fuel consumption. For years, these devices have been incorporated on trailers for the reduction of drag and to deflect the air away from the rear axle and obstructions under the trailers.

Research from Transport Canada which investigated the benefits of the addition of aerodynamic fairings to trailers was conducted between August 2006 and February 2007. This publically available trial program demonstrates that based on their results, fleets have reported fuel consumption savings of 6.4% which translates to 339 less liters of fuel and 925 fewer kilograms of greenhouse gases per tractor-trailer per month. A fleet consisting of 57 trucks saved a total of 7,134 liters and cut their greenhouse gas emissions by 19,475kg during each month of testing [28].

A study by the National Research Council of Canada (NRC) has also investigated the effects of aerodynamic fairings in a full-scale wind tunnel. Their findings indicated that

depending on the type of fairing used, a tractor-trailer can save approximately 2,879 liters of fuel per year. Their results are based on a tractor-trailer traveling an annual distance of 130,000km cruising at 100km/h. For the study, a Volvo VN660 tractor was used with a 28ft trailer and a 40ft trailer [29].

Another study of fairings was conducted to test and compare four different designs. The underbody fairings tested included a long wedge skirt, a short wedge shirt, a short wedge skirt with a center skirt and a straight side skirt. The results indicated that the best design was the wedge type skirt due to its overall better drag reduction. The device itself starts as a point at the kingpin and extends along the length of the trailer until the ends reach the left and right side of the rear axle. The four designs can be observed in Figure 2.13 [30].

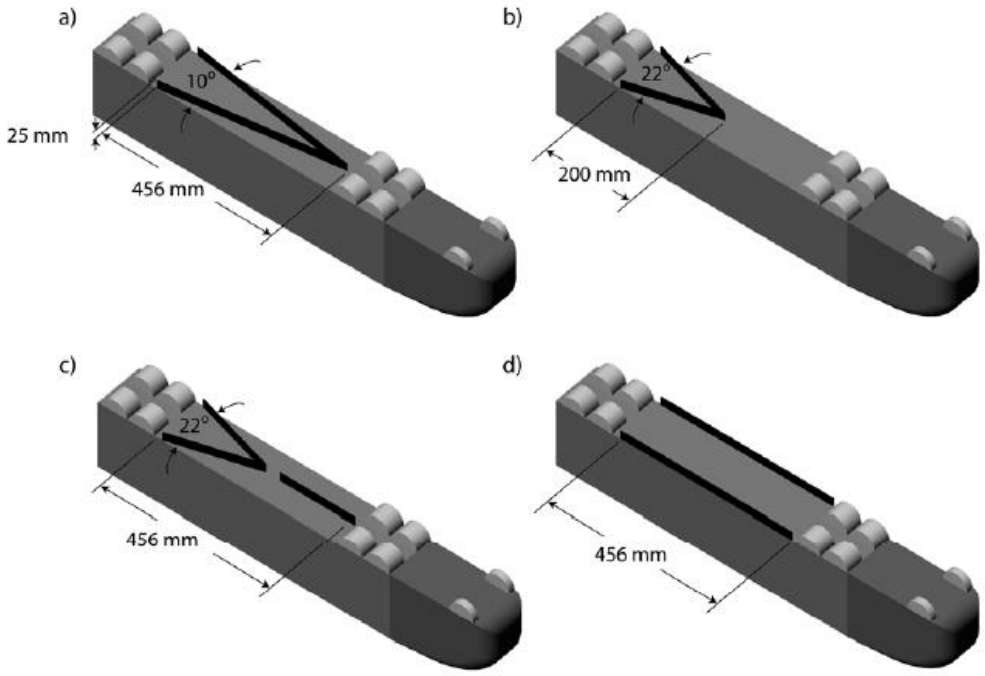

Figure 2.13 - The four designs of the fairing study [30]

CHAPTER 3: RESOURCES AND TEST VEHICLES

3.1 LS-DYNA SOFTWARE PACKAGE

For this research, the LS-DYNA software package is utilized for the collision simulations, topology and multi-objective optimization and the data acquisition. The LS-DYNA PrePost is used to set up the simulations and analyse them once they have been solved. The data can then be extracted, studied and plotted using MatLab. The LS-TaSC program is used to determine optimal load paths to aid the design process of the brackets and SUPD. The LS-Opt program is then utilized to determine shell thickness for the reduction of mass while keeping the robustness of the device. The following gives a basic understanding of the programs and methods used to design and develop the side underride protective devices.

3.1.1 LS-DYNA

Originally developed by the Lawrence Livermore National Laboratory, the DYNA3D software was released in 1976 [31]. This was the program's first iteration. During this time, the program's application was the stress analysis of structures which underwent impact loading. Since then, the program has been modified over the years to improve the software and for the addition of more capabilities. To utilize the software for proper crashworthy assessments, the Livermore Software Technology Corporation was formed in 1988 to continue the development of the product. The name of the software was then changed to LS-DYNA [32].

Today, LS-DYNA is used as a finite element code for multiple applications. These include the analysis of large static and dynamic deformations and the response of structures and structures coupled to fluids. The program is used extensively in the construction, military, manufacturing, aerospace and automotive industries. The origins of the code is highly non-linear. It uses explicit time integration to analyse transient dynamic finite elements. The term nonlinear signifies changing boundary conditions, large deformations or nonlinear materials that do not have ideally elastic behavior. The term

transient dynamic indicates the analysis of simulations that require high speed and short duration when the inertial forces need to be analysed [33]. To simulate collisions, the main solution method is based on the explicit time integration. There is also an implicit solver for the analysis of structures and heat transfer. Most implicit solutions are used with static and quasistatic loading cases to remove the inertial effects. This solver is used in this research when applying the regulation loads to the guards to test for robustness.

3.1.2 LS-PrePost

The Livermore Software Technology Corporation has developed its own pre-processor to create LS-DYNA input files. It allows for pre-processing features such as meshing tools for surface, solid, 2D, block and tool meshing. It also has special applications such as metal forming, airbag folding, dummy positioning, and model checking. Its primary function is to deliver comprehensive LS-DYNA keyword support to create, view and model LS-DYNA files in an interactive manner. Its post-processing features include the plotting of the data, the processing and animation of the output files [34].

3.1.3 Topology (LS-TaSC)

The LS-TaSC software is a topology and shape computational application for LS-DYNA. Its purpose is to optimize structures to reduce the mass of objects while maintaining their structural integrity. The optimizer in the program takes the initial file which contains boundary conditions, design domains and loads then derives the optimal shape, size and gap locations for the object [35]. In this research, this application is used for the shape optimization of the support brackets for the SUPDs.

3.1.4 Optimization (LS-Opt)

The manual for the LS-Opt software describes the conventional design approach such as when an initial design is improved by evaluating its final response then adjusting it and making changes based on experience or intuition. It some cases, this does not always give the desired results or the best possible design. This software aims to use an inverse method to this approach by first allowing the software to apply specific criterions and

then computing the final design. It accomplishes this by having the user input design criterions which are added as constraints and objectives into the optimization problem. Once solved, the finished design is the optimal solution design [36].

3.1.5 SAE CLASS FILTER

The raw data collected from the post-processor must be filtered before being analysed. This data includes the forces experienced during the impacts and the accelerations. In the Manual for Assessing Safety Hardware (MASH), the authors indicated that for the primary reference instrumentation specifications, the optical instrumentation (SAE J211-1 JUL2007 and J211-2 NOV2008) should be used for crash testing. It is recommended that vehicle acceleration data be filtered at 60Hz for the purpose of data representation [37]. This filter is called the SAE Channel Class 60. In a book published concerning the mechanics of a vehicle during a crash, the author states that the necessary filter for vehicle collision simulation is the Channel Class 60. Other classes are necessary when analysing different aspects of the collision [38]. Table 3.1 shows these classification.

Table 3.1 - SAE J211 Channel Class Selection [38]

Channel Class Selection – SAE J211

Typical Test Measurement	Channel Class
Vehicle structural acceleration for use in:	
Total vehicle comparison	**60**
Collision simulation (for example, impact sled) input	60
Component analysis	600
Integration for velocity or displacement	180
Barrier face force	**60**
Belt restraint system load	**60**
Occupant	
Head acceleration	**1000**
Chest acceleration	**180**
deflection	180
Pelvis	
acceleration	**1000**
forces	1000
moments	1000
Femur/knee/tibia/ankle	
forces	**600**
moments	600
displacements	180
Sled acceleration	**60**
Steering column load	**600**
Headform acceleration	**1000**

3.2 TEST VEHICLES

3.2.1 2010 TOYOTA YARIS

This finite element model of a 2010 production Toyota Yaris was developed at the National Crash Analysis Center (NCAC) of the George Washington University (GWU). To create the model, engineers utilized reverse engineering methods to replicate the vehicle from a production model for accuracy and consistency. The reverse engineering process to create the Toyota Yaris consisted of taking apart a production version model, cataloging the parts, scanning them for geometry, measuring their thickness and assessing their material type. The parts were then meshed and assembled on a computer and the car was put together. The model is validated by comparing the simulated crash results to the data obtained from the physical frontal New Car Assessment Program (NCAP) test of the National Highway Traffic Safety Administration (NHTSA). It was created to support finite element crash simulations [39]. Figure 3.1 shows the finite element model of the 2010 Toyota Yaris.

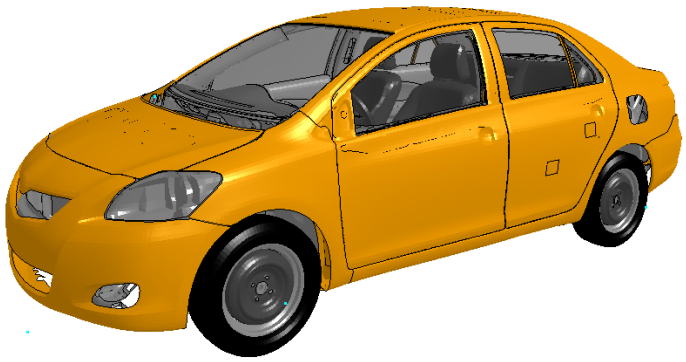

Figure 3.1 - LS-DYNA 2010 Toyota Yaris model

The vehicle in question conforms to the Manual for Assessing Safety Hardware 2009 (MASH) requirements for a small test vehicle. These vehicles weigh approximately 1,100kg and are represented as the 1100C class. This weight was selected by studying the 2nd percentile of vehicle weight for the passenger vehicle types sold in 2002. The results indicated that this vehicle was a small sedan with an approximate weight of

2,420lbs or 1,100kg [37]. Table 3.2 demonstrates the properties of the MASH vehicle classes.

Table 3.2 - Recommended properties of MASH vehicle class 1100C and 1500A [34]

Property	1100C (Small Car)	1500A (Intermediate Car)	2270P (Pickup Truck)
MASS, lb (kg)			
Test Inertial	2420 ± 55 (1100 ± 25)	3300 ± 220 (1500 ± 100)	5000 ± 110 (2270 ± 50)
Dummy	165 (75)	Optional	Optional
Max. Ballast	175 (80)	440 (200)	440 (200)
Gross Static	2585 ± 55 (1175 ± 25)	3300 ± 75 (1500 ± 35)	5000 ± 110 (2270 ± 50)
DIMENSIONS, in. (mm)			
Wheelbase	98 ± 5 (2500 ± 125)	N/A	148 ± 12 (3760 ± 300)
Front Overhang	35 ± 4 (900 ± 100)	N/A	39 ± 3 (1000 ± 75)
Overall Length	169± 8 (4300 ± 200)	N/A	237 ± 13 (6020 ± 325)
Overall Width	65 ± 3 (1650 ± 75)	N/A	78 ± 2 (1950 ± 50)
Hood Height	24 ± 4 (600 ± 100)	N/A	43 ± 4 (1100 ± 75)
Track Width[a]	56 ± 2 (1425 ± 50)	N/A	67 ± 1.5 (1700 ± 38)
CENTER OF MASS LOCATION,[b] in. (mm)			
Aft of Front Axle	39 ± 4 (990 ± 100)	N/A	63 ± 4 (1575 ± 100)
Above Ground (minimum)[c]	N/A	N/A	28.0 (710)
LOCATION OF ENGINE	Front	Front	Front
LOCATION OF DRIVE AXLE	Front	Front or Rear	Rear
TYPE OF TRANSMISSION	Manual or Automatic	Manual or Automatic	Manual or Automatic

3.2.2 2001 FORD TAURUS

The Manual for Assessing Safety Hardware states that a mid-sized test vehicle should be utilized when evaluating the performance stages of energy-absorbing systems. For this, they established the 1500A class of vehicles weighing approximately 3,300lbs or 1,500kg. In this case, a midsized sedan is utilized as most appropriate body style for this class and its specifications are seen in Table 3.2 [37]. By following these guidelines, the 2001 Ford Taurus finite element model was developed. In similarity to the Toyota Yaris model, the Taurus was developed by the NCAC at the George Washington University. The crash data of the model was compared to and validated using the NHTSA actual test data. Additional validation tests were conducted such as a full frontal wall impact, a moving deformable barrier impact, an offset rigid pole impact and an offset deformable barrier collision [40]. Figure 3.2 shows the 2001 Ford Taurus finite element model that will used for the testing of SUPDs.

Figure 3.2 - LS-DYNA 2001 For Taurus model

3.2.3 TRACTOR-TRAILER

The finite element tractor-trailer model utilized for the full dynamic simulations of the SUPDs was developed by a research team. The team consisted the Battelle Memorial Institute (BMI), the Oak Ridge National Laboratory (ORNL) and the University of Tennessee at Knoxville (UTK). The project was sponsored by the National Transportation Research Center Inc. (NTRCI). The vehicle utilized is a 45ft long trailer attached to a day cab tractor model with a 194in wheelbase. The finite element model has a weight of 23,127kg or 50,986lbs [41]. When looking at the tractor-trailer configuration in Figure 3.3, it is evident that there lies a large and unprotected gap between the trailer jack and the rear wheels. This gap has a ground clearance of 1,100mm and a length of 6500mm. This large gap is investigated in this research for the potential benefits of adding and underride guard.

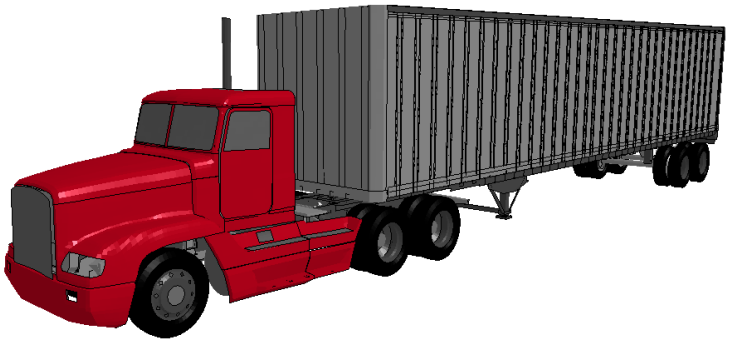

Figure 3.3 - LS-DYNA tractor-trailer model

3.2.4 FORD F800 STRAIGHT TRUCK

The other heavy vehicle investigated in this research for its penitential implementation of an SUPD is the straight truck. The finite element model utilized is a Ford F800 single-unit truck (SUT). The vehicle was developed by the Federal Highway Administration (FHWA) at the National Crash Analysis Center (NCAC). The research geared towards the development of the finite element model was conducted by the same team as the tractor-trailer model. The model has an overall weight of 8,034kg or 17,713lbs [42]. Much like the tractor-trailer, this vehicle has a large unprotected gap that small passenger vehicles can pass under during a side crash. Due to the arrangement of the rear axle, the straight truck can benefit from two guards for each of its sides. The first would be installed between the cabin and the rear axle and the second; between the rear axle and the rear most part of the vehicle. The cargo area has a ground clearance of approximately 1,050mm. The first gap has a length of 3,000mm and the second has a length of 1,800mm. Figure 3.4 shows the straight-truck model that will be utilized in the research.

Figure 3.4 - LS-DYNA F800 straight truck model

3.3 IIHS STRUCTURAL PERFORMANCE RATING

When evaluating the performance of vehicles during collisions, it is important to evaluate the deformation of the occupant compartment. The Insurance Institute for Highway Safety (IIHS) has established guidelines for rating the structural performance of

vehicles during offset frontal collisions. The report states that the injury measures recorded on a dummy are used for evaluating the crashworthiness of a vehicle. Another evaluation metric would be to calculate the collapse or intrusion of the occupant compartment. This method is a good indicator and predictor on the risk of injury on the occupants of the vehicles. In this research, the same evaluation guidelines will be used to investigate and compare underride guards and how their performance is measured from the intrusion point of view. The measurements used are nodal points in the vehicle where the driver is positioned. These points are measured pre and post-crash. The results are then plotted for observation. They consist of seven moving points inside the vehicle and the closing distance between the A and B-pillar. Two of the points are located on the instrument panel below the steering wheel. These are used to measure the deformation of the driver's knee area. There are four points located in the footwell area. The points are located on the footrest, the left toepan, the center toepan and the right toepan. The last point is located on the brake pedal. The results are then plotted in the graph of Figure 3.5 for evaluation. The values are rated on a Good, Acceptable, Marginal and Poor scale [43].

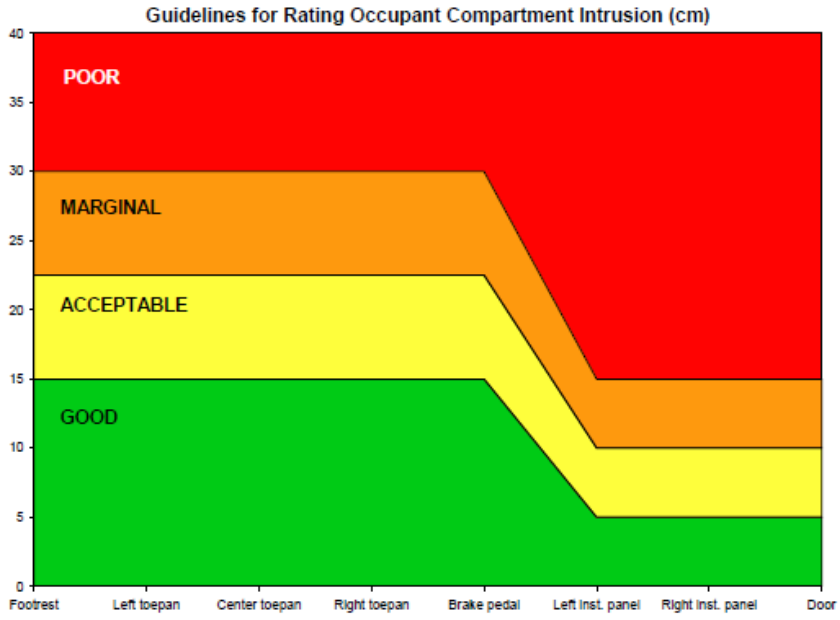

Figure 3.5 - IIHS Guidelines for rating Occupant Compartment Intrusion (cm) [43]

The collision is conducted with a vehicle colliding into a deformable barrier with an initial velocity of 64km/h. The vehicle is positioned so that 40% of its front end makes contact with the barrier. The barrier is positioned with a ground clearance of 20cm [44]. The tests are conducted with the Toyota Yaris and the Ford Taurus. The LS-DYNA software package has a card which allows for the evaluation of the IIHS guidelines. To determine the proper node selection of the LS-DYNA vehicles, simulated tests were conducted and compared to the actual test data results for accuracy.

3.3.1 IIHS TOYOTA YARIS VALIDATION

The NCAC Toyota Yaris report has the results of their intrusion measurements. Their data however only consists of the four footwell points [39]. The IIHS has published the data of the physical crash test. The identification of this test is CEF0610 [45]. The results are shown in Table 3.3.

Table 3.3 - Intrusion values for the 2010 Toyota Yaris

Test Results	NCAC Simulated Results	IIHS CEF0610 Physical Test Results
Footwell intrusion		
Footrest (cm)	85	30
Left (cm)	118	100
Center (cm)	101	60
Right (cm)	75	50
Brake Pedal Movement		
Brake Pedal (cm)	N/A	40
Instrument panel rearward movement		
Left (cm)	N/A	10
Right (cm)	N/A	10
A-pillar rearward movement		
A-pillar (cm)	N/A	10

In order to validate the LS-DYNA simulation, the collision had to be replicated in the program with a deformable barrier. The barrier is publically available online on the LS-DYNA website [46]. The first step was to determine the appropriate nodal points inside the vehicle. The Yaris model does not have a brake pedal therefore, a point located on the footwell was chosen to represent it. Figure 3.6 shows the location of these points on the finite element model.

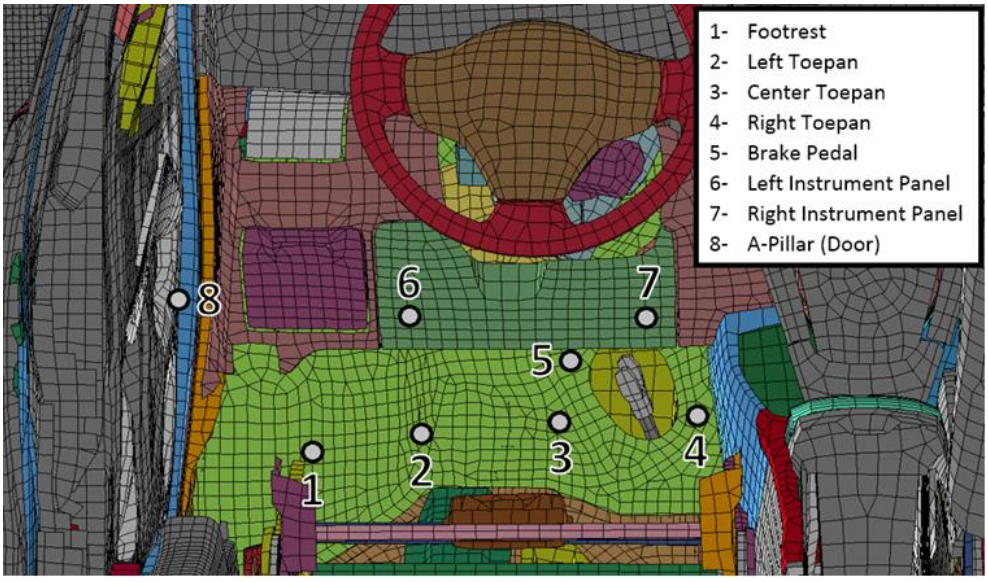

Figure 3.6 - Determined Yaris IIHS measurement points

A visual demonstration of the result of the test is shown in Figure 3.7. The Yaris, with an initial velocity of 64km/h collides with the deformable barrier. The measurements from the selected nodes are then calculated with the IIHS feature built into the PrePost and the results are shown in Figure 3.8. The data is compared to the NCAC simulation results and the CEF0610 physical data results.

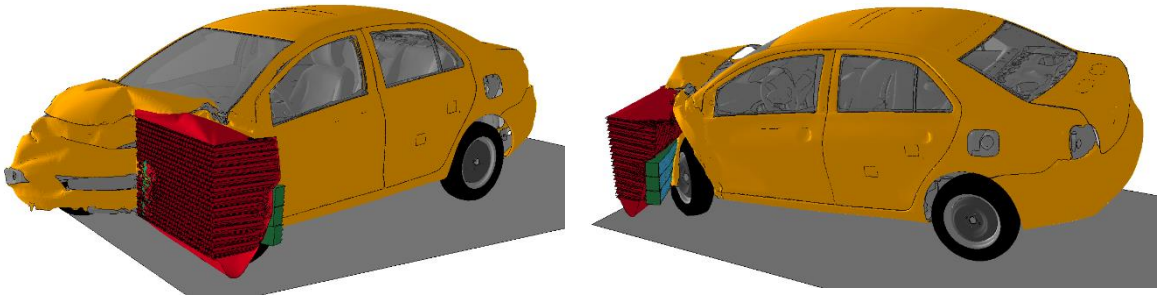

Figure 3.7 - Yaris IIHS simulation into deformable barrier

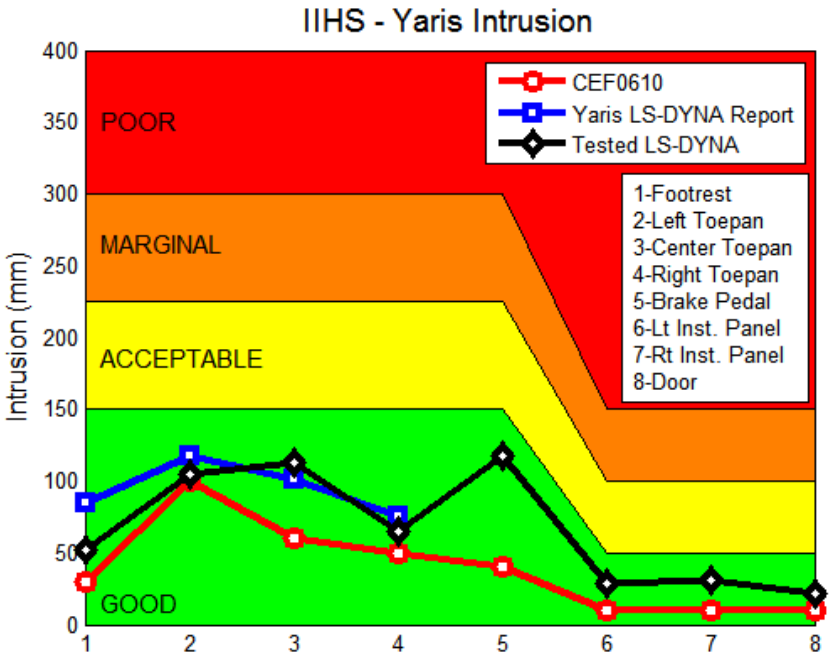

Figure 3.8 - Yaris IIHS test comparisons

The final results are very favorable compared to the actual data obtained from the physical crash test. The footrest deformation is slightly higher than the CEF0610 test. The left and right toepan were very similar. The center toepan had slightly higher values than expected however, the result was still acceptable. Since the finite element Yaris had no brake pedal, the results are much higher than the actual data. The final three points were also very accurate when compared to the actual data, yielding only slightly higher values. The Toyota Yaris model will be used to investigate and compare how different side underride guards affect the intrusion of the vehicle. Because of this, the achieved simulated data is acceptable and will be utilized in this research.

3.3.2 IIHS Ford Taurus Validation

The NCAC Taurus report has the results of their obtained simulated data for points located on the footwell [40]. The IIHS has the data of their physical test; CF00010, listed online [47]. The data of both these tests is listed in Table 3.4.

Table 3.4 - Intrusion values for the 2001 Ford Taurus

Test Results	NCAC Simulated Results	IIHS CF00010 Physical Test Results
Footwell intrusion		
Footrest (cm)	105	80
Left (cm)	166	120
Center (cm)	161	140
Right (cm)	156	130
Brake Pedal Movement		
Brake Pedal (cm)	N/A	140
Instrument panel rearward movement		
Left (cm)	N/A	20
Right (cm)	N/A	10
A-pillar rearward movement		
A-pillar (cm)	N/A	30

To replicate the simulation in LS-DYNA, the nodal following points were chosen and are shown in Figure 3.9. A visual representation of the simulated collision is demonstrated in Figure 3.10.

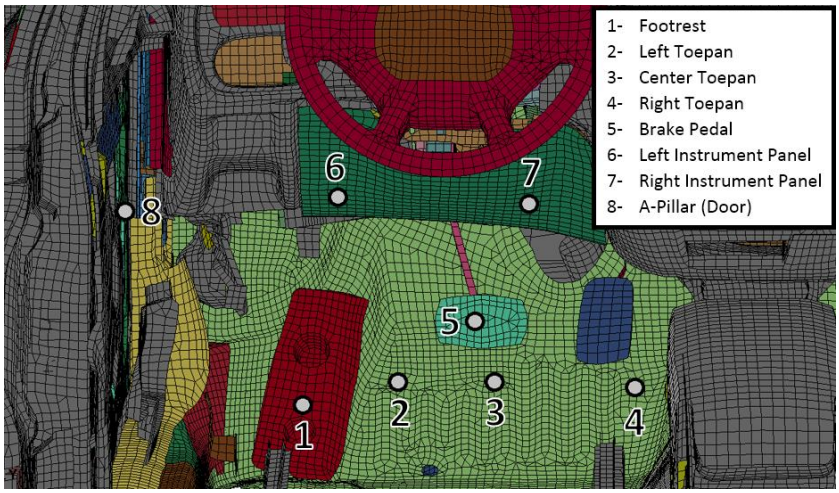

Figure 3.9 - Determined Taurus IIHS measurement points

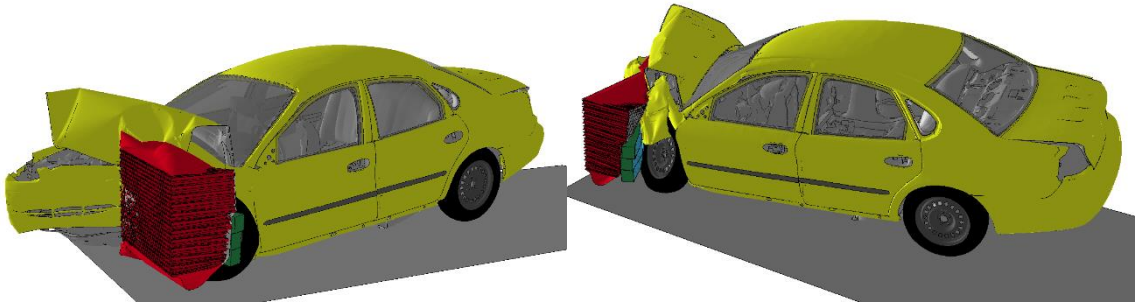

Figure 3.10 - Taurus IIHS simulation into deformable barrier

The results are shown and compared to the physical tests in Figure 3.11. The first four points are very similar when compared to the CF00010 test results. The brake pedal moved approximately 100mm more in the simulated collision. The final three points are slightly higher than the actual data however, they follow the same trend. Since the data achieved is acceptable, the LS-DYNA Taurus will be utilized as a comparison for different underride guards.

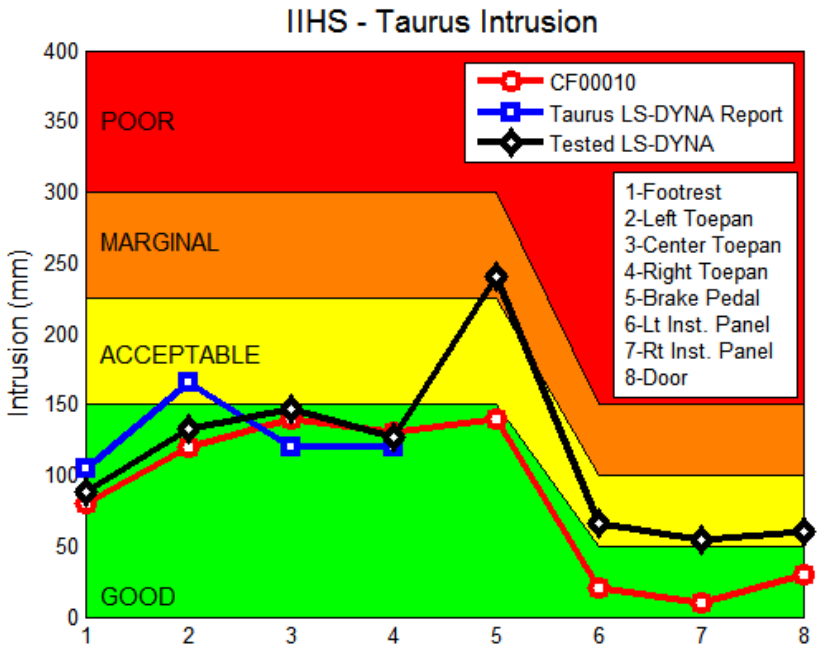

Figure 3.11 - Taurus IIHS test comparisons

CHAPTER 4: DEVELOPMENT OF A REGULATION

Acknowledgement:

This is an Author's Original Manuscript of an article whose final and definitive form, the Version of Record, “Development of a Regulation for Testing the Effectiveness of a Rigid Side Underride Protection Device (SUPD)”, has been published in the International Journal of Crashworthiness, December 11, 2013, © 2013 Taylor & Francis, available online at:

http://www.tandfonline.com/doi/abs/10.1080/13588265.2013.868083#.Us16TbSftNU

All of the writing, testing and research conducted in this paper was done by the author. The co-authors reviewed the work and gave technical support when needed.

4.1 MOTIVATION AND OVERVIEW OF THE REGULATION

The development of a side underride protection device (SUPD) is a crucial aspect for improving the safety of small car to tractor-trailer collisions. Devices such as rear underride guards are already implemented and regulated in North America and many places around the world along with front underride devices, which are regulated in Europe. The large and unprotected gap between the rear axle and the kingpin of the trailer remains a hazard for small passenger vehicles passing underneath. To develop devices to prevent such accidents, a regulation for testing the underride guards must be implemented to determine their feasibility. This section utilizes the background information and testing procedures of the existing regulations for front, side and rear underride guards previously explained in the “Standards and Regulations” section to help develop the side regulation. A finite element tractor-trailer model is presented and a component model based on the trailer is created and validated to be used for simulations. Collisions with small passenger cars such as the National Crash Analysis Center’s Toyota Yaris and Ford Taurus into rigid walls are conducted and methods are introduced to obtain a quasistatic model from the dynamic crash. Device dimensions are determined using tractor-trailer models in TruckSim to obtain the maximum

allowable ground clearance of the devices. Feasible rigid guards are then created and tested with the proposed quasistatic regulation and compared to the results obtained from the dynamic tests.

4.2 PASSENGER VEHICLE SPECIFICATIONS

The two finite element vehicle models chosen for the testing and validation of the regulation are the Toyota Yaris and the Ford Taurus. As previously mentioned, the Toyota Yaris is based on a 2010 production model and weighs 1262.37kg. This model conforms to the Manual for Assessing Safety Hardware (MASH) definition of a small passenger vehicle; the 1100C class, which weighs approximately 1100kg [39]. The Ford Taurus is based on a 2001 production model which is in the range for the MASH 1500A class with an approximate weight of 1500kg. The LS-DYNA model weighs 1634.58kg [40]. The dimensions and heights of the front rails and absorber bars are shown in Figure 4.1 and Figure 4.2. These lengths and heights will be important to the development of the testing method and will be considered in this chapter.

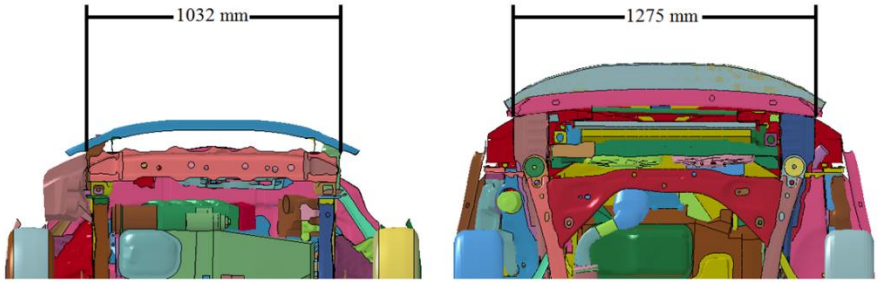

Figure 4.1 - Distance between the front rails

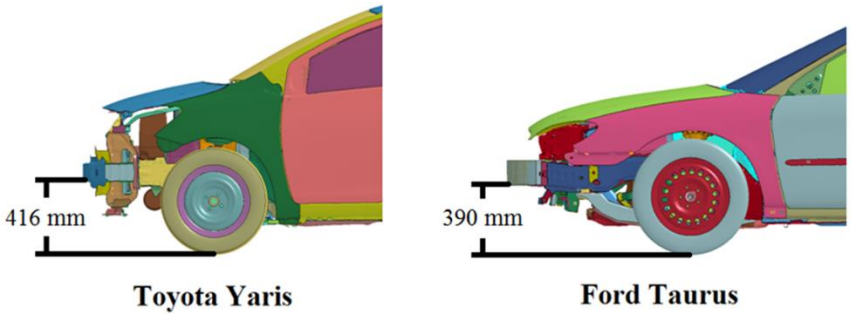

Figure 4.2 - Ground clearance of front rails and absorber bars

4.3 TRACTOR-TRAILER AND COMPONENT LEVEL VALIDATION

To carry out tests both dynamically and quasistatically, a component level of the tractor-trailer must be created and validated. This component level allows for faster solve times, which greatly reduces computational cost. The tractor-trailer model utilized was previously explained and was created by the Battelle Memorial Institute, the Oak Ridge National Laboratory and the University of Tennessee under the sponsorship of the National Transportation Research Center Inc. (NTRCI) [41]. Two basic component levels were created for testing. The first includes the I-beams, which are located under the trailer and fixed at both ends. The second is created from the same I-beams; however, in this case, they are rigid. The rigid test fixture resembles the requirements of the rear guard regulation. A basic underride guard was welded to the tractor-trailer and both component devices were tested with the 2010 Toyota Yaris travelling at speeds of 56km/h, 64km/h and 80km/h. Figure 4.3 to Figure 4.8 shows the impact force experienced during the collision, along with the displacement of the guard, for each individual speed.

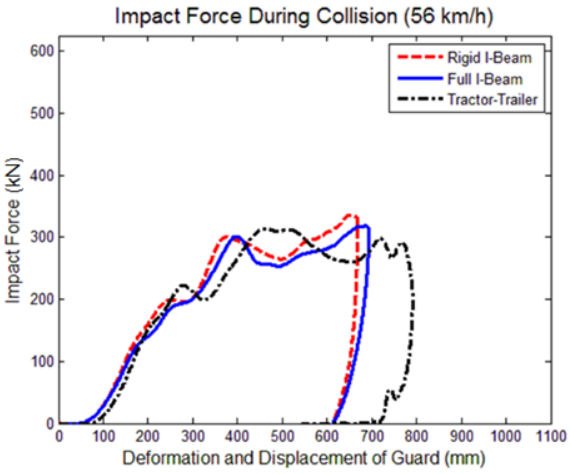

Figure 4.3 - 56km/h force graph

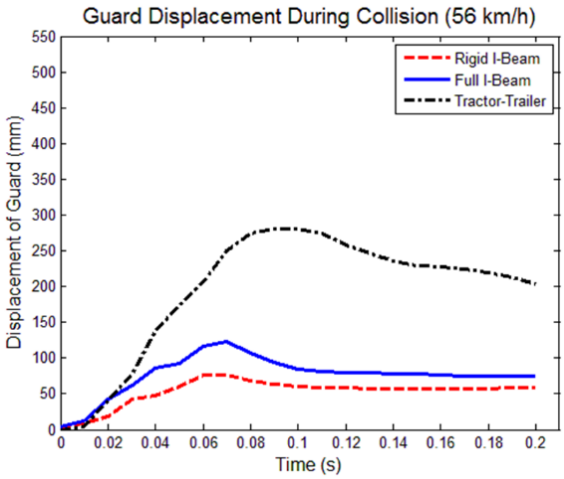

Figure 4.4 - 56km/h guard displacement

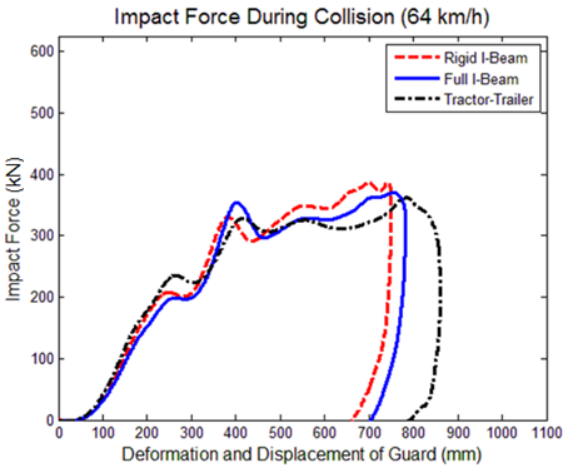

Figure 4.5 - 64km/h force graph

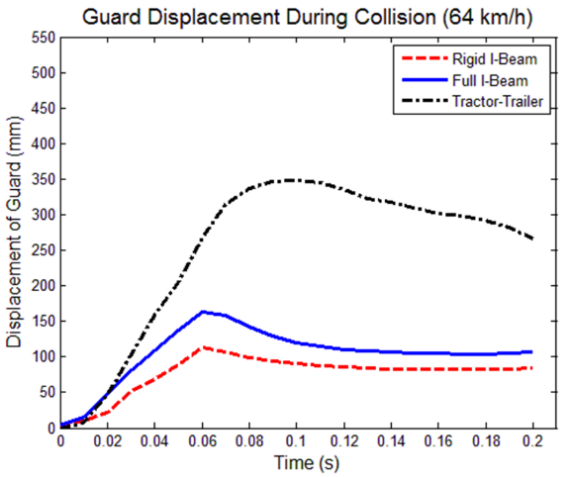

Figure 4.6 - 64km/h guard displacement

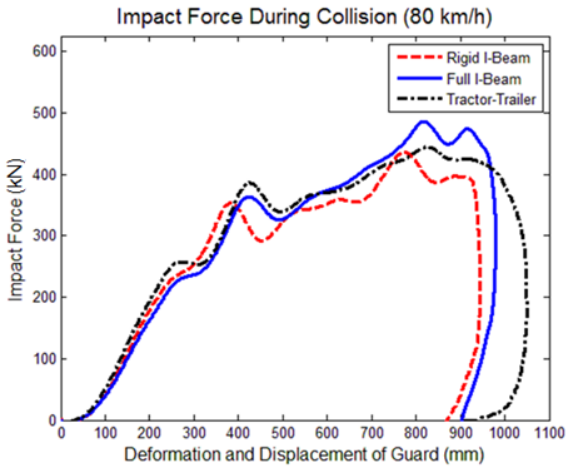

Figure 4.7 - 80km/h force graph

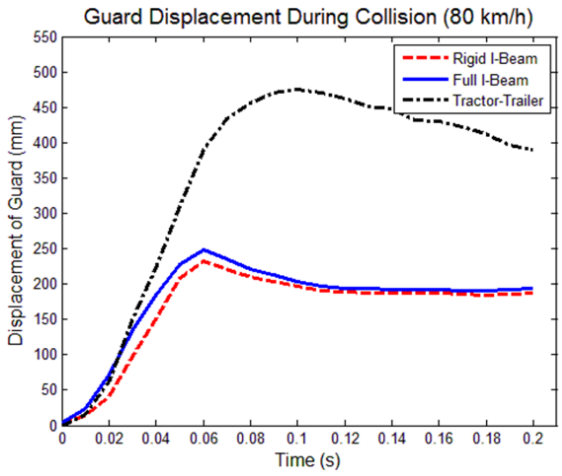

Figure 4.8 - 80km/h guard displacement

When looking at the impact force during the collision of all three speeds and all three test configurations, the results appear to be very similar in terms of the amount of force experienced. When the full tractor-trailer is analysed, the deformation and displacement of the guard is slightly larger in all three cases due to the displacement of the entire trailer during the crash. When the car makes contact with the full tractor-trailer, the trailer experiences some lateral displacement as it slides on the ground along with some deformation. In the same graphs, towards the end of the data, there is some amount of return in the deformation of the guard along with the displacement of the guard. This is the vehicle bouncing back from the guard after the collision with a negative velocity since the data is calculated from its centre of gravity.

When the guard displacement during the collision is observed, the results between the rigid and fixed I-Beams are very comparable. The tractor-trailer configuration experiences about double the guard displacement. This again is due to the fact that the trailer is not fixed, and the collision causes the trailer to slide sideways. During these collisions, the guard deformation of all three configurations was visually very comparable. To dramatically reduce computational cost, and with the results of these runs, it is confirmed that the use of either the rigid or fixed I-Beam model is acceptable for the testing and development of a side underride guard. As a final step to the design process, the final guards should however be tested dynamically with the full model to validate their feasibility.

4.4 SIDE GUARD DIMENSIONS

4.4.1 BASIC DIMENSIONS

To create a regulation for side guards, proper dimension guidelines must be followed. The length of the device must be considered. Section 2.2.3 explains the regulation of lateral protection devices for unprotected road users. Figure 2.5 shows some dimensions, including the distance between the wheels and the device. To stay compliant with this regulation, the same maximum distance of 300mm should be utilized. To determine if this amount was feasible, dynamic tests with the Yaris and a test guard were conducted and the results demonstrated that this value was in fact acceptable. In comparison to Figure 2.5 which shows a gap between two axles, many guards in North American would be installed to tractor-trailers which have a trailer jack in this gap. Because of this and to leave adequate room for the jack operation, the edge of the guard must be within 300mm from the outer edge of the lifting device.

In the same figure, the depth of the device is also shown. For this regulation, the entire device should not be placed more than 30mm from the outside edge of the trailer, resembling the European regulation. The device must also not add to the overall width of the trailer or straight truck.

4.4.2 TRAILER GROUND CLEARANCE

The proposed regulation for side guards must have a basis for minimal possible ground clearance of the guard. The guard must be low enough to be feasible for stopping cars, however, must be high enough to clear road obstacles such as curbs and grade crossings. To begin, the ground clearance for road obstacles must be observed. To achieve the minimal possible clearance, the largest tractor-trailer wheelbase configuration was chosen from the Ontario Traffic Act, which would allow for the smallest clearance gap when driving over grade crossings which is displayed in Figure 4.9 [48].

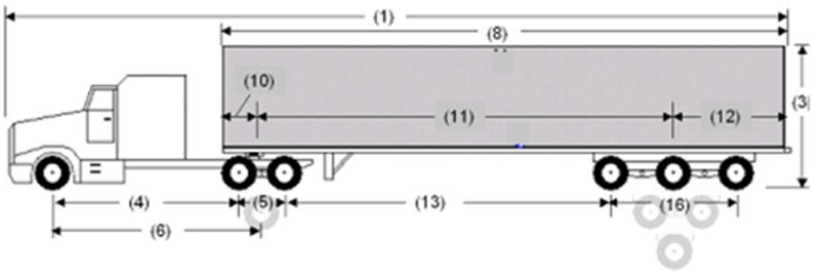

Reference	Length (m)
(4)	5 (max)
(5)	1.2 (min)
Tractor Wheelbase	6.2
Kingpin (4)+((5)/(2))	5.6
(11) Wheelbase	12.5 (max)
(13) Inter-Vehicle-Unit Distance	11.3
Kingpin to First Axle	11.9
Kingpin to Second Axle	13.1
Trailer Ground Clearance	1.1

Figure 4.9 - Tractor-trailer configuration [48]

For these simulations, the TruckSim program was used to measure the ground clearance in comparison to the road profile. The first road profile was taken from the Railway-Highway Crossing at Grade Regulation report. This profile is described as 1m of height for every 20m of horizontal length of the approaches [49]. The second profile is taken from the Draft Canadian Railway-Roadway Grade Crossings Standard (CRRGCS) report. This profile consists of a ratio of 1:50 within the first 8m of the rail and 1:20 for the next 10m [50].

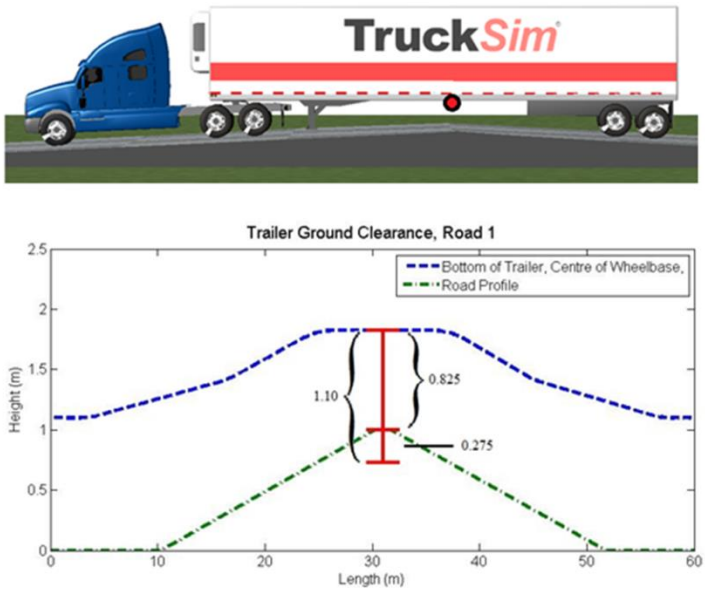

Ground Clearance=(trailer ground clearance on flat ground) -
(distance between road profile and trailer bottom at the highest point)

Minimum Ground Clearance = 1100mm – 825mm

Minimum Ground Clearance = 275mm = 27.5cm

Figure 4.10 - Road profile 1 ground clearance

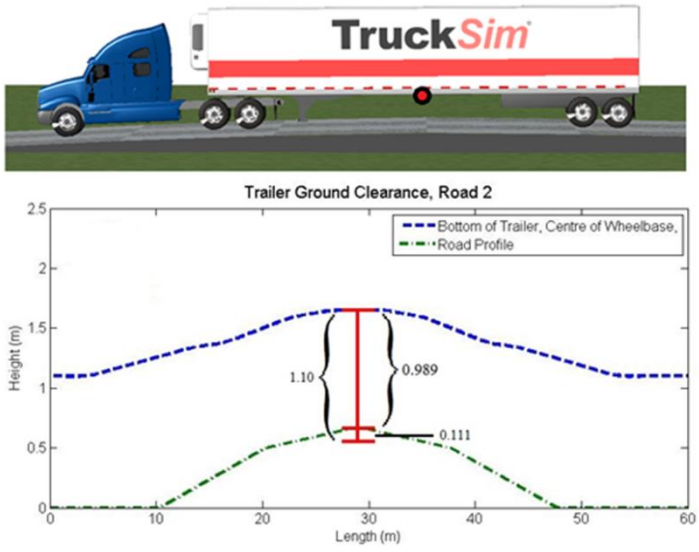

Ground Clearance=(trailer ground clearance on flat ground) -
(distance between road profile and trailer bottom at the highest point)

Minimum Ground Clearance = 1100mm – 989mm

Minimum Ground Clearance = 111mm = 11.1cm

Figure 4.11 - Road profile 2 ground clearance

In Figure 4.10 and Figure 4.11, it is shown that the minimal ground clearance required to pass the first road profile is 275mm and the second one is 111mm. In addition to this, the Australian government also has restrictions to road profiles. Their regulation states that the slope must be 1:15 [51]. Running this road profile in the same manner as the previous two profiles yields a minimal clearance of 366mm. Other countries throughout the world have their own standards and regulations for minimal clearance on tractor-trailers. In Europe, to minimise the risk of the bottom of a trailer hitting railway crossings, the government has issued some rules. If the interaxle spacing is between 6 and 11.5m, the clearance must be 160mm. If the axle spacing is larger than 11.5m, the clearance must be 190mm [52]. In New Zealand, the ground clearance for heavy vehicles must be 100mm or at least 6 percent of the distance to the nearest axle of where the clearance is measured [53]. If the trailer mentioned above is to comply with this law, the clearance would have to be 339mm.

4.5 VEHICLE FORCES AND ROBUSTNESS

To fully investigate the effect that the height of an underride guard can have on a vehicle, the following tests were conducted. For compatibility of the underride guards, the Toyota Yaris and the Ford Taurus were utilized with numerous tests. The first test consisted of colliding the cars into a rigid wall, a 200mm rigid bar, a 300mm rigid bar, and a 400mm rigid bar. The reason for this test was to investigate the effect of the vehicle colliding with different sizes of impact areas. The bars were tested at different ground clearance intervals such as; 300mm, 350mm, 400mm, 450mm and 500mm. The goal is to determine which configuration resembles the rigid wall test since this is when the vehicle's optimal crashworthiness is observed. Other tests consisted of comparing the force over deformation graphs of vehicles in the same class along with testing the different types of classes. Lastly, the peak and average height of the impact force is investigated to establish proper testing measures for the regulation.

4.5.1 TOYOTA YARIS - GROUND CLEARANCE

This initial test consisted of colliding the 2010 LS-DYNA Toyota Yaris model into a rigid wall and into rigid bars of heights 200mm, 300mm and 400mm. Figure 4.12 to Figure 4.14 shows the results of these collisions while changing the ground clearance of the bars. The tests are conducted at 64km/h.

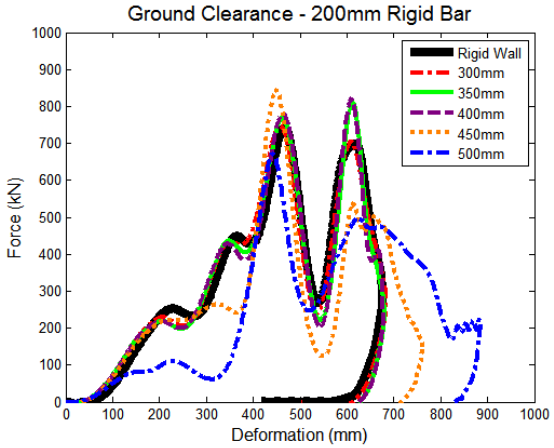

Figure 4.12 - Ground clearance with a 200mm rigid bar (Yaris)

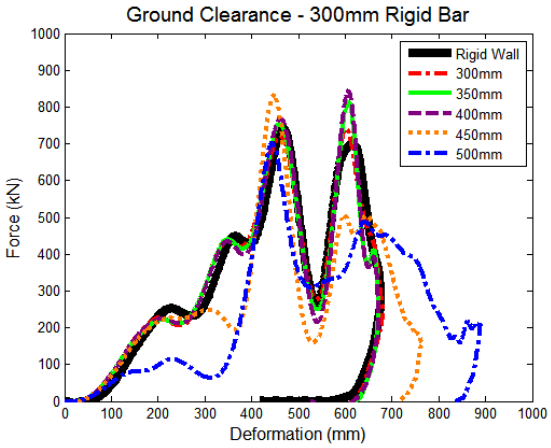

Figure 4.13 - Ground clearance with a 300mm rigid bar (Yaris)

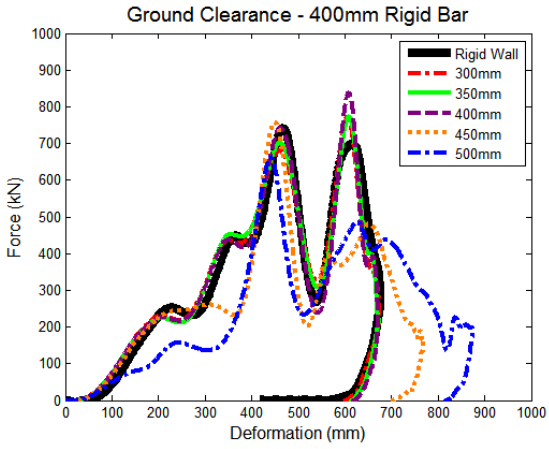

Figure 4.14 - Ground clearance with a 300mm rigid bar (Yaris)

When looking at the 200mm rigid bar, the data shows that at ground clearance heights of 300 to 400mm, the system resembled the data from the Yaris contacting the rigid wall. This is due to the alignment of the front rails and the engine coming into contact directly with the bar. The 450 and 500mm clearances show that in these cases, the vehicle would underride the bar, causing the greater intrusion. The 300 and 400mm

bars showed very similar results to the 200mm bar. The rails would make contact with the device until the 450mm clearance, where the car would underride regardless of the section height of the bars.

4.5.2 TOYOTA YARIS - RIGID BAR HEIGHTS

The graphs in this section rearrange the plots from the previous section. Here, we compare how the ground clearance is affected by the section height of the bar. The data is also compared to the rigid wall data. Figure 4.15 to Figure 4.19 shows this data.

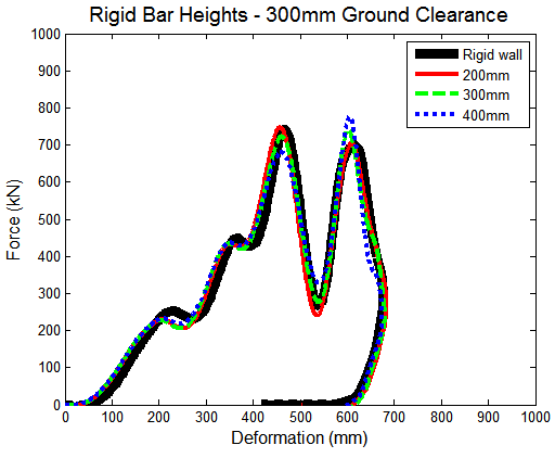

Figure 4.15 - Rigid bar heights with a 300mm ground clearance (Yaris)

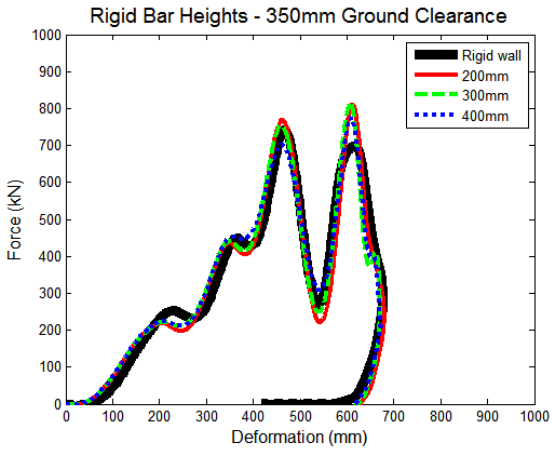

Figure 4.16 - Rigid bar heights with a 350mm ground clearance (Yaris)

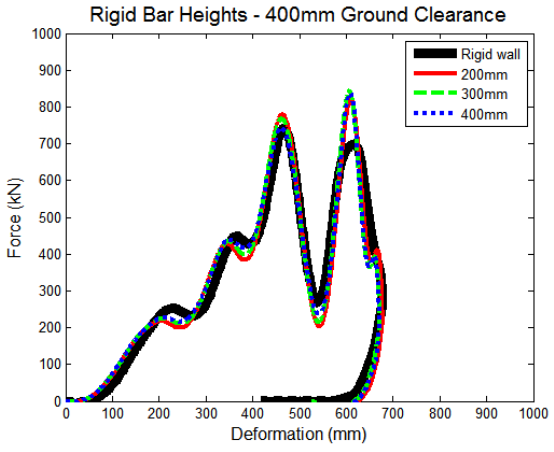

Figure 4.17 - Rigid bar heights with a 400mm ground clearance (Yaris)

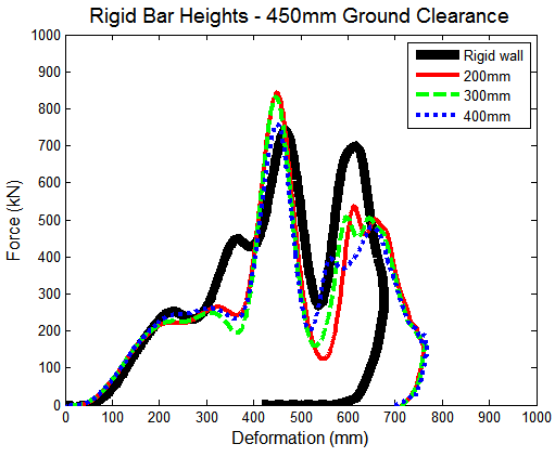

Figure 4.18 - Rigid bar heights with a 450mm ground clearance (Yaris)

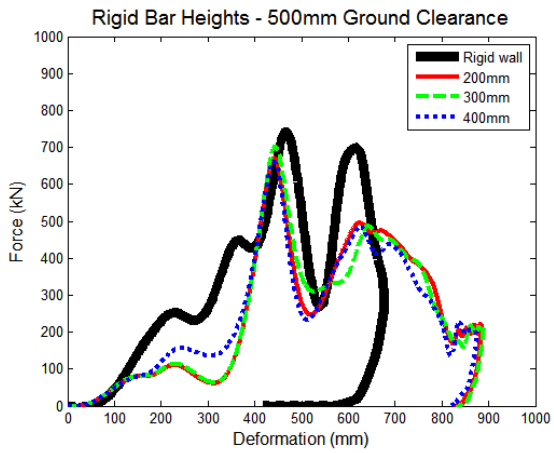

Figure 4.19 - Rigid bar heights with a 500mm ground clearance (Yaris)

Similarly to the conclusions from the first graphs, the section height has little to no effect in the 300 to 400mm clearance heights. It is more evident in these graphs that at the 450mm clearance, the car begins to underride the bars by comparing the curves to the rigid wall curve. The same is observed in the 500mm graph. To properly design a guard, the force graphs should resemble the rigid wall as close as possible to utilize the vehicle's crashworthy properties during the collisions.

4.5.3 Ford Taurus - Ground Clearance

The Ford Taurus data is now compared. Much like the results for the Toyota Yaris, the 300 to 400mm ground clearance best resembled the rigid wall curve. The section height of the bars had little to no impact when comparing the 200, 300 and 400mm sections to a rigid wall. At the 450 and 500mm clearances, underride can be observed since the vehicle has larger deformations, showing that it is passing under the bars. Figure 4.20 to Figure 4.22 shows these results.

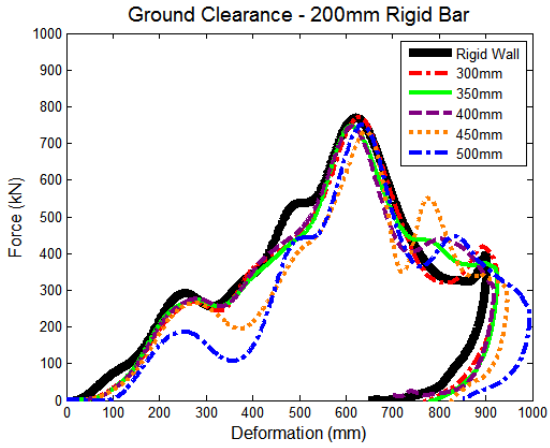

Figure 4.20 - Ground clearance with a 200mm rigid bar (Taurus)

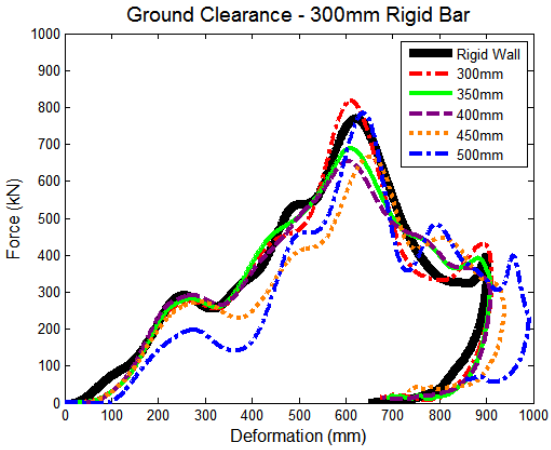

Figure 4.21 - Ground clearance with a 300mm rigid bar (Taurus)

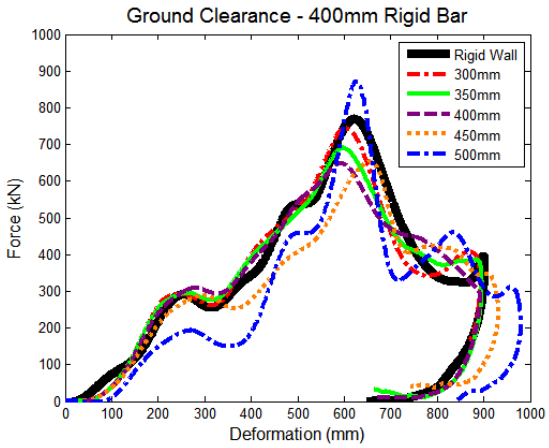

Figure 4.22 - Ground clearance with a 400mm rigid bar (Taurus)

4.5.4 FORD TAURUS - RIGID BAR HEIGHTS

In this section, the plots are rearranged to investigate the effect of section heights on different ground clearances. The same conclusions can be drawn from these graphs. The data greatly resembles the rigid wall collision in the 300 to 400mm ground clearance heights. The vehicle begins to underride in the 450 and 500mm cases. Figure 4.23 to Figure 4.27 shows the results of the Taurus hitting the bars at different ground clearances along with comparing the data to the rigid wall tests.

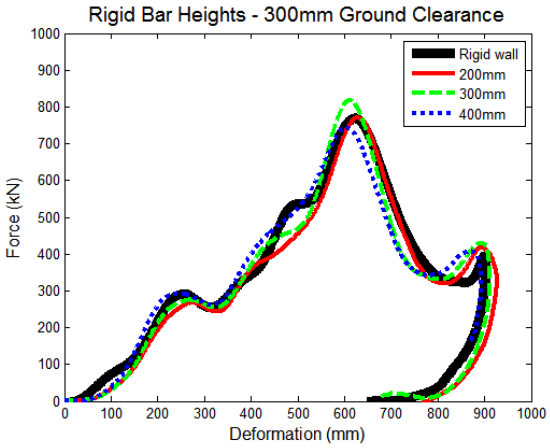

Figure 4.23 - Rigid bar heights with a 300mm ground clearance (Taurus)

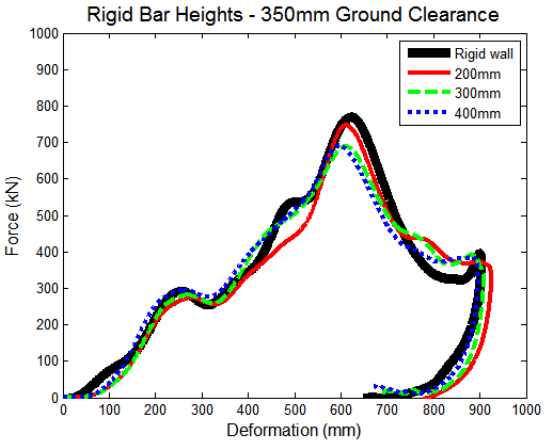

Figure 4.24 - Rigid bar heights with a 350mm ground clearance (Taurus)

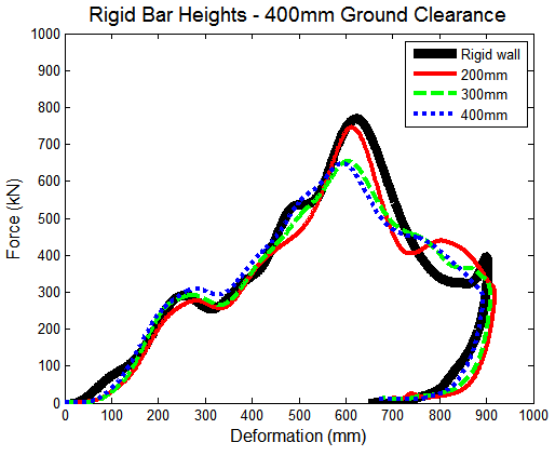

Figure 4.25 - Rigid bar heights with a 400mm ground clearance (Taurus)

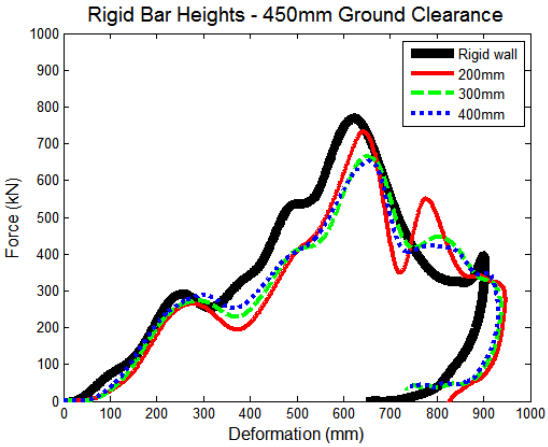

Figure 4.26 - Rigid bar heights with a 450mm ground clearance (Taurus)

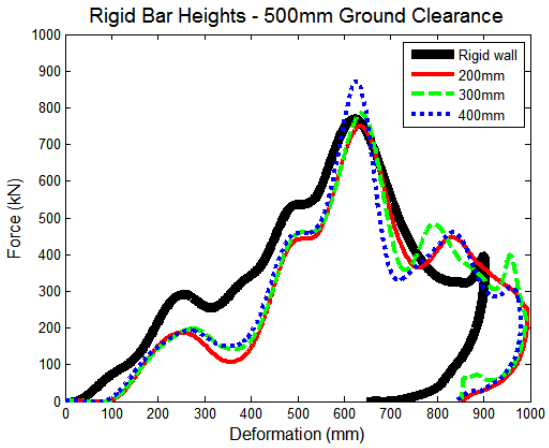

Figure 4.27 - Rigid bar heights with a 500mm ground clearance (Taurus)

When investigating all of the data in this section, one can conclude that the side underride guard should utilize a maximum ground clearance of 400mm to prevent vehicle underride of small and medium sized passenger vehicles.

4.5.5 CLASS COMPARISON

The section above compares the data of the subcompact and midsize car classes since those are the publically available LS-DYNA vehicle models. In the United States, vehicle classes are specified in terms of their interior volumes in cubic feet. The Subcompact cars are categorized as cars with interior volumes greater than 85 cubic feet but smaller than 100 cubic feet. The compact car class must have an interior greater than or equal to 100 cubic feet but no larger than 110 cubic feet. The midsized car segment is classified as having greater than or equal to 110 interior cubic feet volume and is limited to a maximum of 120 cubic feet volume [54]. In addition to cars, three SUV classes were also compared. These include the Compact SUV, the Midsized SUV and Full Sized SUV segment. The Light Duty Truck Class 1 and Light Duty Truck Class 2 vehicles are also compared along with the Minivan segment. The Class 1 consists of all trucks with a gross vehicle weight rating of 6,000lbs or less and the Class 2 is all trucks between 6,001 and 10,000lbs [55]. Figure 4.28 to Figure 4.36 shows these classes along with their appropriate vehicles. The vehicles that have an asterisk beside them are vehicle which are available for LS-DYNA and additional tests are conducted with them following this section. The data is obtained from the National Highway Traffic Safety Administration website [56]. The vehicles in these collisions have an initial velocity of 56km/h.

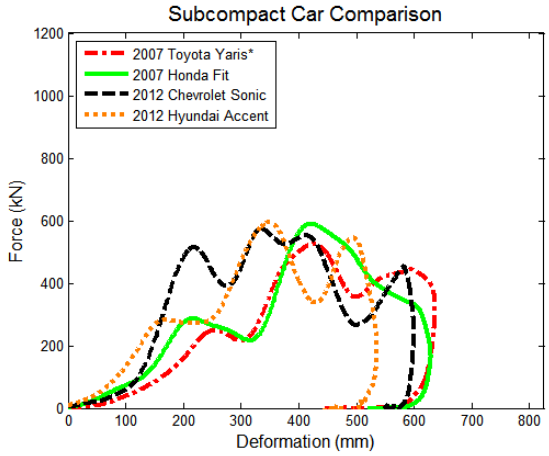

Figure 4.28 - Subcompact car collision comparison

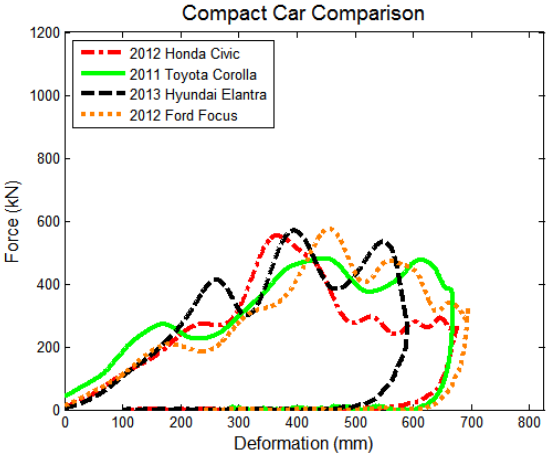

Figure 4.29 - Compact car collision comparison

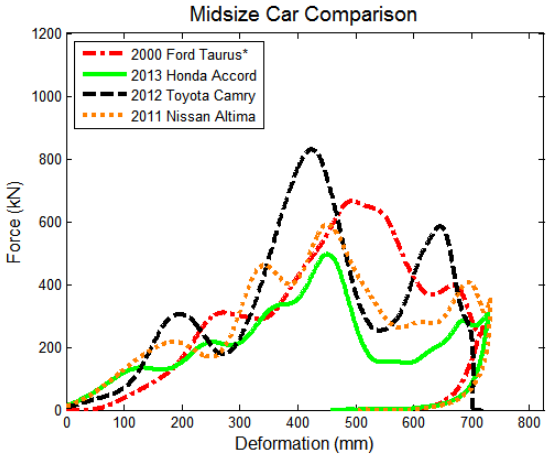

Figure 4.30 - Midsize car collision comparison

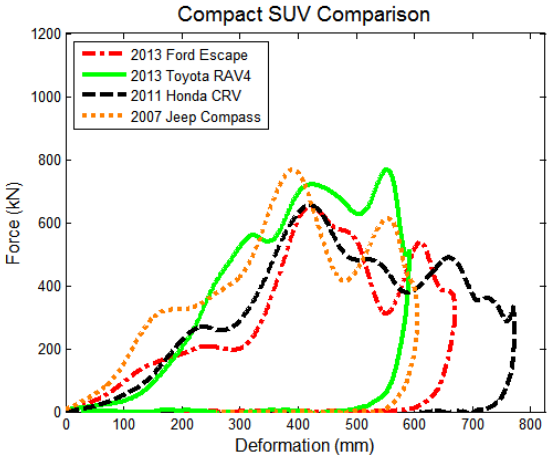

Figure 4.31 - Compact SUV collision comparison

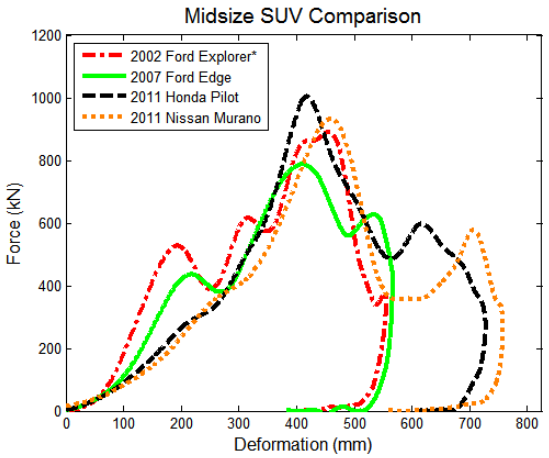

Figure 4.32 - Midsize SUV collision comparison

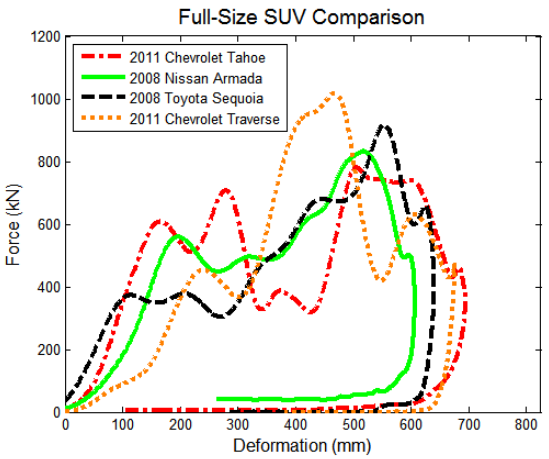

Figure 4.33 - Full-Size SUV collision comparison

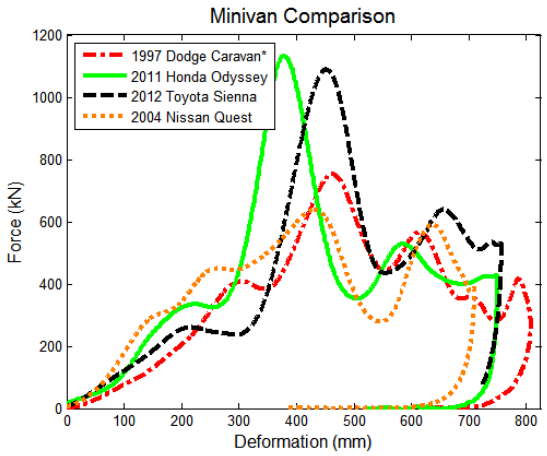

Figure 4.34 - Minivan collision comparison

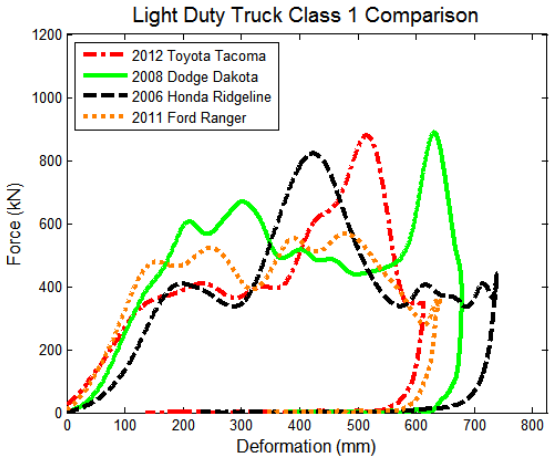

Figure 4.35 - Light Duty Truck Class 1 collision comparison

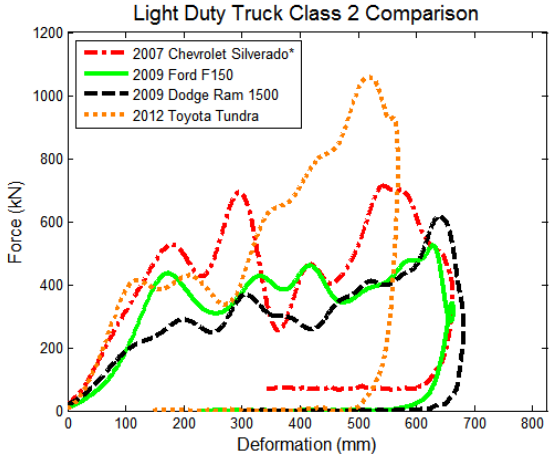

Figure 4.36 - Light Duty Truck Class 2 collision comparison

As the vehicle class augments, one can see that the impact forces of the vehicles are increased due their increase in weight. Each vehicle reacts differently when colliding with a rigid wall depending on their configuration and style. It may however be noted that for each class, the vehicle's reaction profiles are similar.

Figure 4.37 and Figure 4.38 compares the vehicles with an asterisk beside them from the graphs above. Figure 4.37 compares their actual physical data and Figure 4.38 shows their established data in an LS-DYNA collision.

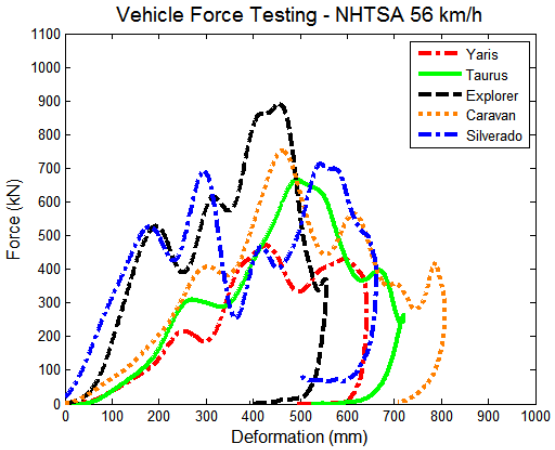

Figure 4.37 - Actual data of LS-DYNA vehicle collisions

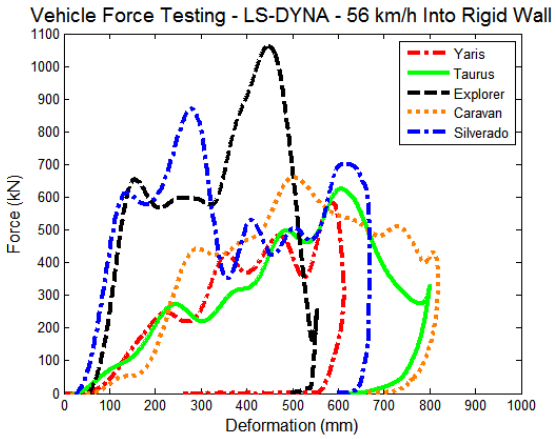

Figure 4.38 - LS-DYNA simulated vehicle collisions

4.5.6 LS-DYNA Models Vs. Actual Data

The data from the actual crash tests and the data obtained from the LS-DYNA for the vehicles is now compared in Figure 4.39 to Figure 4.43.

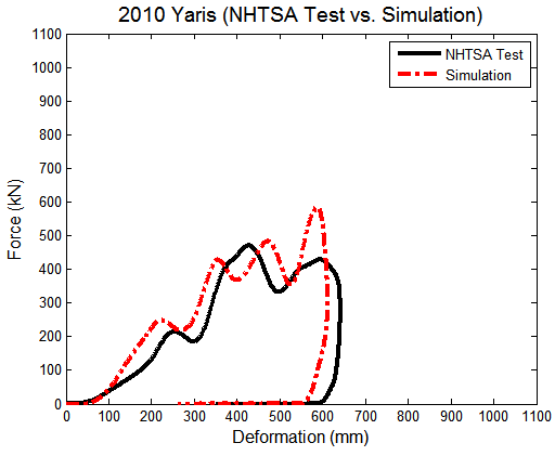

Figure 4.39 - 2010 Yaris NHTSA and simulation comparison

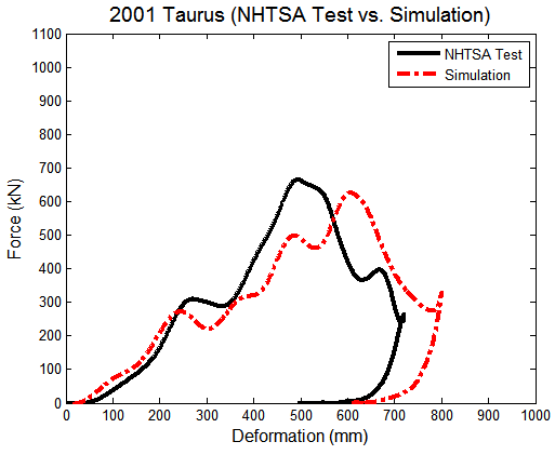

Figure 4.40 - 2001 Taurus NHTSA and simulation comparison

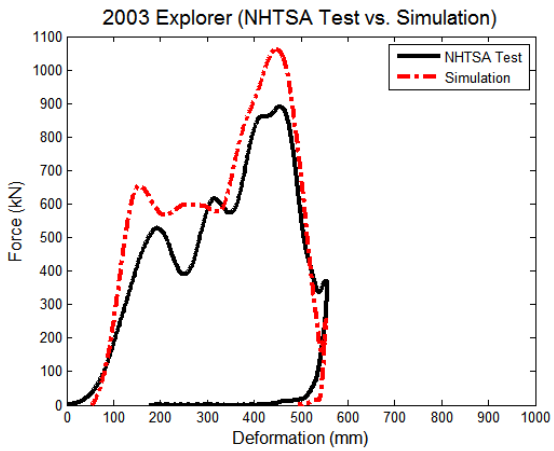

Figure 4.41 - 2003 Explorer NHTSA and simulation comparison

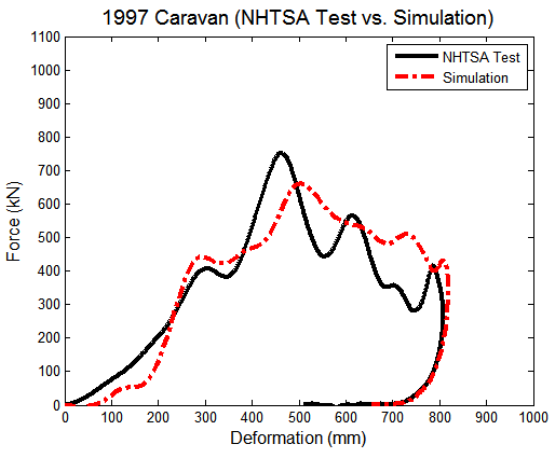

Figure 4.42 - 1997 Caravan NHTSA and simulation comparison

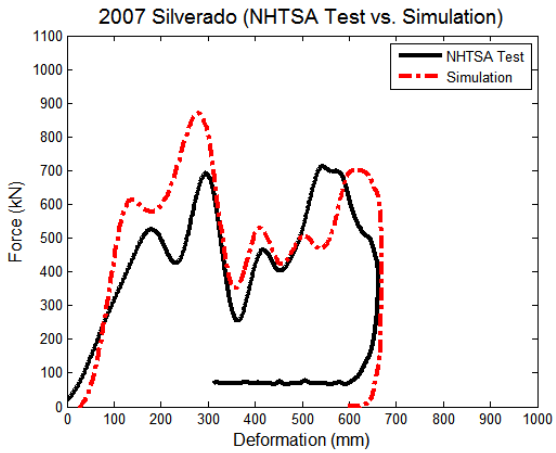

Figure 4.43 - 2007 Silverado NHTSA and simulation comparison

The graphs above display the accuracy of the LS-DYNA simulations and models. The data obtained from the actual crash tests is very comparable to the LS-DYNA simulations. Again, as previously noted, when the vehicle becomes larger, the impact force increases. Figure 4.44 shows the LS-DYNA vehicle collisions with an initial velocity of 64km/h for reference.

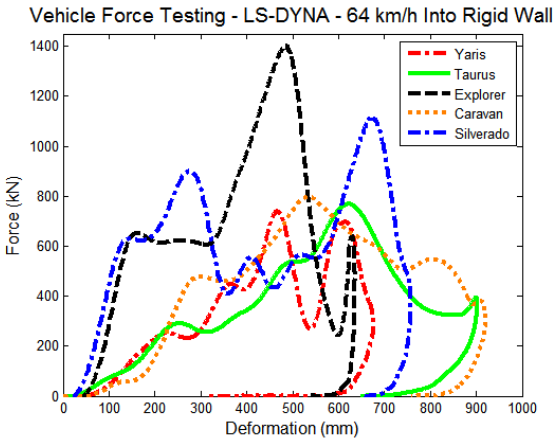

Figure 4.44 - LS-DYNA vehicles into rigid wall at 64km/h

A visual representation of the data of the LS-DYNA with an initial velocity of 64km/h is shown in Table 4.1. The pictures are taken when the vehicle experiences its maximum deformation when colliding with the rigid wall. The table shows how the vehicles react and the severity of such accidents.

With the data obtained from the NHTSA for the different vehicle classes, Figure 4.45 is created. Plotted in this figure is the peak and average height of the force of each vehicle during their collision with a rigid wall for comparative purposes. This image is revisited when establishing the testing parameters for the regulation.

Table 4.1 - LS-DYNA vehicles into rigid wall at 64km/h

Toyota Yaris 64km/h	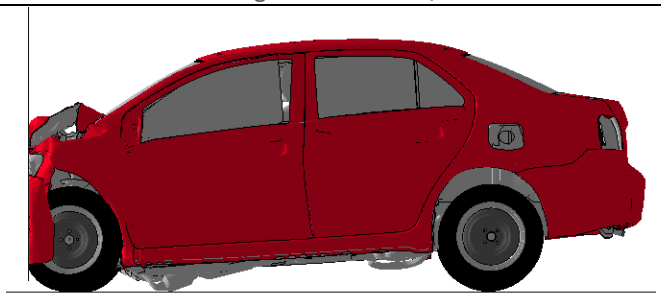
Ford Taurus 64km/h	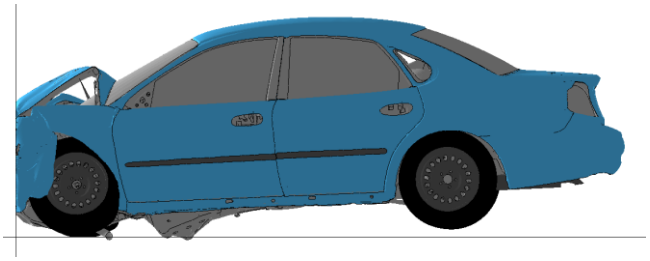
Ford Explorer 64km/h	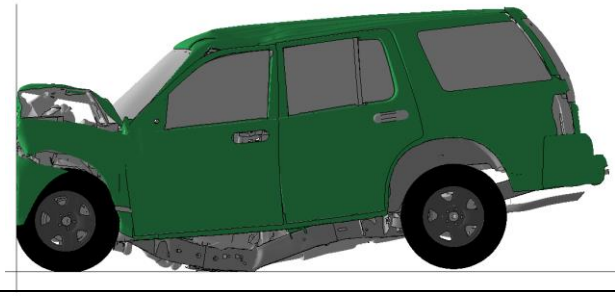
Dodge Caravan 64km/h	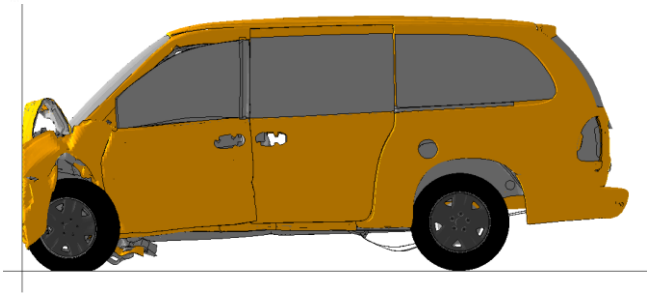
Chevrolet Silverado 64km/h	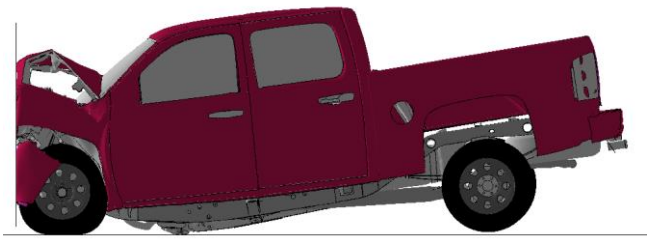

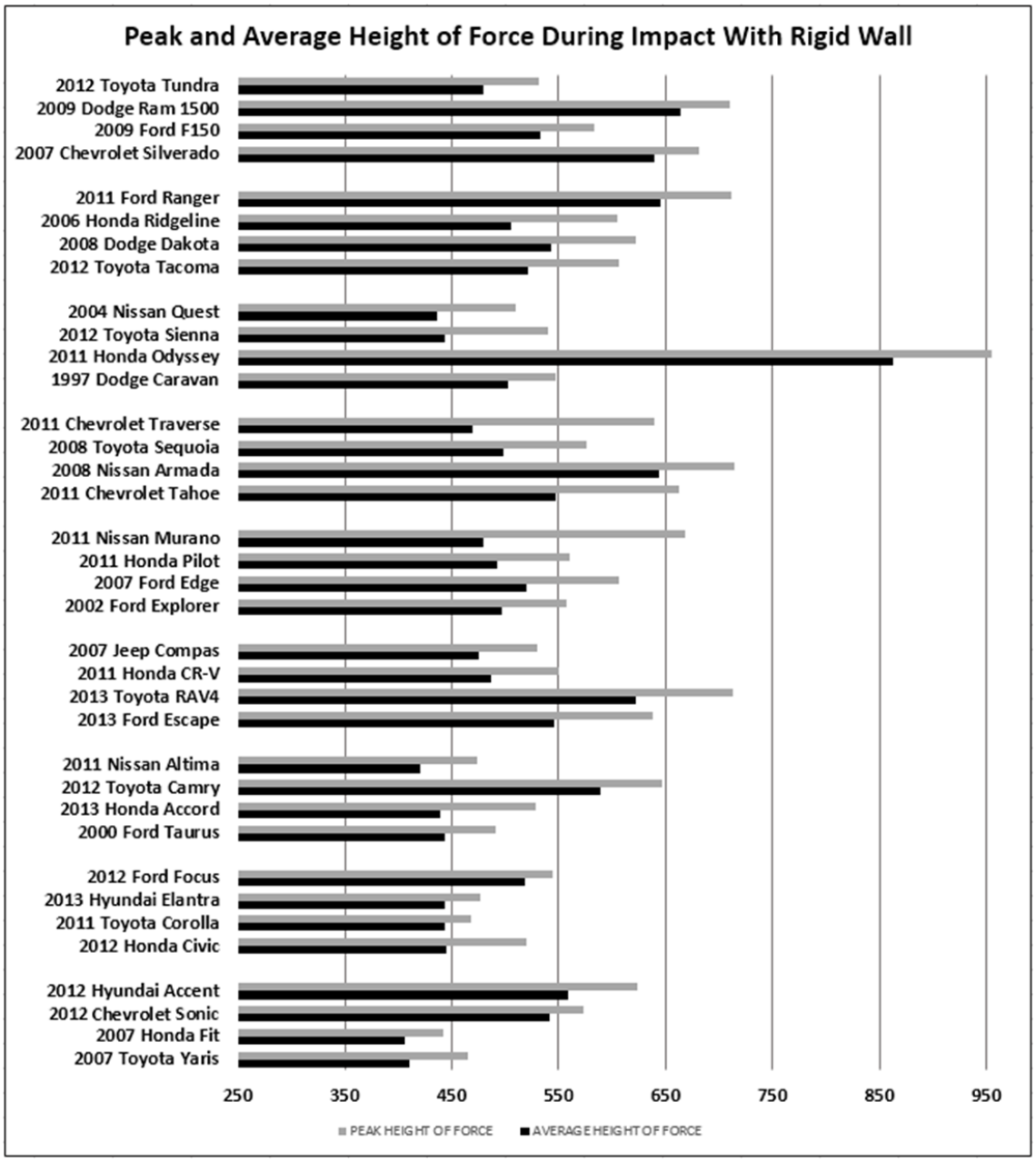

Figure 4.45 - Peak and average height of force during impact with rigid wall

With the above mentioned the ground clearance for an effective side underride guard while still having the ability to go over crossings without damaging the device would have to have a minimum height of 350mm with a maximum height of 400mm. This would allow small passenger cars to make full use of their crashworthiness properties during underride.

4.6 FORCE APPLICATION DEVICE

Unlike the testing methods for front and rear guards explained earlier in this thesis, side underride guards cannot utilize the same approach of testing which consists of applying a small disk with a force to the bracket of the guard. This reasoning is due to the fact that the side guard is much longer, and the brackets may be positioned differently depending on the design and configuration of the guard and the trailer. With this in mind, the proposed approach utilizes a large plate which resembles the front rails and absorber bar of a small passenger vehicle during a crash as seen in Figure 4.46. Figure 4.1 and Figure 4.2 demonstrates some basic dimensions that can be derived to create the appropriate force plate which is observed in Figure 4.46.

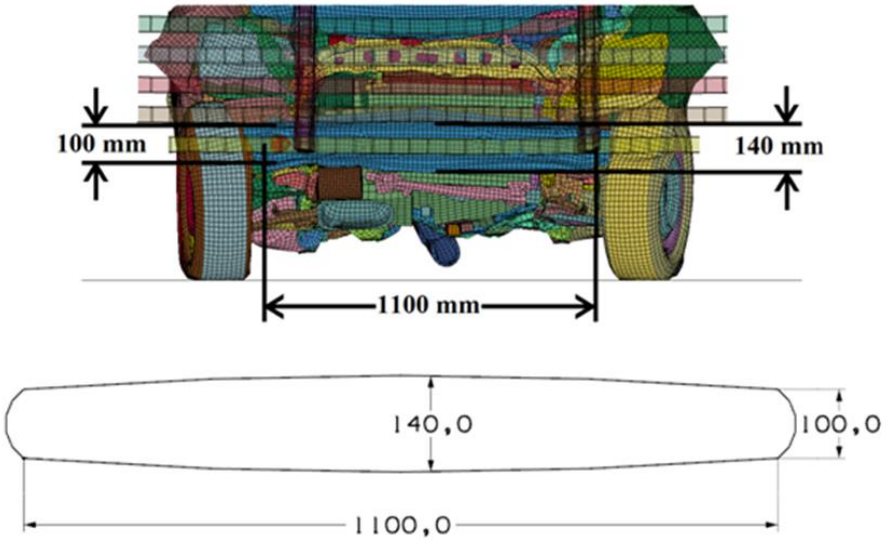

Figure 4.46 - Force application device dimensions

The final dimensions of the plate are as follows: a length of 1100mm, a centre height of 140mm at its centre and a height of 100mm at its extremities. The proposed approach is to apply this plate with a force quasistatically. Since the guard is long and can vary from trailer to trailer or straight truck configuration, the centre of the plate is to be positioned in the centre of the guard and tested at increments of 500mm until the plate reaches at least 50% overhang at the edges which can be seen in Figure 4.47. If the guard is symmetric, only half the guard may be tested, otherwise, both sides from the centre

must be analysed. Observed in Figure 4.2 are the heights of the front rails. Those values show that the centre of the plate should be placed at a height of 450mm from the ground, allowing for some variance and tolerance for other types of vehicles.

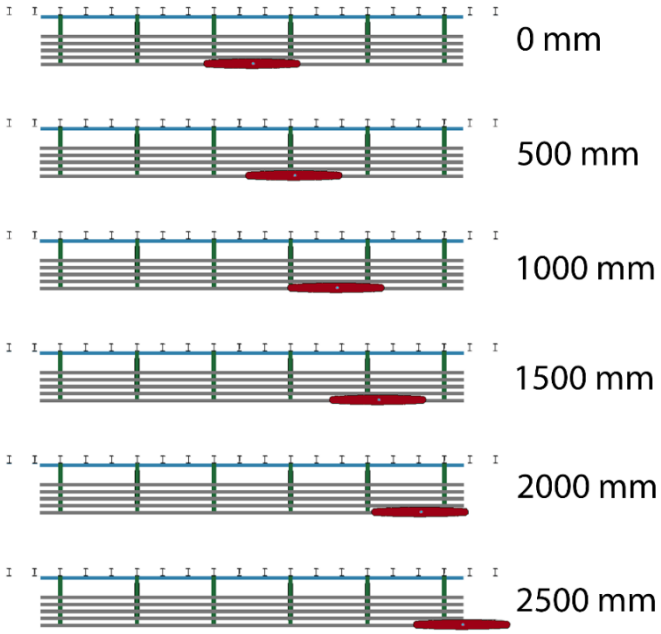

Figure 4.47 - Offset positioning explained

4.7 PROPOSED GUARDS

To test the outlined method above, three underride protection devices were created. The guards were each built differently to test the method for the regulation to establish consistency. The brackets supporting the guards are welded to the lateral I-beams of the trailer. Figure 4.48 shows these three proposed guards.

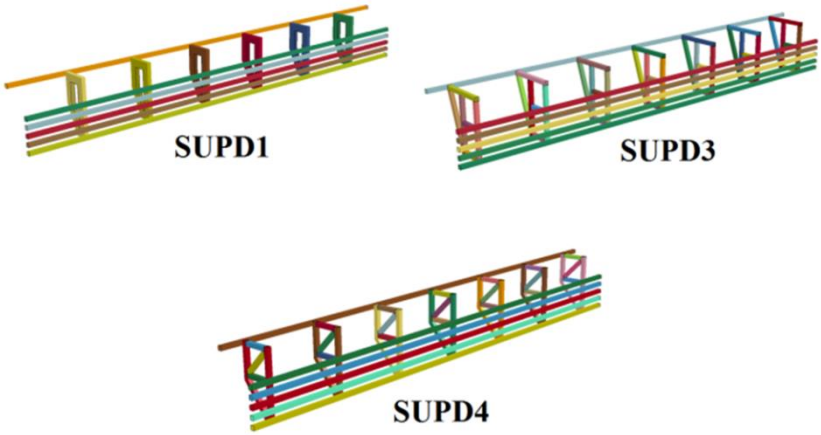

Figure 4.48 - SUPD1, SUPD3, SUPD4

As explained previously in the ground clearance section, these guards are designed to have a clearance of 350mm. Also, as explained, the most feasible design would be to have the impact area resemble a wall in order to take full advantage of the vehicle's crashworthiness. This chapter described the use of 200, 300 and 400mm rigid bars as impact area heights. The results for these were similar and the 200mm bar proved to be adequate. Because of this, side guards should be designed to have an impact area of at least 200mm. To benefit a greater variety of vehicles, the side guard should have an impact area height of 400mm. To be compliant with the European regulation, the guard must also have a maximum gap distance between the upper most impact bar and the bottom of the trailer of 350mm. We can now modify Figure 4.45 to show where the impact area lies within the vehicle data. Figure 4.49 shows these results.

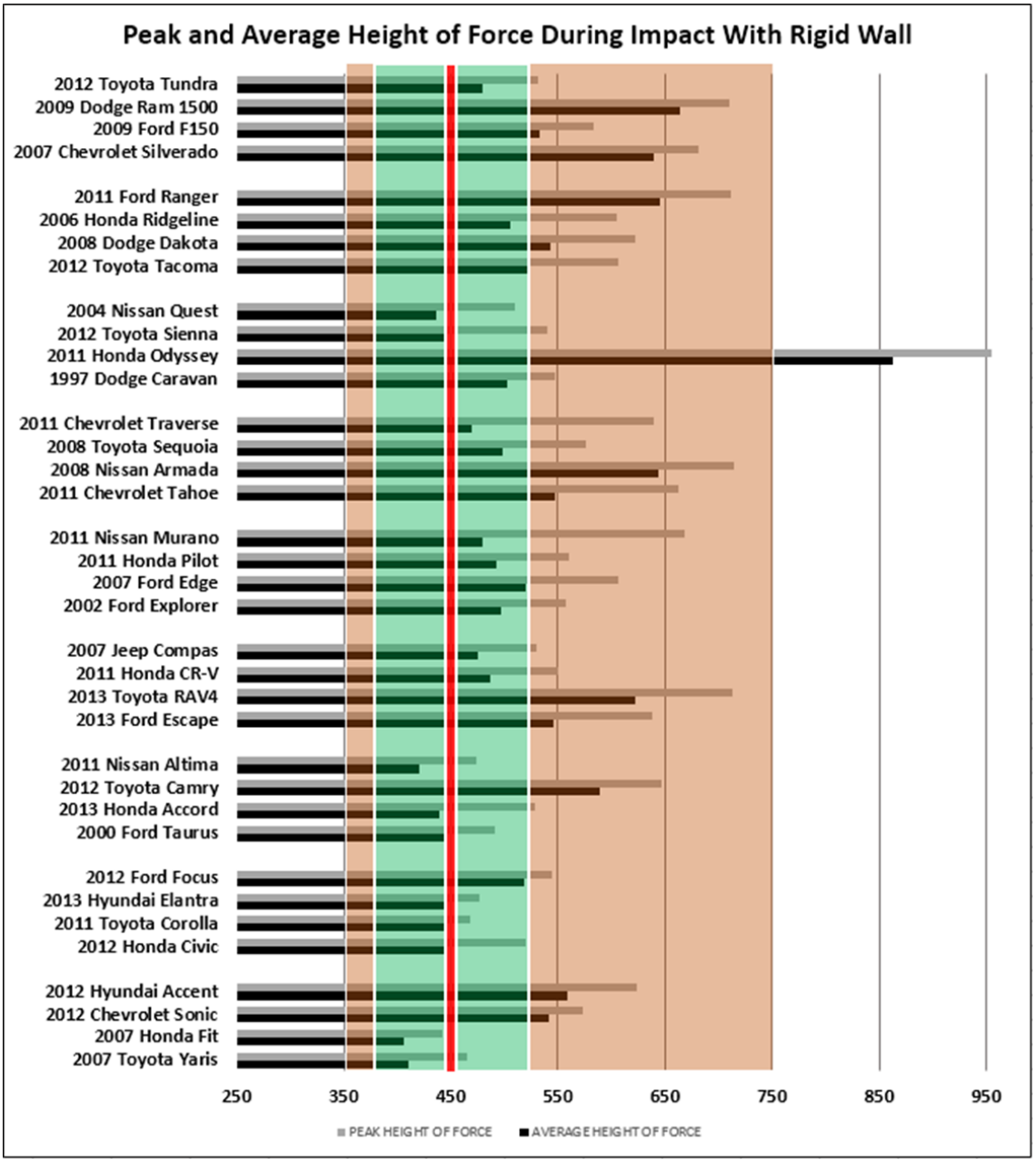

Figure 4.49 - Peak and average height of force with SUPD dimensions

The larger colored in area represents the impact area of the guard which is chosen to be 400mm. The ground clearance is set to 350mm. The smaller colored section is the area spawned by the force application device when it is applied to the guard. The line in the middle represents the height of the center of the application device. From this figure, it is evident that the 400mm impact area height along with the positioning and size of the application device is favorable for multi vehicle compatibility.

Since this regulation aims towards designing guards that stay rigid during impact, the maximum deformation must be established. In the literature review, the rear underride guard is described as being a rigid guard, with a maximum allowable deformation of 125mm [8]. The front regulation describes a maximum deformation of 400mm, measured from the front of the tractor [15]. To develop a true rigid underride device for the side of trailers and straight trucks, the proposed maximum deformation under testing conditions will be set to 100mm.

4.8 TESTING AND ANALYSIS

To determine the appropriate approach of applying a quasistatic force to the underride guard for testing, many methods were considered. Firstly, the dynamic force during a collision must be determined and converted to a quasistatic force for testing. One of the first proposed methods for this analysis was by Beerman in 1984 [57].

4.8.1 BEERMAN METHOD

To implement the Beerman method, an equation derived by Murray in 1988, which can be observed in many papers concerning underride guards, can be utilized and is displayed in the following equation. In this equation, "F" represents the average force acting between the two vehicles, "m1" is the mass of the car, "m2" is the mass of the tractor-trailer, "V" is the closing speed of the vehicle and "s" is the crush distance [58] [59].

$$F = \frac{m_1 m_2 V^2}{2(m_1 + m_2)s}$$

The first test used a car mass of 1,100kg to be compliant with the MASH small car testing criteria and this car is considered to be the Yaris. The other vehicle tested was the Taurus, and its chosen mass was 1500kg to be compliant with the medium sized car category in MASH. The crush distance "s" was determined by crashing the cars into a rigid wall using the LS-DYNA software and measuring the deformation. This was an accurate approach since the guards are designed to be rigid. The mass of the second

vehicle “m2” is equal to the mass of the tractor-trailer. For the tests, the mass was taken from 18,143.7kg (40,000lbs) to 36,287.4kg (80,000lbs) in increments of 4,535.9kg (10,000lbs). An additional mass was added, the one of the LS-DYNA tractor-trailer, which was 23,127kg (50,986lbs). In Figure 4.50, the masses are expressed in units of kilograms.

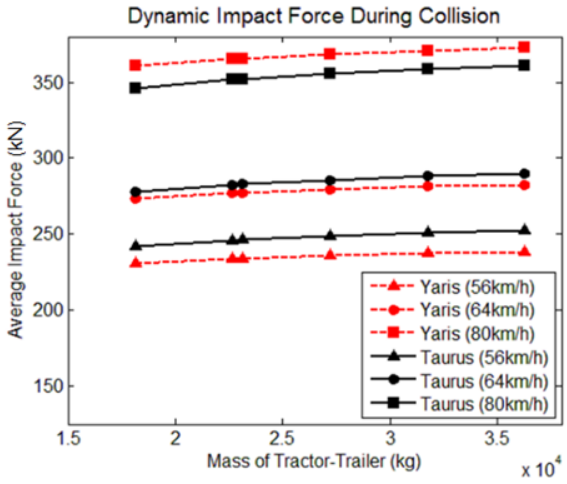

Figure 4.50 - Average dynamic impact force during collision

Beerman’s method determined that the ratio of dynamic to quasistatic crushing loads was around 1.5. This was found for both the axial buckling and bending collapse of thin walled members. Figure 4.51 shows the average quasistatic force required for testing rigid side underride guards.

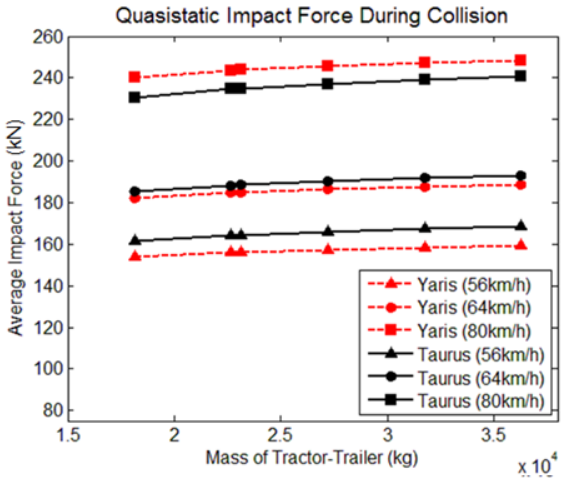

Figure 4.51 - Average quasistatic impact force during collision

4.8.2 RIGID WALL VEHICLE TESTS

Although the Murray and Beerman method were used as a simplified approach to determine the testing force for underride guards, today there are methods which can replicate a crash in a simulated environment in order to obtain sophisticated results. Figure 4.52 and Figure 4.53 shows the Toyota Yaris and Ford Taurus impact force graphs over the deformation of the car calculated from the centre of gravity, respectively. In addition to the graphs, the average force of the collision is added in a table.

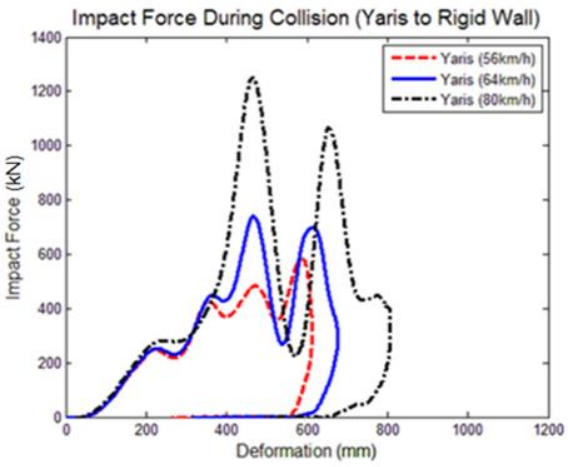

Crash Configuration	Average Force (kN)
Yaris (56km/h)	207.82
Yaris (64km/h)	246.36
Yaris (80km/h)	282.36

Figure 4.52 - Yaris into rigid wall collision data

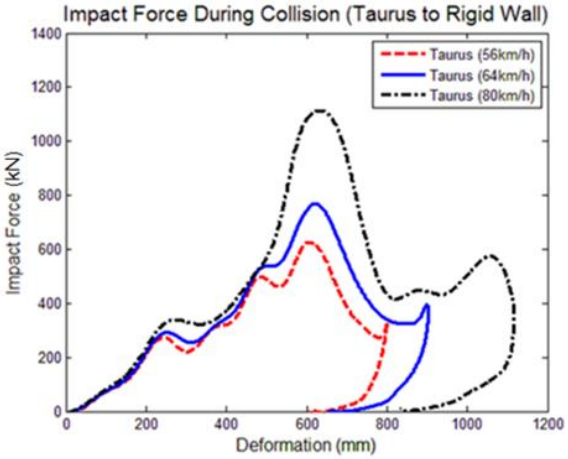

Crash Configuration	Average Force (kN)
Taurus (56km/h)	230.87
Taurus (64km/h)	262.92
Taurus (80km/h)	316.61

Figure 4.53 - Taurus into rigid wall collision data

By comparing these average values to the ones determined by the Murray and Beerman method, a few observations can be made. Since the graphs show full vehicle collisions, they can only be compared to the dynamic impact force graph from the previous section. In every instance, the calculated method resulted in slightly higher values than the simulated method. At 64km/h, the Yaris had an average impact force of 246.36kN and the Taurus had an average impact force of 262.9kN. The calculated method showed the Yaris having an average force of approximately 275kN and the Taurus, a force of 280kN. With these results, one can conclude that by using the average of all these values, the force of the collision of both the vehicles would be approximately 265kN. By

converting this with the Beerman ratio of 1.5, the average quasistatic force required to test a side underride guard is 180kN.

4.8.3 DYNAMIC VS. QUASISTATIC

To properly test the proposed method of using a plate which resembled the testing approach of rear guards in Canada, the deformation of the guard had to be compared with both quasistatic forces and a dynamic analysis. The deformations of the guards were compared until an appropriate force was chosen for the regulation. All three proposed guards were utilized for these tests. The tests were conducted by colliding the Toyota Yaris and Ford Taurus into the center of the guard installed on the rigid component I-Beam model at a velocity of 64km/h. This speed was chosen as the benchmark for designing rigid guards. The time of the simulation was then adjusted for comparison purposes. With the same guards, quasistatic forces were applied in increments of 100KN until a comparable value was found. The simulations were tested until the guard had reached equilibrium. The results of the test are shown in Figure 4.54 to Figure 4.56.

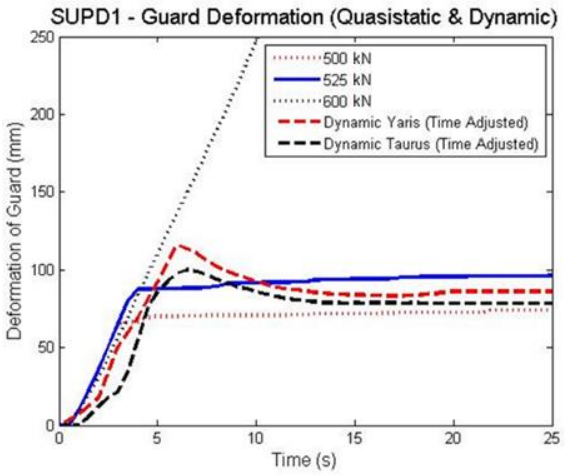

Figure 4.54 - SUPD1 guard deformation

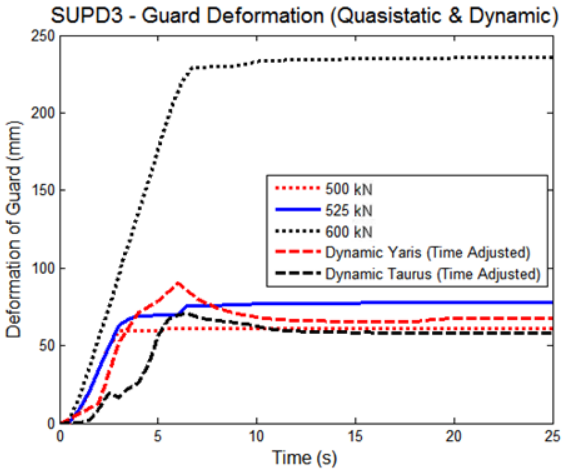

Figure 4.55 - SUPD3 guard deformation

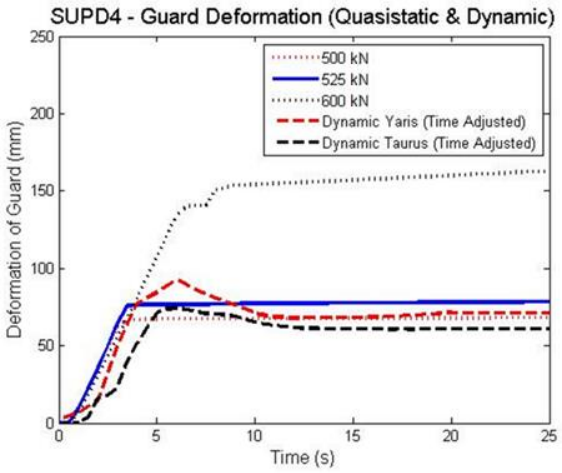

Figure 4.56 - SUPD4 guard deformation

The graphs show the results of the dynamic crashes, along with the applied forces of 500kN, 525kN and 600kN. Since the forces were set in increments of 100kN, it was observed that in order to match with a small safety factor the deformation of the guards, 500kN was not enough, and 600kN was too much. In all three cases, 525kN was tested and proved to be an effective force. The guard's displacement would settle at a value slightly above the dynamic tests. Since it was proposed that the guards have a maximum deformation of 100mm to be considered a feasible rigid system, using a force of 525kN with the rigid plate proved to be an effective method. When an actual collision occurs, the guard will also stay rigid, with an approximate maximum deformation of 100mm. These results demonstrated that the Murray and Beerman method did not yield high enough values to be used to design proper rigid side guards with the planned force application device method.

4.8.4 Offset Testing

The proposed 525kN force was only applied in the 0mm offset setting, meaning directly in the middle of the guard. Offset testing needed to be conducted to confirm the feasibility of the amount of force along with the testing method. This method involved moving the force plate by increments of 500mm until the centre of the plate has reached the end of the guard. After every test, a new guard must be utilized because of the deformation created from the previous test. Since the guards tested were

symmetric, the offset testing only needed to be conducted on one side of the guard. As seen earlier, each guard utilizes their own individual bracket throughout the entire device. Because of this, the brackets installed on each end of the guard are made stronger since they would have to hold the entire 525kN load during the final offset test. In a crash situation, the sole bracket would have to stop the entire vehicle if the collision was offset. To accomplish this, the end brackets were thicker than the others, making them more rigid. Figure 4.57 to Figure 4.59 shows all three guards along with the offset deformation comparisons of the dynamic and quasistatic tests.

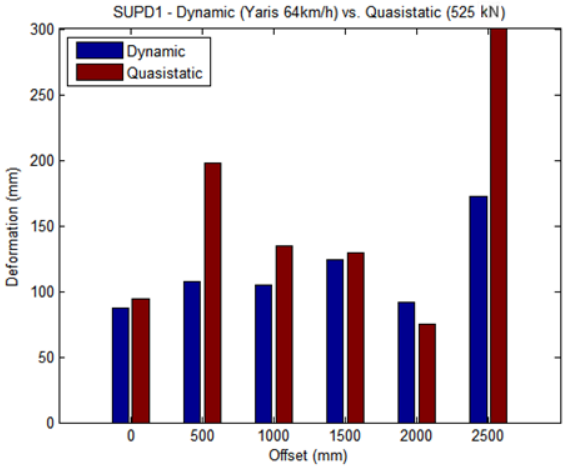

Figure 4.57 - SUPD1 offset testing deformation

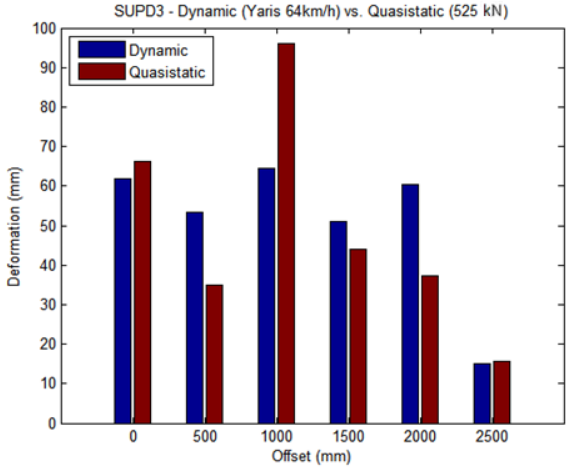

Figure 4.58 - SUPD3 offset testing deformation

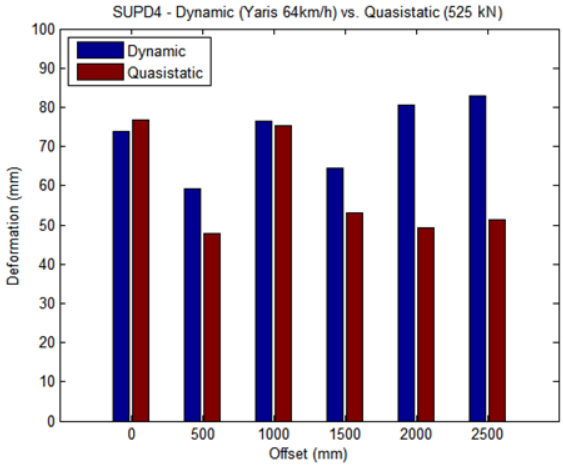

Figure 4.59 - SUPD4 offset testing deformation

In the case of SUPD1, although the guard's deformation was smaller than 100mm at zero offset, some tests failed at other increments. However, the quasistatic force of 525kN proved to be feasible since the results only showed marginal error. In the final offset of 2500mm, the quasistatic attempt failed to find equilibrium, meaning that the guard had buckled. The force application device deformed the bracket to the point where it was no longer capable of holding the load. Even with this, the guard still proved to have sufficient strength to stop the vehicle.

When looking at SUPD3, none of the trials achieved a greater deformation than 100mm. This guard is, therefore, a feasible design for a side underride guard. In terms of comparison between the achieved deformations of quasistatic versus dynamic, it is observed that in three out of the six cases, the quasistatic approach was greater than the dynamic crash. In the other cases, the results were very similar, only varying by about 20mm.

SUPD4 showed very similar results to SUPD3. The device did not exceed a deformation of 100mm and all of the trials were very comparable to one another.

In all of the graphs shown in this section, some dynamic deformations are greater than the quasistatic deformations. This occurs due to the deformation and buckling properties of the brackets and guards in question. During the quasistatic tests, a constant load is applied on the guards which allows for consistent results. During the dynamic tests when the car comes in contact with the guard, there are peaks and variations observed in the impact forces. This causes the guards to slightly buckle or deform in a different manner. If the deformation during the quasistatic test is kept under 100mm, the dynamic results would yield similar results.

With the results shown above, it is feasible to claim that a force of 525kN with the recommended plate with a maximum deformation of 100mm tested at intervals of 500mm on the guard is a sufficient regulation to design proper rigid side underride guards. If the guards stay within the 100mm maximum deformation in the quasistatic

tests, the dynamic deformation will not vary by any significant margin and the guards are still considered to be rigid.

4.8.5 ANGLE CRASHES

Further testing was conducted to determine how the guards would react during angle crashes compared to a perpendicular crash. Each of the three guards were tested with the Yaris impacting the guards at angles of 15, 30, 45 and 60 degrees. Figure 4.60 to Figure 4.62 shows the deformations of the guards for each crash configuration. When comparing these results to the perpendicular (90 degree) crashes listed in the previous section, it becomes apparent that the guards experienced much smaller deformations, and were still rigid enough to stop the car. As the angle increases, the deformation becomes larger, showing that the perpendicular (90 degree) crash was the worst condition for maximum deformation of the guard.

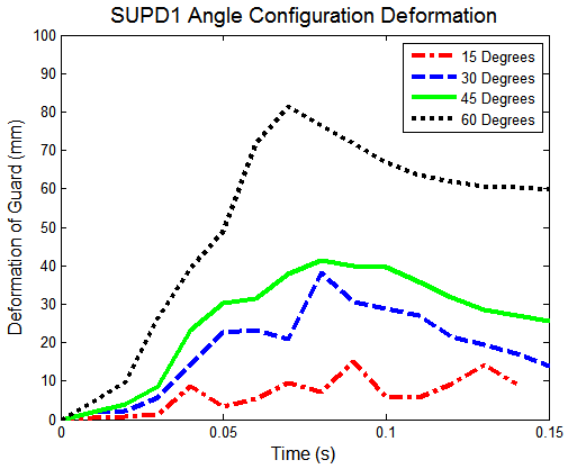

Figure 4.60 - SUPD1 angle configuration deformation

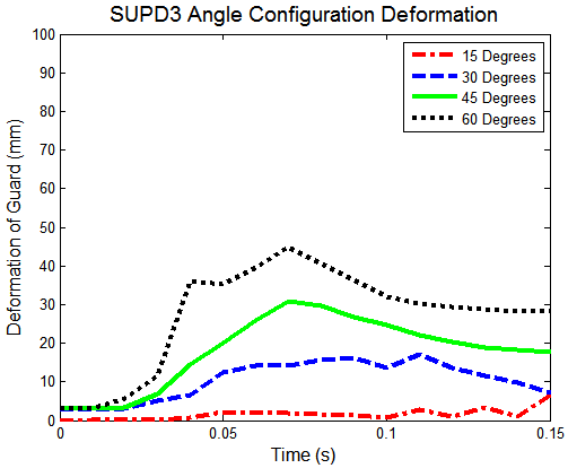

Figure 4.61 - SUPD3 angle configuration deformation

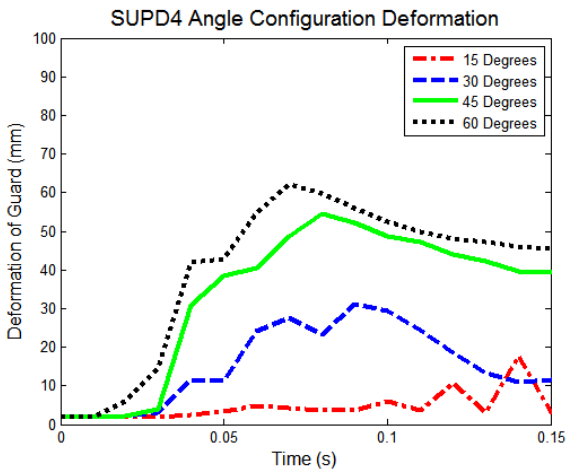

Figure 4.62 - SUPD4 angle configuration deformation

4.9 CONCLUSION OF REGULATION

This work has shown an overview of a regulation for testing the effectiveness of rigid side underride protection devices. The following initial comments, required guard dimensions and testing procedures have been determined in each section of this chapter and some findings are displayed in Figure 4.63:

Initial Comments:

- A large force application device is feasible for use on underride guards since it is currently regulated in Canada for rear guard testing
- The European regulation for side underride guards is only for unprotected road users and is not sufficient for passenger car collisions
- Rigid I-Beams are sufficient components for the testing of SUPDs, or in cases of different trailer configurations; rigid structures
- If the guard is not symmetric, it must be tested on both sides of the guard's centre axis

Guard Dimensions (Figure 4.63):

- The ground clearance must be at a minimum of 350mm with a maximum of 400mm in order to clear obstacles while still being able to use the crashworthy properties of the vehicles

- The device must not be more than 300mm from the wheels or the jack
- The device must not be placed more than 30mm inward from the outside edge of the trailer
- The guard's impact area height must be at least 400mm and have a maximum clearance from the bottom of the trailer of 350mm

Testing Procedures:

- The force application device should have the dimensions shown in Figure 4.46 and during testing, its centre must be 450mm from the ground
- The force application device is to be tested with a force of 525kN in increments of 500mm from the centre of the guard until the centre of the application device reaches the end of the guard
- A new guard must be utilized for every 500mm offset test
- The force application device must have a forward displacement during testing, and must be guided to prevent rotation
- The maximum deformation of the guard under any test must be 100mm in order to have rigid guard properties when the collisions occur dynamically

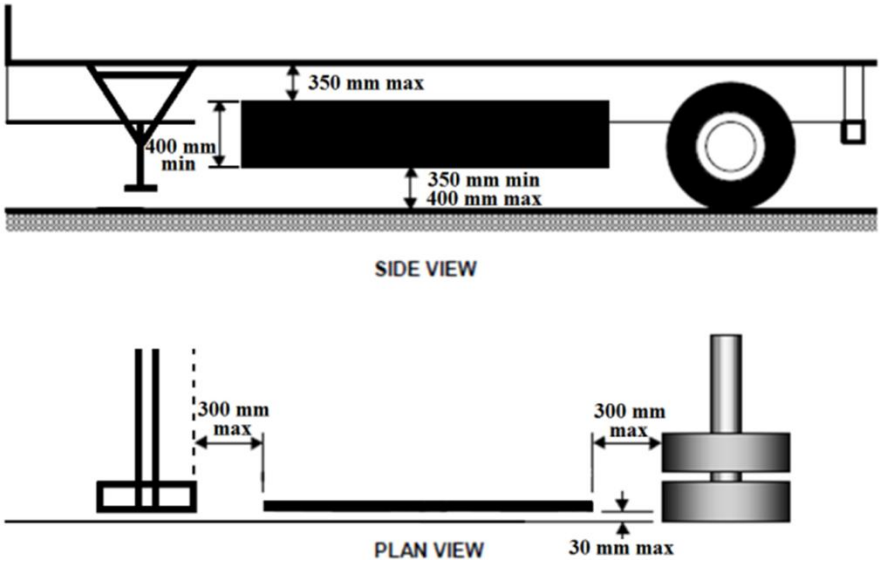

Figure 4.63 - Rigid SUPD dimension requirements (figure modified from [15])

With the regulation dimensions and testing methods outlined herein, other side underride guard concepts can now be developed. The same method may be utilized for other types of trailers and for straight trucks. In the cases investigated above, SUPD1 failed the regulation. SUPD3 and SUPD4 both proved to be feasible and passed both the quasistatic and dynamic tests. Since their deformation was smaller than 100mm during the quasistatic tests, it further solidified the claim that a force of 525kN was feasible for this type of crash and that the dynamic results would yield similar results. Utilizing optimization and topology software, rigid, lightweight and feasible guards can be created to protect not only unprotected road users, but also the occupants of small passenger vehicles.

CHAPTER 5: DESIGN VIA TOPOLOGY AND OPTIMIZATION

With the regulation for testing the effectiveness of side underride guards now developed and proven effective, the design and optimization of side guards is investigated in this chapter. The LS-DYNA software package is employed along with the topology optimizer LS-TaSC and the multi-objective optimizer LS-Opt. The first program is utilized to carve out the appropriate load paths of the brackets and the second, to optimize the thickness and allow node transformation to reduce the overall mass of the systems. Figure 5.1 shows a proposed design roadmap to aid in designing the most optimal and lightweight guards while retaining the overall robustness of the devices.

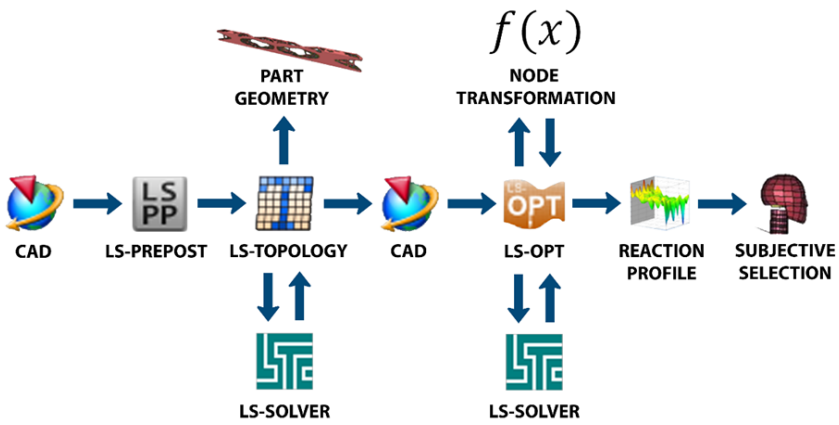

Figure 5.1 - SUPD design map utilizing topology and multi-objective optimization

The road map starts with initial parts created with the Unigraphics NX software. In this case, a block is created to be used in the LS-TaSC software for the brackets along with an impact area to cover the unprotected gap of the trailers and straight trucks. The parts are then imported in the LS-DYNA PrePost software. They are then meshed accordingly and assigned materials. The proper cards are implemented to ensure proper simulation and to establish the appropriate contacts. Next, the topology software is utilized for reduction of the bracket blocks to determine their load path. This is done using the force application device with the 525kN of force from the regulation at the proper intervals. When the final design is established, the part is recreated in Unigraphics NX using shell elements. The model is then imported in LS-Opt for optimization. The solver

is then used for the multiple iterations and node transformations to reduce the mass of the system. The results of each iteration are plotted and the final design is selected. The designs and optimizations of the SUPDs are shown below by utilizing this approach.

5.1 TOPOLOGY OPTIMIZATION (LS-TASC)

The process of determining the load paths on the brackets using LS-TaSC is outlined in Figure 5.2. In this picture, the bracket for SUPD5 (tractor-trailer SUPD) is designed. After each iteration, the program removes unnecessary material while keeping the robustness of the system until it reaches the stopping criteria defined by the user. This criteria is the mass fraction which is a value inputted during the initialization of the program. The simulation stops once the bracket reaches the assigned fraction of its initial mass.

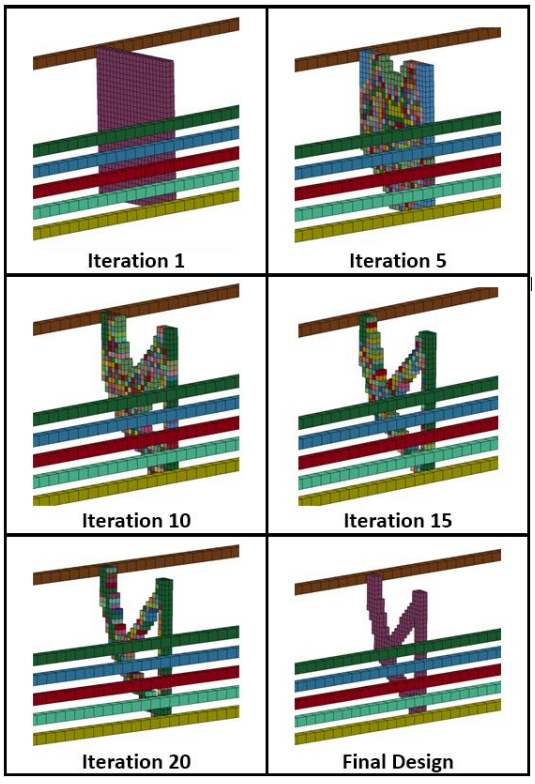

Figure 5.2 - LS-TaSC iteration process of an SUPD bracket

As outlined in the regulation, the devices are tested using the force application device with a quasistatic force of 525kN at intervals of 500mm until the application device

reaches 50% overhang. The bracket is given a specific design envelop which in these cases is a rectangular prism. For the tractor-trailer SUPD5, the dimension of this prism is given an appropriate height to stay within the 350 and 400mm ground clearance of the regulation. The width is that of the structural I-beams of the trailer. The depth is determined by the program to be the most effective while minimizing the mass. Figure 5.3 shows the final load path of the SUPD5 bracket along with the setup of the force application device.

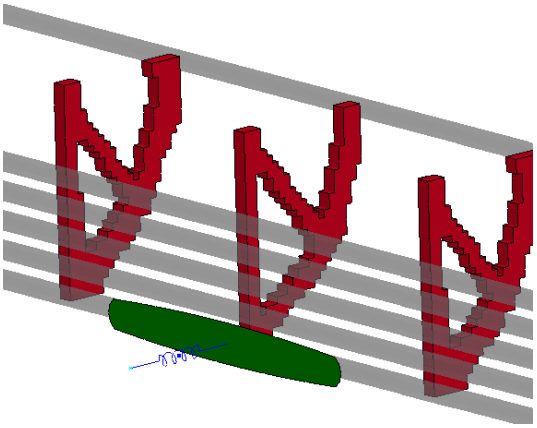

Figure 5.3 - Load path for the tractor-trailer SUPD bracket using LS-TaSC

When designing the brackets for the straight truck, the large C-beam which crosses the entire length of the vehicle can be utilized as an anchor point for the SUPD. The optimal SUPD-ST1 (straight truck SUPD) bracket load path is shown in Figure 5.4.

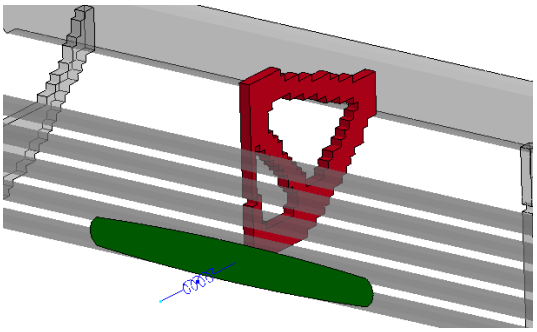

Figure 5.4 - Load path for the straight truck SUPD bracket using LS-TaSC

5.2 MULTI-OBJECTIVE OPTIMIZATION (LS-OPT)

At this point in the SUPD design process, the guards are created and tested using the proposed regulation. Multi-objective optimization is utilized to reduce the mass of the devices by changing the thickness of the parts along with shifting nodes to create the most efficient shapes. For this section, two types of frontal impact areas were investigated. The first utilized a guard rail type design. Normally, a guard rail will have two "humps" when looking at its side profile. To stay compliant with the regulation which states that a 400mm impact area must be used, a third "hump" was added and the overall shape was resized to accommodate this height. The second design uses 5 rectangular tubes spanning the entire length of the guard. This tube has the ability to shift its nodes to become wider or narrower. This function is added in the optimizer as an objective and the best possible size is determined. Both of the designs' side profiles can be seen in Figure 5.5. This same figure shows how the nodes of the square tubes were able to translate. The side profile of the force application device and its position is also outlined.

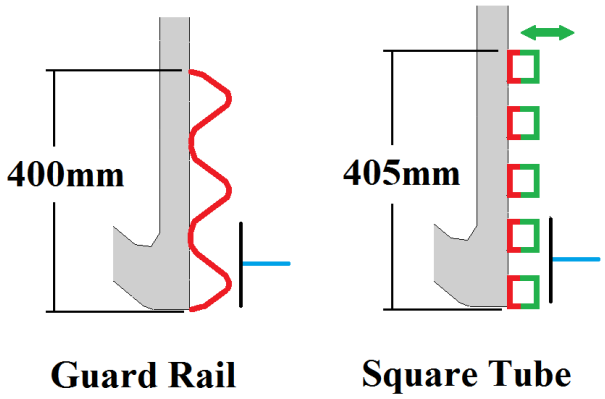

Figure 5.5 - Frontal crash area designs side profile

As previously indicated, SUPD5 is referred as the guard compatible with the LS-DYNA tractor-trailer and SUPD-ST1 is the guard designed for the Ford F-800 straight truck. Due to the 6500mm gap length of the tractor-trailer, two possible bracket placement configurations were investigated. The first includes having 7 brackets spaced out evenly across the entire device. Each part of the brackets can have a different thickness. The

values are determined using the optimizer. Both end brackets will have a larger thickness compared to the other brackets since they must hold the 525kN force at the 50% overlap. The other design consists of using 9 brackets. The middle brackets are spaced out evenly and at the ends, two brackets are placed in close proximity. Both of these are tested with the guard rail and the square tube frontal area designs and can be seen in Figure 5.6 and Figure 5.7.

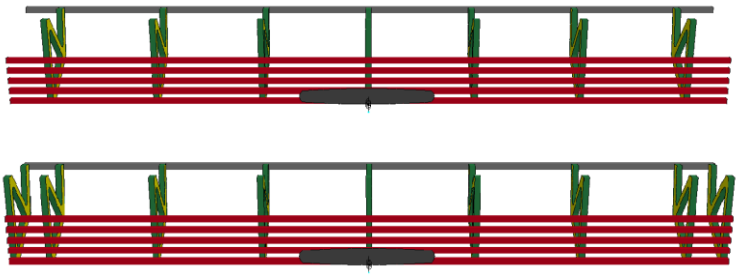

Figure 5.6 - SUPD5 with thicker and double end brackets designs with square tubes

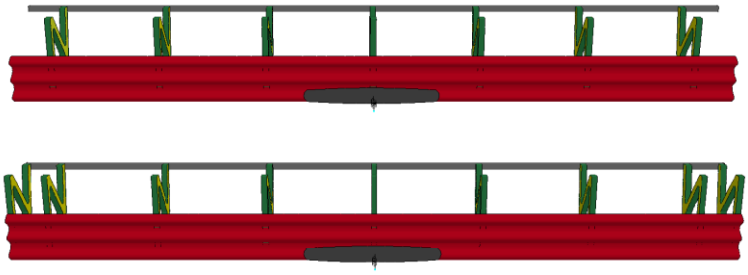

Figure 5.7 - SUPD5 with thicker and double end brackets designs with a guard rail

For the straight truck, the same principle of impact area was used. It is outlined in Figure 5.8. Since two guards are needed per side; one before and one after the rear axle, only one bracket configuration is considered. However, in this case, two bracket designs are tested and they can be seen in Figure 5.9.

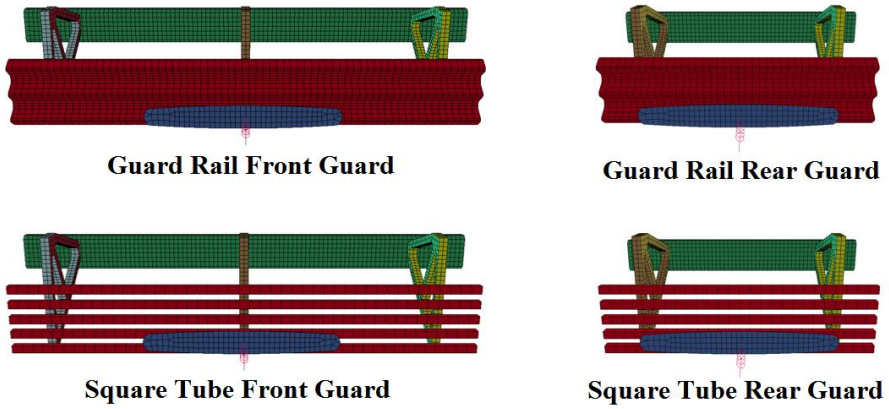

Figure 5.8 - SUPS-ST1 with guard rail and square tube impact areas

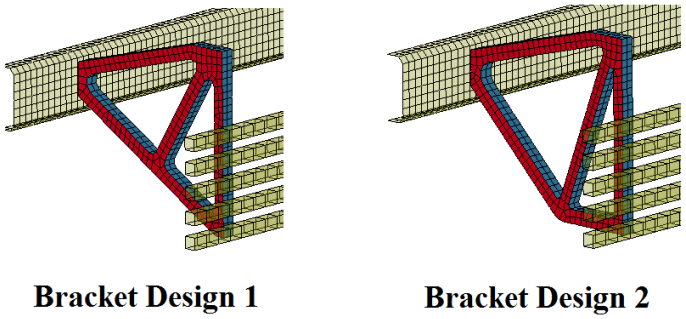

Figure 5.9 - SUPD-ST1 bracket design 1 & 2

For all cases outlined above, the material utilized for all of the parts of the SUPDs is an ASTM A653/A653M structural quality grade 80 steel. This material is used for the lateral cross I-beams of the LS-DYNA tractor-trailer model [41]. It is a structural steel with a high strength and a low-alloy composition [60]. Other materials could be utilized for the guards which would yield different results. A material selection could be implemented in the optimizer as a function to determine the lightest possible weight. However, without an appropriate cost function, it is difficult decide which material would be best since the manufacturability of some materials and their costs can render the underride guard unfeasible. That aspect is out of the scope of this research at this point and is considered in the future work section.

Several algorithms are embedded within the LS-OPT software to solve multi-objective optimization problems. A couple algorithms were trialed as possible solving methods for

the SUPDs. A direct simulation genetic algorithm was tested as a possible algorithm however, the most effective algorithm was the Hybrid Adaptive Simulated Annealing (HASA). This algorithm was a more effective and robust method of solving. The HASA is a combination of two optimization methods to aid in finding and converging quickly to the global optimum solution. The first of the two is an Adaptive Simulated Annealing (ASA) stochastic algorithm used to find the global optimum solution. Alone, this algorithm can become computationally expensive to find the solution since determining the proper stopping criterion can be difficult. It is then paired with a gradient based optimization method such as the Leaf Frog Optimizer (LFOPC). The addition of the LFOPC permits the optimizer to converge to a global optimum solution in a much more quick and efficient manner especially with very large optimization problems. The benefits of using the HASA over the genetic algorithm was that it allowed for diversity when exploring the design space when employing the LFOPC and allowed the continuation of the solution when some models would not find an equilibrium and fail [36].

In the case of optimizing for a device such as an SUPD or when a physical object must be created, certain aspects of the optimization procedures must be taken into account. Unlike mathematical optimization when the very best solution is determined using bounds when the parameterization is determined, the optimization of mechanical objects must consider the feasibility of manufacturability and cost. In other words, when determining the thickness of a specific part, it is insufficient to claim that the final values have multiple decimal points. Standard manufactured parts and thicknesses must be utilized when building the item. Because of this, the design space bounds must be assigned with discrete variables. When designing the SUPDs, the bounds had discrete variables set at intervals of 0.5mm. This would allow for feasible designs with realistic shell thicknesses. The final solution is therefore not necessarily the most optimal solution however, it is the most feasible optimal solution when considering engineering intuition for manufacturability and cost.

In the case of the SUPD5 and SUPD-ST1 optimization, the parameterization included the shell section thickness and the node transformation. Material may also be added with an appropriate understanding of cost and manufacturability as mentioned above. The optimizer would increase or decrease the thickness of each component of the brackets and front impact area to determine the most lightweight design while staying compliant with the regulation. The node transformation of the square tubes was explained above. The objective is to reduce the mass of the devices while having minimal deformation. The maximum allowable deformation which was determined in the proposed regulation is 100mm.

When setting up the simulations, a simultaneous loading technique was utilized. This consisted of having all of the load case increments of the regulation within a single simulation file. Pictures of this technique are shown in the coming sections. The purpose of this was to ensure that the guard would not deform more than 100mm in any of the offset cases. By having all of the cases in the same simulation, this would identify if any of the cases fail which would be considered a failed attempt by the program. The guard would be considered feasible if all of the load cases passed within a single simulation.

5.2.1 TRACTOR-TRAILER SUPD5

From the proposed regulation, the guard must resist a force of 525kN placed at the 0mm offset; the middle of the guard. The tests are then repeated at increments of 500mm until the force application devices reaches 50% overhang of the guard. Figure 5.10 shows this method along with the simultaneous loading conditions. As stated in the regulation, since the guard is symmetric, only half of the device needs to be tested.

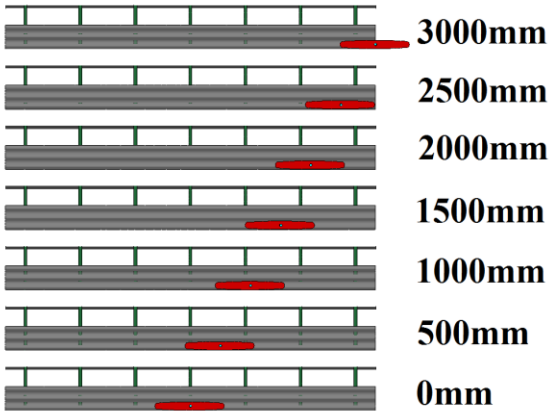

Figure 5.10 - Force application device loading conditions of SUPD5

Table 5.1 shows the results of the SUPD5 optimization along with the tested configuration including the thicker and double end brackets with the square tube and guard rail impact areas. The final masses of the devices are outlined. The final values are multiplied by two since a guard must be installed on both sides of the trailer.

Table 5.1 - Final Results of the SUPD5 optimization

Tractor-Trailer SUPD Design Type		Weight (kg)	Weight (lbs.)
Guard Rail	Double End Bracket Support	(192.296 x 2) = 384.592	(423.940 x 2) = 847.880
	Thicker End Bracket Support	(184.917x 2) = 369.834	(407.672 x 2) = 815.344
Square Tube	Double End Bracket Support	(185.889 x 2) = 371.778	(409.815 x 2) = 819.630
	Thicker End Bracket Support	(186.776x 2) = 373.552	(411.771 x 2) = 823.542

The most feasible and lightweight design was determined to be the thicker end bracket support system with the guard rail front impact area. The total weight of the device was 184.9kg. All of the designs yielded very similar results. The next step consisted of testing the guard with the 2010 Toyota Yaris and the 2001 Ford Taurus with the appropriate increments. When looking at the end load cases; the 2500mm and the 3000mm offsets, the bracket would tend to bend inward towards the center of the guard. To eliminate this, a square tube cross bar was added connecting the two outer most brackets together for added rigidity.

Figure 5.11 to Figure 5.14 shows the impact force over deformation graphs of the 0, 500, 1000 and 1500mm offset configuration collisions. The graphs consist of simulations with a Yaris and a SUPD5 installed on a component level test fixture, a Yaris and a SUPD5 with the added bar between the two end brackets, a Taurus and a SUPD5 with added bar and a full simulation consisting of a tractor-trailer, a SUPD5 with bar and a Toyota Yaris. The initial velocity of each simulation was 64km/h. In these cases, the force over deformation curves when comparing the Yaris with and without the bar were very similar. During these offsets, the bar has little effect since it is only installed between the outer two most brackets. The profiles of all four graphs is slightly different. This is dependent on the positioning of the car, whether it makes direct center contact with one bracket or whether the contact is made between two brackets. The deformation of the Taurus is much greater compared to the Yaris. This is due to the larger deformation of the front end during a collision, which is seen in Section 4.5.5. During the full simulation, the deformation is much greater and the force is reduced. In these cases, when the Yaris collides with the trailer, the force is enough to push it along the ground, causing it to skid. The trailer also experiences some deformation and twist due to the collision, which adds to the deformation of the Yaris since its value is measured from its center of gravity. This results in a reduction of peak impact force.

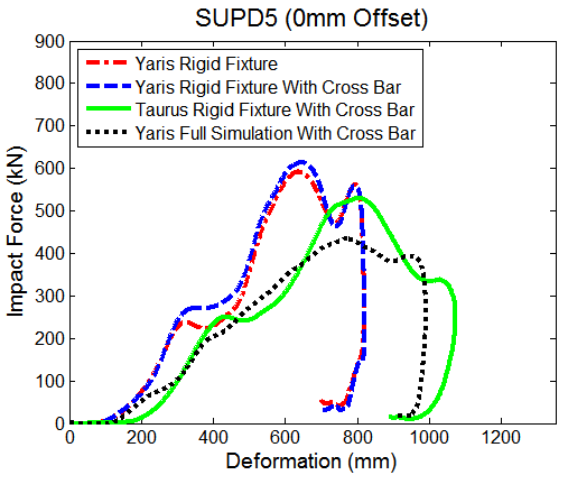

Figure 5.11 - SUPD5 impact force graph at 0mm offset

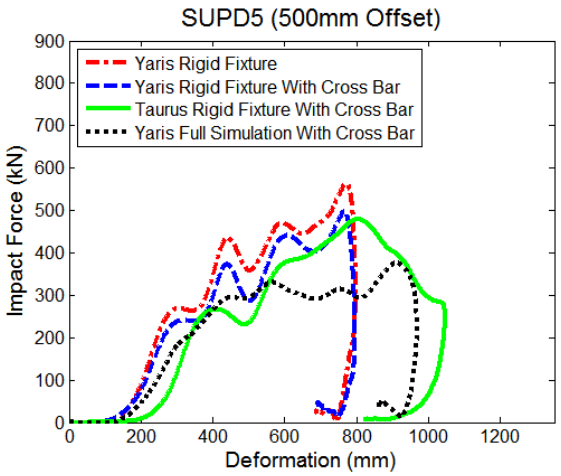

Figure 5.12 - SUPD5 impact force graph at 500mm offset

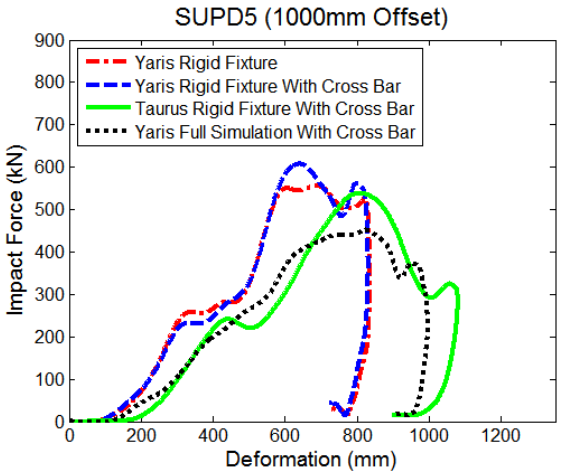

Figure 5.13 - SUPD5 impact force graph at 1000mm offset

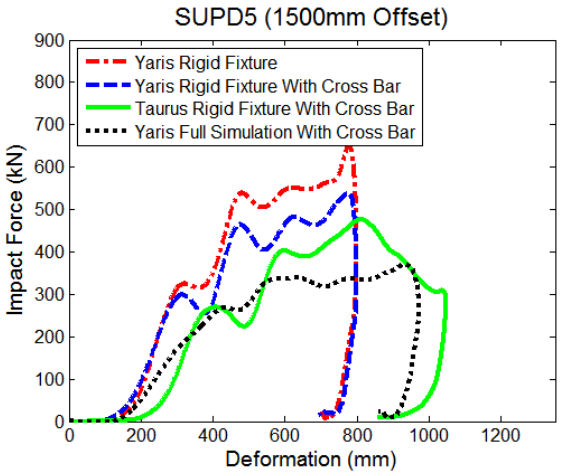

Figure 5.14 - SUPD5 impact force graph at 1500mm offset

Next, the 2000 and 2500mm offset graphs are investigated in Figure 5.15 and Figure 5.16. In these simulations, the vehicle is offset towards the end of the guard. The more the offset, the more overlap exists between the car and the edge of the guard. This leads to larger deformations of the car since the crush zone is reduced. The addition of the bar to the guard becomes apparent in these simulations. The overall deformation is about 50mm smaller indicating that the bar added to the rigidity and robustness of the guard.

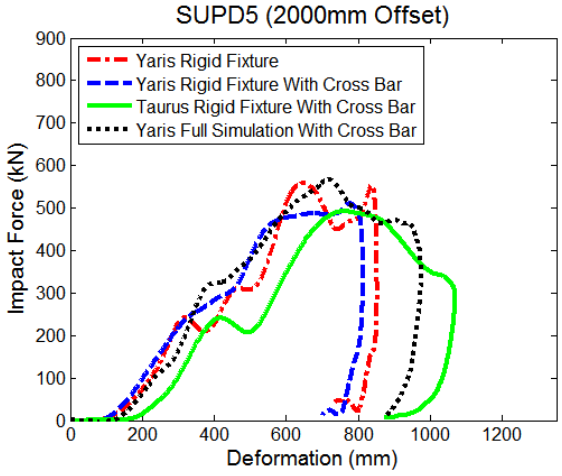

Figure 5.15 - SUPD5 impact force graph at 2000mm offset

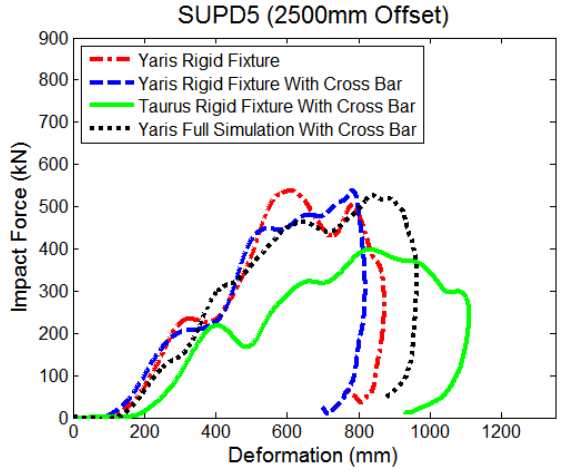

Figure 5.16 - SUPD5 impact force graph at 2500mm offset

In the final 3000mm offset case, an additional full tractor-trailer simulation was conducted. At one end of the guard, the +3000mm offset, the trailer rear axle and wheel interfere with the collision. At the other end, the -3000mm offset, the trailer jack or landing gear interferes in a different manner with the collision. Because of this, both were conducted and plotted in the graph. At this offset, the addition of the bar is also apparent and helps to stop the vehicle by keeping the guard rigid. In the component level tests, the car would deflect off the guard and continue to travel and experience larger deformation. In the +3000mm offset, the rear wheel aided the car in coming to a full stop much quicker. In the -3000m, the trailer jack also helps to stop the vehicle however, being much smaller, this effort is reduced.

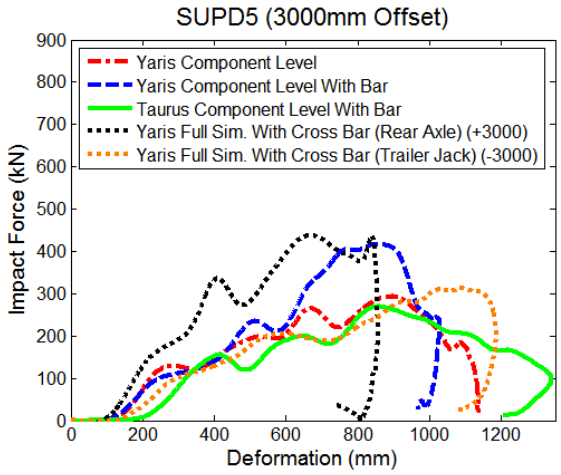

Figure 5.17 - SUPD5 impact force graph at 3000mm offset

The final design is demonstrated in Figure 5.18. The guard rail impact area is made semi-transparent to show the bars that were added to increase the rigidity of the guard. The final weight of the device with the added bars is 198.1kg. Since a guard is to be installed on each side of the trailer, the weight of two devices added to a trailer to prevent underride from both sides is 396.2kg. Figure 5.19 shows a comparison of the SUPD at the 3000mm interval without and with the cross bar. When no bar is installed, the outer most bracket tends to get pushed inward towards the center of the guard. In this figure, it is evident that the bar stops this from occurring, creating a more rigid device.

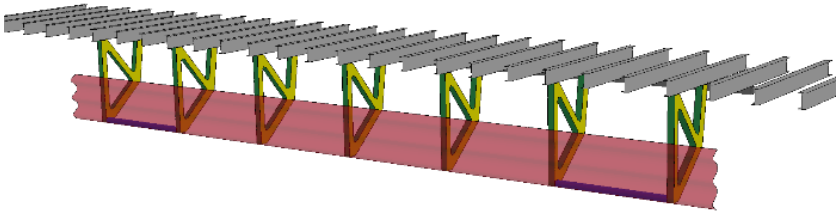

Figure 5.18 - Final SUPD5 design

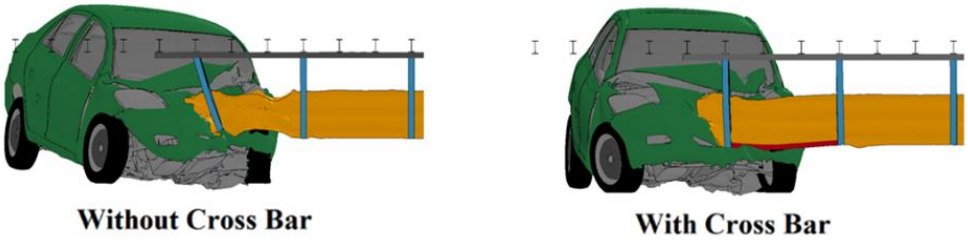

Figure 5.19 - Comparison of SUPD5 without and with the cross bar

The regulation states that if the guard is tested with an applied force of 525kN at certain intervals, the dynamic tests will yield similar results and the guard will stay rigid with minimal deformation. Figure 5.20 shows the deformation of the guard when hit by the Yaris and the Taurus. The graphs prove the claim made by the regulation. In most cases, the deformation is well below the 100mm mark. The only case where the deformation is larger than 100mm is when the Ford Taurus impacts the guard at the 500mm offset. The value of this collision is 107mm which is still considered an acceptable value. The graph also demonstrates the comparison between a compact car and a midsize car when hitting the guard. The results are very similar and comparable. The guard stays rigid during the collision from small to medium passenger vehicles and prevents them from underriding.

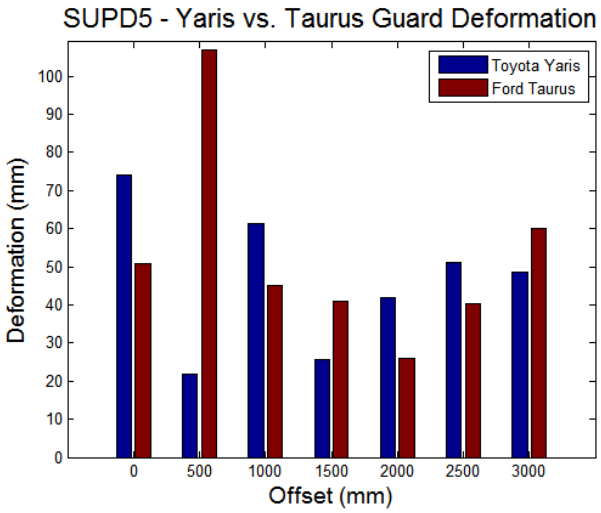

Figure 5.20 - SUPD5 Yaris vs. Taurus deformation

To show how underride is prevented with a guard when a vehicle collides with a tractor-trailer, Figure 5.21 is observed. In the graph, the displacement and deformation of the Yaris with the guard is approximately 1050mm. This indicates that the vehicle comes to a complete stop and does not underride the trailer and explains why the force is much greater. When no guard is installed, the displacement and deformation is about 2750mm. The impact force in this case is much smaller, but the vehicle completely passes under the trailer and finally comes to a stop when the B-pillars collide with the trailer. A visual representation of these scenarios is shown in the figure.

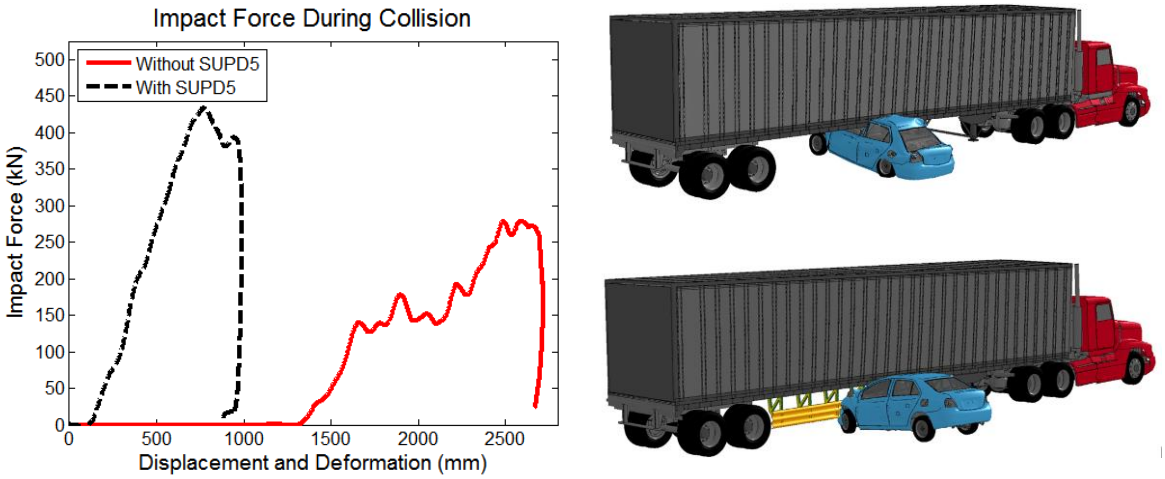

Figure 5.21 - Comparison of collision with and without SUPD5

5.2.2 STRAIGHT TRUCK SUPD-ST1

Similarly to what was conducted for the SUPD of the tractor-trailer, the guard for the straight truck is now optimized and evaluated. Since the rear axle of the straight truck is positioned further away from the back of the truck, two guards are to be utilized per side of the vehicle. The first is positioned between the cab and the rear axle and the second between the rear axle and the rear most point of the vehicle. By following the regulation, Figure 5.22 shows the force application device offset cases. Since two guards are utilized, the device is placed on the first guard and its position is incremented until it reaches 50% overhang of the device. The second guard is tested in the same manner.

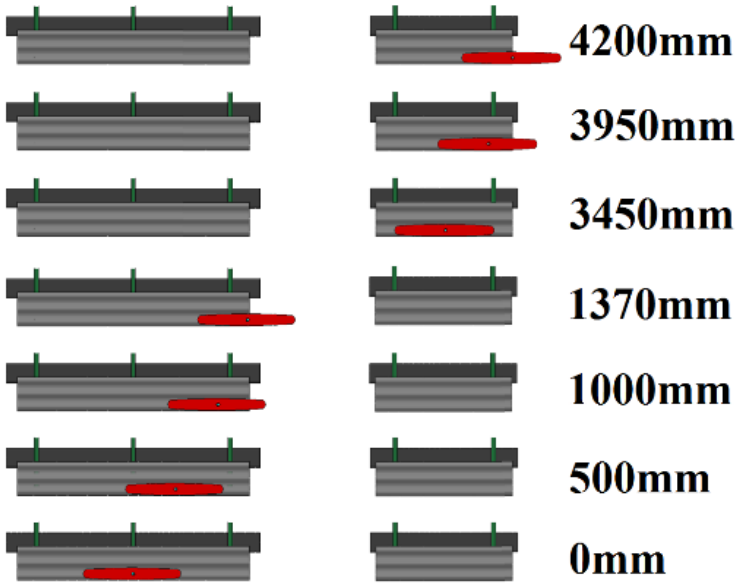

Figure 5.22 - Force application device loading conditions of SUDP-ST1

Table 5.2 and Table 5.3 show the final results of the optimization of the front and rear guard. Both bracket designs were tested with the guard rail and square tube impact areas. The results show that for the front guard, the guard rail type design with the Bracket Design 1 was the lightest guard able to withstand the forces applied with the regulation. For the rear guard, the guard rail with the Bracket Design 2 was the most effective however, to stay consistent with the front guard, Bracket Design 1 is utilized for the remainder of this section. This guard weighed 0.569kg more than the lightest design.

Table 5.2 - Final results of SUPD-ST1 front guard optimization

Straight Truck SUPD Design Type (In Front of Rear Axle)		Weight (kg)	Weight (lbs.)
Guard Rail	Bracket Design 1	(79.786 x 2) = 159.572	(175.898 x 2) = 351.796
	Bracket Design 2	(84.257 x 2) = 168.514	(185.755 x 2) = 371.510
Rectangular Tube	Bracket Design 1	(85.747 x 2) = 171.494	(189.040 x 2) = 378.080
	Bracket Design 2	(90.688 x 2) = 181.376	(199.933 x 2) = 399.866

Table 5.3 - Final results of SUPD-ST1 rear guard optimization

Straight Truck SUPD Design Type (Behind Rear Axle)		Weight (kg)	Weight (lbs.)
Guard Rail	Bracket Design 1	(52.933 x 2) = 105.866	(116.697 x 2) = 233.394
	Bracket Design 2	(52.364 x 2) = 104.728	(115.443 x 2) = 230.886
Rectangular Tube	Bracket Design 1	(57.630 x 2) = 115.260	(127.052 x 2) = 254.104
	Bracket Design 2	(63.415 x 2) = 126.830	(139.806 x 2) = 279.612

As observed with SUPD5, the brackets would tend to fold inward during dynamic simulations with the Yaris and Taurus. This same deformation was observed with SUPD-ST1. Because of this, the same method of adding a cross bar to the device was utilized. This added rigidity to the guard which reduced the deformation of the device.

When looking at the graphs of Figure 5.23 to Figure 5.25, the addition of the bar becomes apparent. The forces experienced during the collisions were much greater when the bar was installed and the deformation was reduced. This shows that the guard's rigidity had increased. The vehicle comes to a complete stop much faster with the bar. Due to the positioning of the brackets, the forces experienced differ from one another depending on offset of the vehicle. The vehicle may have a head on collision with a bracket or be between two brackets. This will alter the results of the simulation and will result in different guard deformation values.

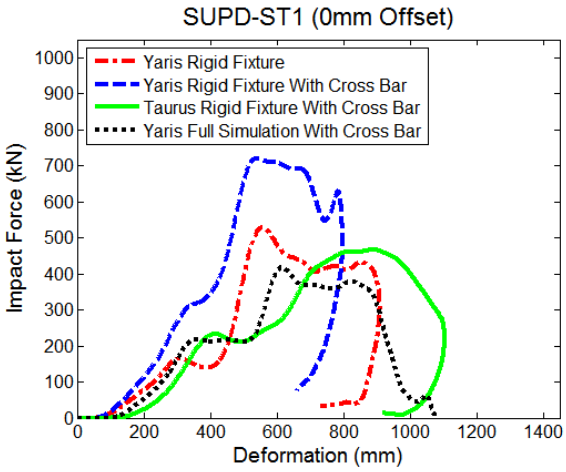

Figure 5.23 - SUPD-ST1 impact force graph at 0mm offset

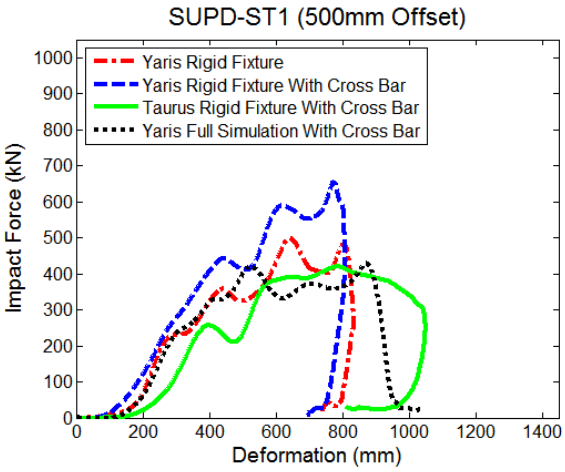

Figure 5.24 - SUPD-ST1 impact force graph at 500mm offset

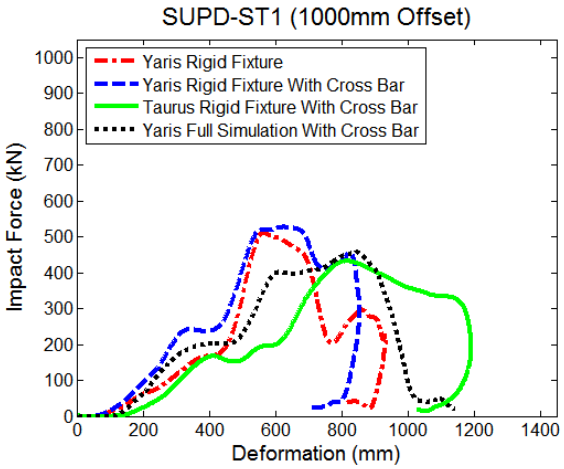

Figure 5.25 - SUPD-ST1 impact force graph at 1000mm offset

In the 1370mm offset case, the car has 50% overhang over the edge of the guard in the rigid fixture tests. In the full simulation tests, the car makes contact with the wheels on the rear axle. The forces experienced are much smaller and the deformation is larger due to the car making contact with the edge of the guard and deforming around it. In the full simulation, the straight truck is pushed along the ground due to the impact in the direction of travel of the vehicle. This is observed in Figure 5.26.

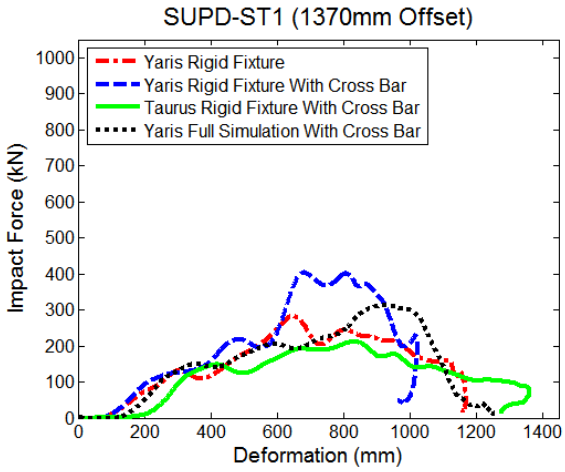

Figure 5.26 - SUPD-ST1 impact force graph at 1370mm offset

The rear guard located between the rear wheels and the rear most point of the straight truck can now be analysed. In the 3450 and 3950mm offset cases, shown in Figure 5.27 and Figure 5.28, several observations can be made. The 3450mm offset has the car positioned in the center of the guard, between two brackets. Both vehicles have a higher impact force and a smaller deformation compared to the 3950mm case, which has a bracket placed in front of the car. In the 3950mm case, there is also a small amount of overlap of the cars to the guard. The deformation is greater since the vehicle tends to wrap around the guard. When investigating the full simulation, since the collision takes place behind the rear axle, the straight truck's rear end will swing out due to the impact force, resulting in greater displacements and deformations of the vehicles. The graphs show that the vehicles continue to travel and do not actually come to a complete stop. The guards did however prevent underride.

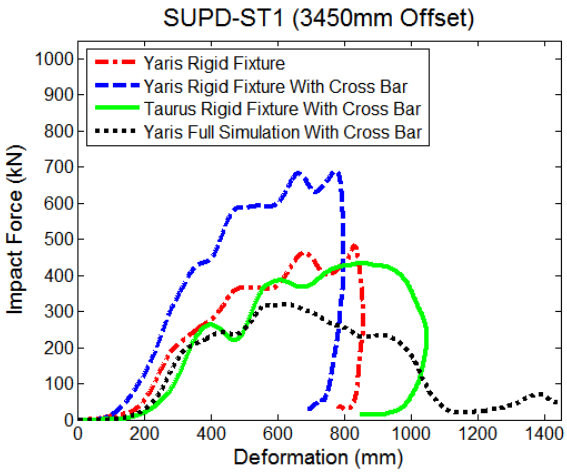

Figure 5.27 - SUPD-ST1 impact force graph at 3450mm offset

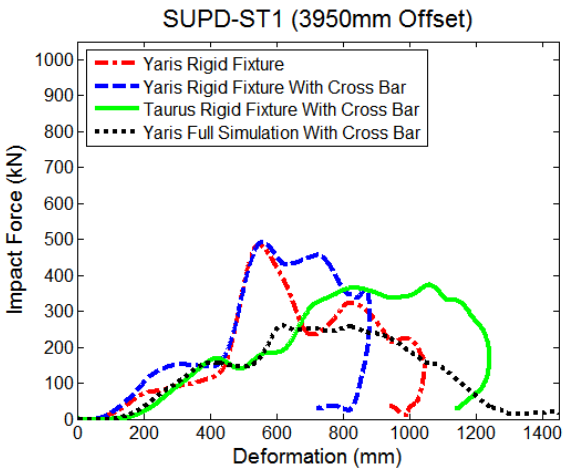

Figure 5.28 - SUPD-ST1 impact force graph at 3950mm offset

In the case of the 4200mm offset, shown in Figure 5.29, the same conclusion can be drawn as in the 3950mm case. The vehicle collides with the straight truck, pushes it along the ground, rebounds off the side and continues to travel since the collision takes place behind the rear axle.

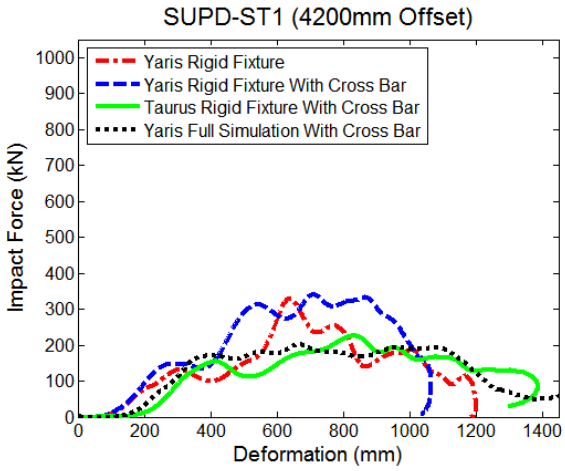

Figure 5.29 - SUPD-ST1 impact force graph at 4200mm offset

In all seven cases, the Ford Taurus data is also compared with the Toyota Yaris collisions. Due to the higher deformation of the vehicle during a collision, the impact force is reduced. The guards were still rigid enough to stop the heavier vehicle from underriding. Figure 5.30 demonstrates the final SUPD-ST1 guard installed on the rigid

test fixture. With the cross bar, the front and rear guards have a combined weight of 148.1kg. Since both sides of the truck require guards, the total weight to fully envelop the vehicle is 296.2kg. The guard rail is shown as semi-transparent to show the cross bar that was added. Figure 5.31 shows how the addition of the cross bar aids in the rigidity of the system during the collision in the offset position.

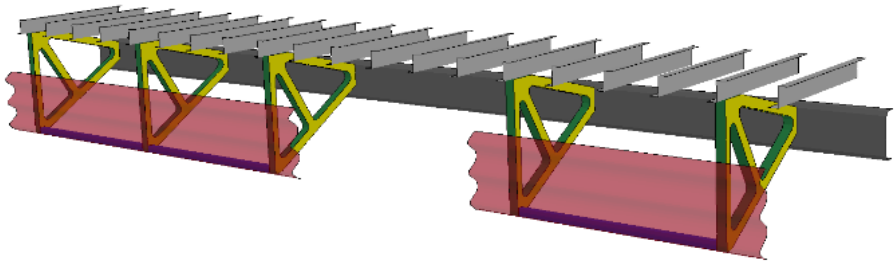

Figure 5.30 - Final SUPD-ST1 design

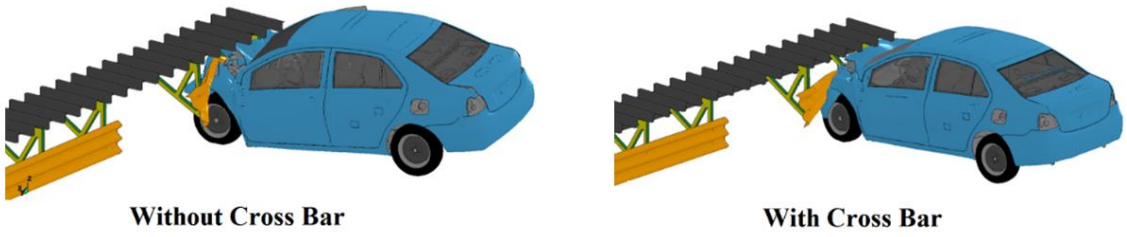

Figure 5.31 - Comparison of SUPD-ST1 without and with the cross bar

Figure 5.32 demonstrates the guard deformation when hit by the Yaris and the Taurus at its multiple offsets. Again, as previously concluded in the SUPD5 section, the guard was able to successfully prevent underride and stop the vehicles. In this case, some of the deformations were slightly larger than 100mm. The values were still deemed acceptable and the guards remained rigid.

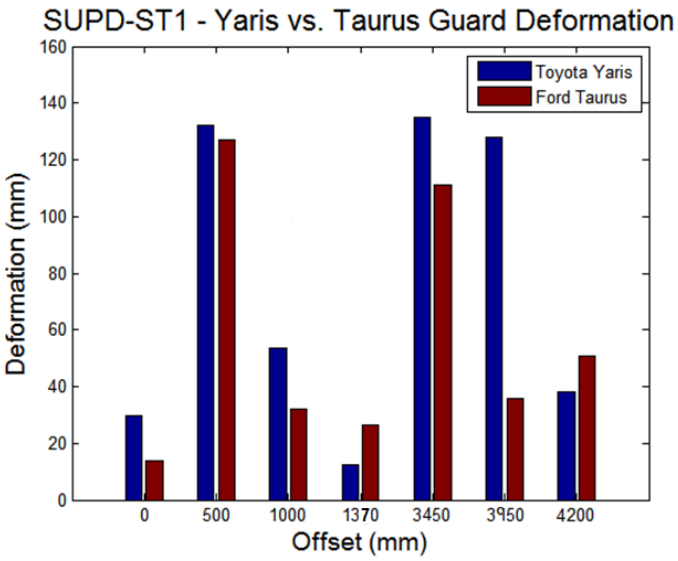

Figure 5.32 - SUPD-ST1 Yaris vs. Taurus deformation

A graphical and visual comparison of the benefits of having an underride guard on straight trucks is shown in Figure 5.33. In this case, the forces are relatively the same since during the simulation without a guard, the vehicle collides with the C-beam located under to heavy vehicle then comes to a full stop. Underride however still occurs as deformation of the A-pillar is observed and the vehicle has a potential of being struck by the rear wheels. The graph shows that the car comes to a complete stop when the guard is installed and that there is no underride.

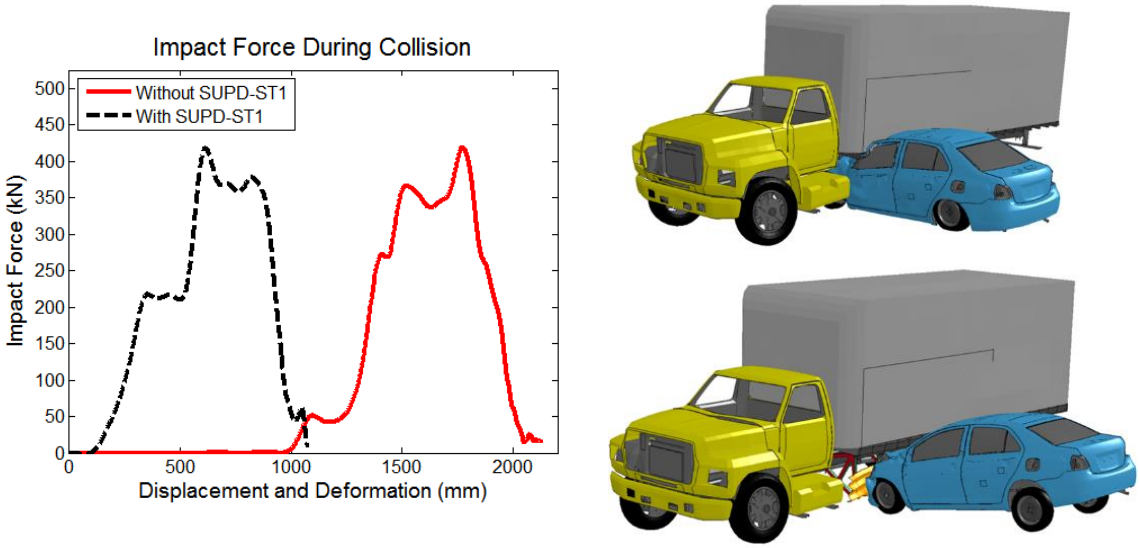

Figure 5.33 - Comparison of collision with and without SUPD-ST1

This section has shown the topology and multi-objective optimization procedures utilized to create the most feasible and lightweight underride guards for both tractor-trailers and straight trucks. Guards for both of these heavy vehicles were created and shown to be effective to stop vehicle underride when colliding with the sides of the heavy vehicles. The final mass of SUPD5 for both sides of the trailer was 396.2kg and the final mass for SUPD-ST1 was 296.2kg.

CHAPTER 6: FINAL DESIGN AND CONSIDERATIONS

With the investigative aerodynamic research conducted in the literature review, it was evident that the design of SUPD5 was lacking a drag reducing shape. The designs simply consisted of a flat surface, which as described in the aerodynamic fairing section, was not necessarily the most efficient shape for air deflection. As seen, many shapes are possible and each have advantages and disadvantages [30]. Kronos, a fairing company, points out a few of their fairing advantages on their website. They state that a fairing should be curved at the front and angled towards the inside of the jack mounts. This deflects the air coming from the rear tires of the truck to the outside of the trailer and fairing [61]. Figure 6.1 from the company's website demonstrates the advantage of having the curve at the front of the device.

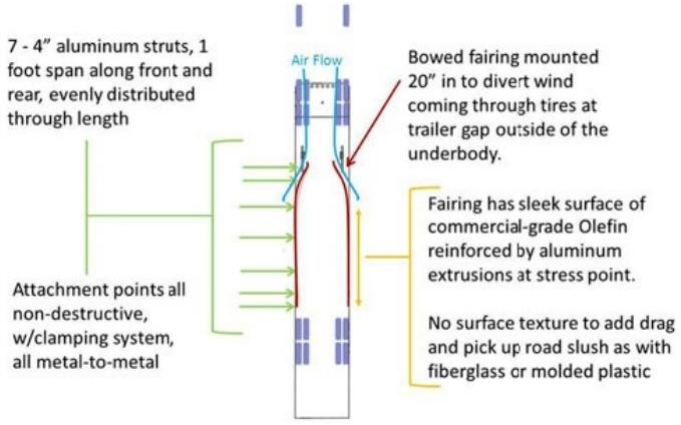

Figure 6.1 - Kronos fairing shape and explanation [61]

Another company explains the benefits of having a toe-in or gear wrap curve at the front of the fairings, coming to the same conclusions as Kronos. Aerofficient claims that when the tractor's wheels are spinning, they create a vortex air flow which needs to be pushed outside of the trailer [62]. If the fairing is simply a flat drop down, the turbulent air coming from the driving wheels will remain under the trailer and cause drag until it exits the rear of the trailer [61].

6.1 TRACTOR-TRAILER SUPD6

The toe-in curve principle was implemented to the SUPD to demonstrate the aerodynamic advantage of an underride guard. To accomplish this feat, the regulation was reinvestigated since the initial claim was that the guard must not be positioned more than 30mm away from the outer edge of the trailer. Utilizing the same design approach as SUPD5, a new guard called SUPD6 is created. Towards the front of the device, the guard is curved 250mm inward. The following tests will determine if the chosen parameters are feasible and if the regulation can be adjusted to accommodate for more aerodynamic underride guards.

The same brackets as SUPD5 were utilized since the topology processes had already been conducted and the brackets proved to be effective. Next, the design of the impact area was investigated. From the previous design, the guard rail type design proved to the lightest. However, after several tests, square tubes were added to the guards to make them more rigid and prevent the brackets from folding towards the inside. To prevent this from happening, the double end bracket system was reinvestigated to strengthen the 3000mm offset load case. The new design would also require a sleek surface to deflect the air with minimal drag. With engineering intuition and the above mentioned, a three bar design was chosen with sheet metal placed between the gaps and the brackets had a double end bracket type configuration. The purpose of this design is to eliminate the addition of the cross bar by having three interconnected bars.

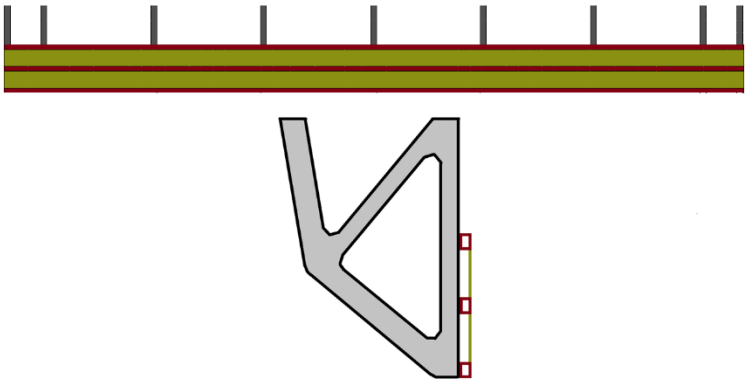

Figure 6.2 - SUPD6 bracket configuration and impact area design

Multi-objective optimization was then utilized with the regulation implicit loading of 525kN to reduce the weight while maintaining structural robustness. The parameterization of the simulation included the thickness of each member of the device and the node transformation of the sheet metal and rectangular tubes. The regulation states that the force application device must be positioned in front of the guard and tested at its multiple intervals of 500mm. When a curved device is tested, the angle of the application device had to be considered. During testing, the device was still guided to prevent rotation however, it was placed perpendicular to the tangent of the guard at the 2500mm and 3000mm offsets. The application device still had its intended forward displacement as can be seen by the position and direction of the springs in Figure 6.3. This figure shows the 2000, 2500 and 3000mm offsets along with the position and angle of the force application device.

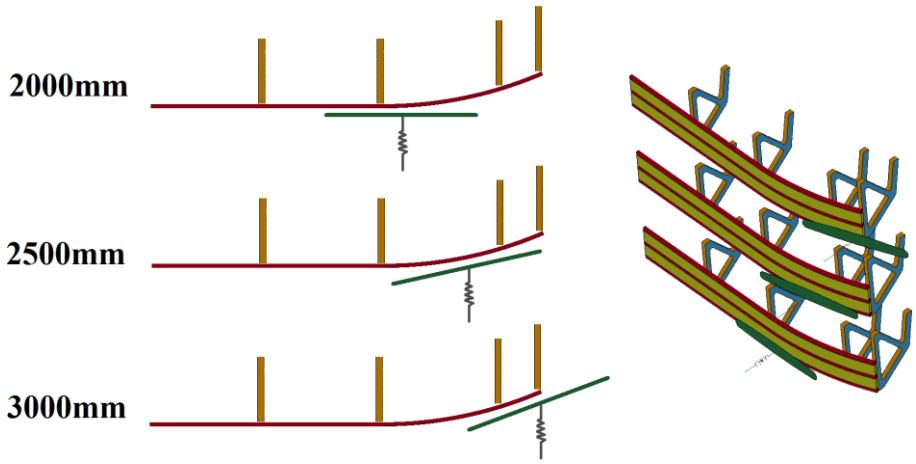

Figure 6.3 - Force application device angle at 2500 and 3000mm offset

The final design is seen in Figure 6.4 and has a weight of 198.9kg which is 0.8kg more than SUPD5 with added cross bar. A piece of plastic was added between the upper most bar of the impact area and the bottom of the trailer. This piece's sole purpose was to cover the gap to complete the aerodynamics of the device.

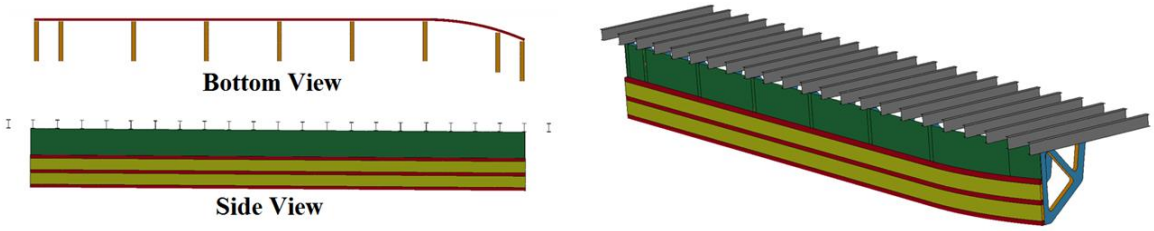

Figure 6.4 - Final SUPD6 design

The explicit testing of the device is now investigated. The regulation states that half the device may be tested if it is symmetrical. In the case of SUPD6, the guard is symmetrical until the 2500 and 3000mm offsets due to the curve. Because of this, two additional offset tests were conducted which included the -2500 and -3000mm cases. For this guard, the negative offset cases are near the rear axle. The guard was tested and installed on the rigid test fixture and on the tractor-trailer for a full simulation with the Toyota Yaris and the Ford Taurus.

Figure 6.5 to Figure 6.9 shows the results of the 0mm to the 2000mm offset tests. Much like the results obtained from SUPD5, the deformation was greater when the tractor-trailer was involved since the vehicle would push it along the ground and would cause the trailer to twist. This occurs since the data is taken from the center of gravity of the passenger vehicle. Although the vehicle is hitting a uniform impact area, the data is different from offset to offset due to the positioning of the brackets. The data of the 0 and 1000mm cases are similar since the vehicle's center axis is making direct contact with a bracket. In the 500 and 1500mm cases, the passenger car is making contact with the impact area positioned between two brackets.

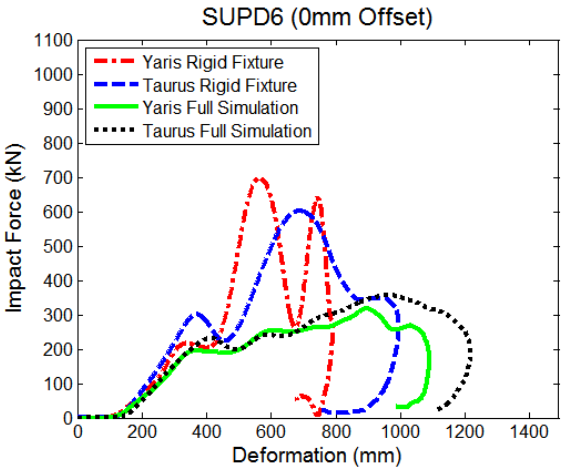

Figure 6.5 - SUPD6 impact force graph at 0mm offset

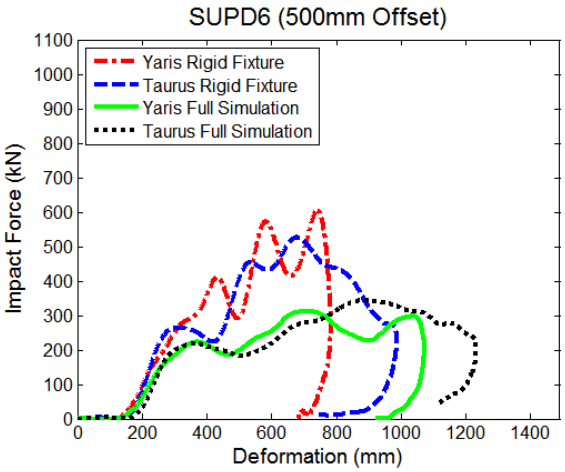

Figure 6.6 - SUPD6 impact force graph at 500mm offset

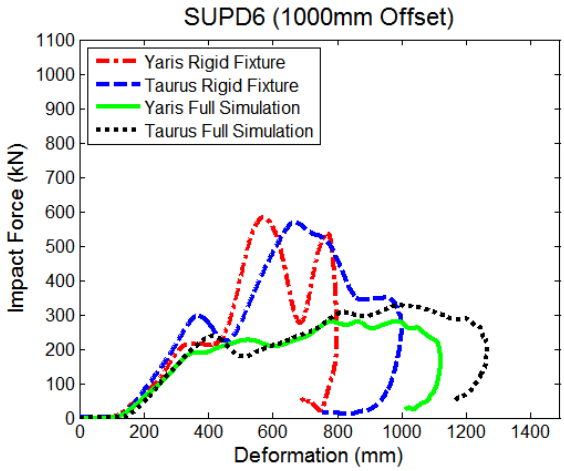

Figure 6.7 - SUPD6 impact force graph at 1000mm offset

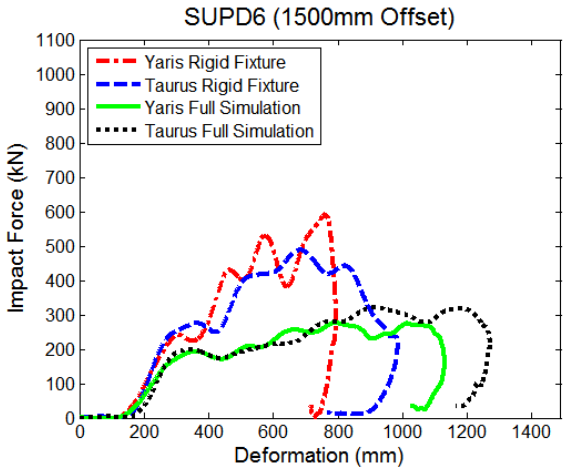

Figure 6.8 - SUPD6 impact force graph at 1500mm offset

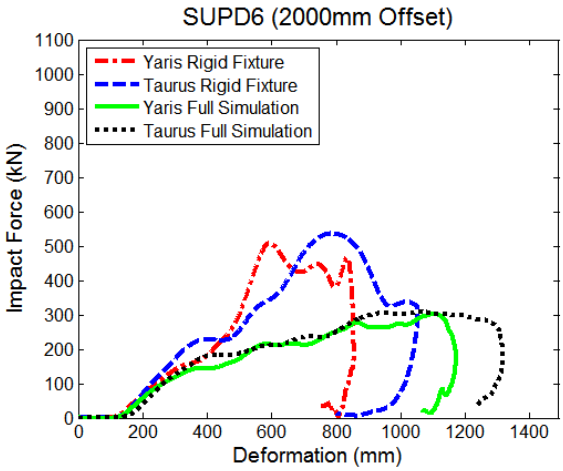

Figure 6.9 - SUPD6 impact force graph at 2000mm offset

Figure 6.10 to Figure 6.13 shows the 2500 and 3000mm offsets near the trailer jack and the -2500 and -3000mm offsets near the rear axle. In the positive cases, the guard is curved inward to meet the trailer jack and deflect the air from the tractor wheels outside of the trailer. In all cases, the vehicle's distance from the guard is the same. In the 3000mm case, one can see that impact does not occur until the 275mm range since the car must travel further to reach the guard due to the curve. The jack also plays a lesser role when it comes to stopping the vehicle, which was shown in the SUPD5 section. At the other end of the guard; the -2500 and 3000mm cases, the vehicle reached a complete stop much quicker. The guard is flat at this offset and the car makes contact with the wheels on the rear axle.

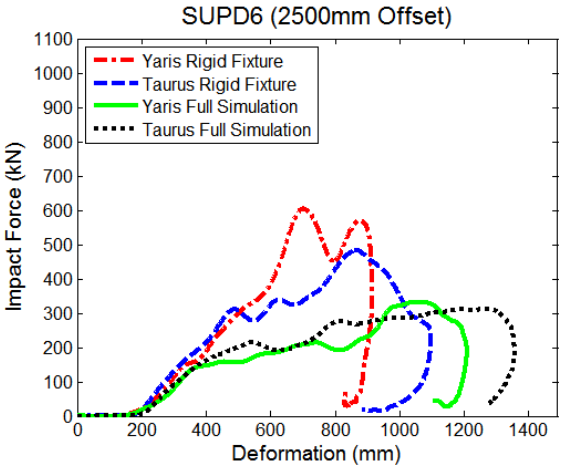

Figure 6.10 - SUPD6 impact force graph at 2500mm offset

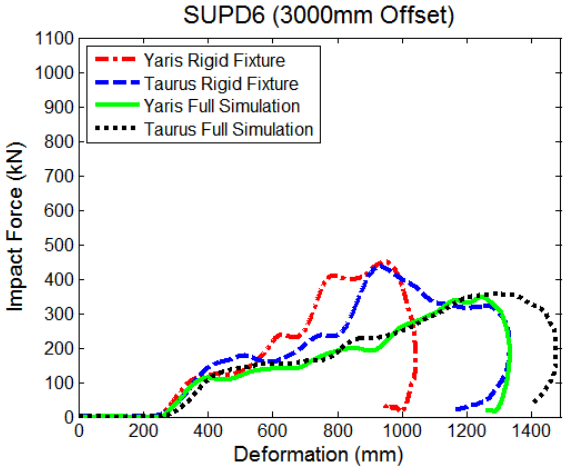

Figure 6.11 - SUPD6 impact force graph at 3000mm offset

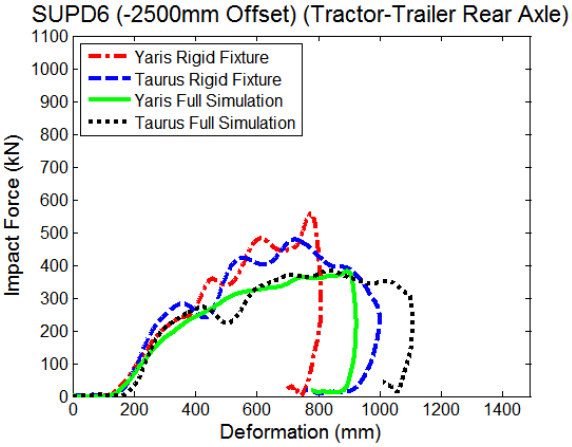

Figure 6.12 - SUPD6 impact force graph at -2500mm offset

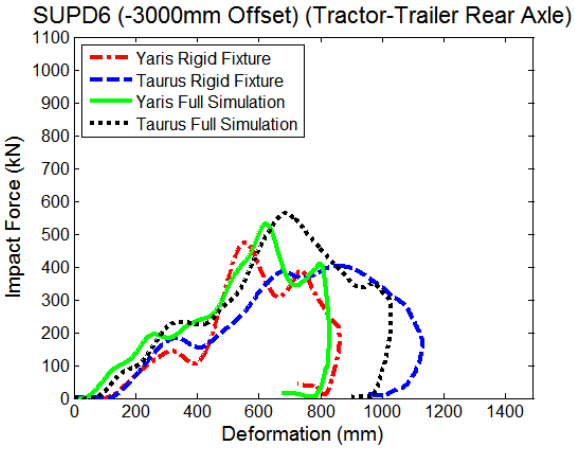

Figure 6.13 - SUPD6 impact force graph at -3000mm offset

From the rigid test fixture collisions, the guard deformation is now examined in Figure 6.14. In the 2000 to 3000mm cases, the deformation passes the 100mm threshold established in the regulation. This occurs since the impact area deforms more in these locations due to the vehicle making contact with the brackets which are placed further back. At the -2500 and -3000mm offsets, the values are acceptable and do not greatly exceed the 100mm deformation point. Because of this, Figure 6.15 was created to show the deformation of the brackets to show their rigidity. From the graph, at the 2500 and 3000mm offsets, the bracket deformation is between 20 and 40mm depending on the vehicle and the configuration. The guard is therefore still considered to be rigid.

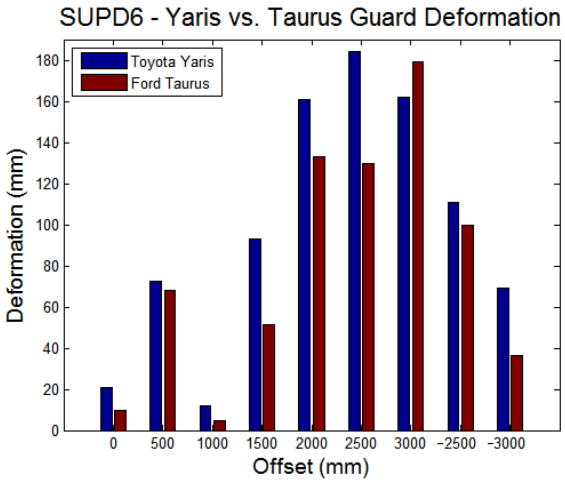

Figure 6.14 - SUPD6 Yaris and Taurus guard deformation

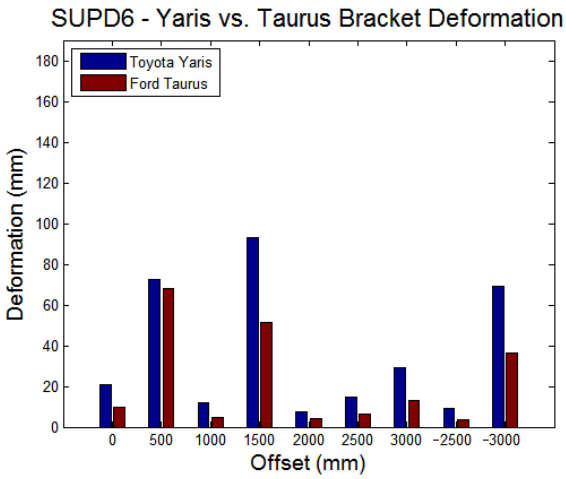

Figure 6.15 - SUPD6 Yaris and Taurus bracket deformation

Utilizing the IIHS compartment intrusion test, SUPD5 with the cross bar can now be compared to SUPD6 when mounted to a rigid test fixture. To show how a guard mounted to a tractor-trailer yields different intrusion values, SUPD6 with the full simulation is also plotted. The results in Figure 6.16 and Figure 6.17 are the two major offset cases of SUPD6 where the car would experience the largest intrusion since it overlaps the SUPD. When comparing SUPD5 with a rigid bar to SUPD6 in both cases, one can see that the results are very similar. The severity of the intrusion is greater in the 3000mm case since the car has more overlap. In this offset, the frontal area of the driver is taking the full impact against the guard which results in larger intrusion values.

The figures also demonstrate that when the guards are mounted on a tractor-trailer instead of a rigid fixture, the severity of the intrusion is greatly reduced.

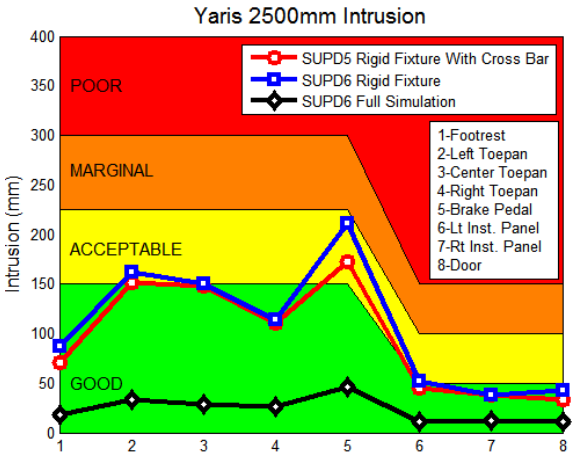

Figure 6.16 - SUPD Yaris 2500mm intrusion graph

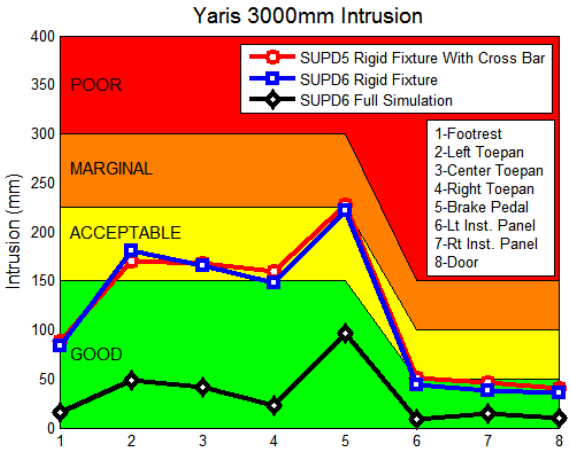

Figure 6.17 - SUPD Yaris 3000mm intrusion graph

Figure 6.18 and Figure 6.19 shows the results of the Taurus collisions for the 2500 and 3000mm offsets, respectively. Again, the results of the 3000mm offset are far more severe than the 2500mm offset. In the 3000mm case, the data from SUPD5 is higher than SUPD6, indicating that the design was more rigid, which caused more damage to the Taurus. When mounted on the tractor-trailer, the results yielded "good" values for all data points. The intrusion is much smaller since the tractor-trailer absorbs some of the impact force for the collision.

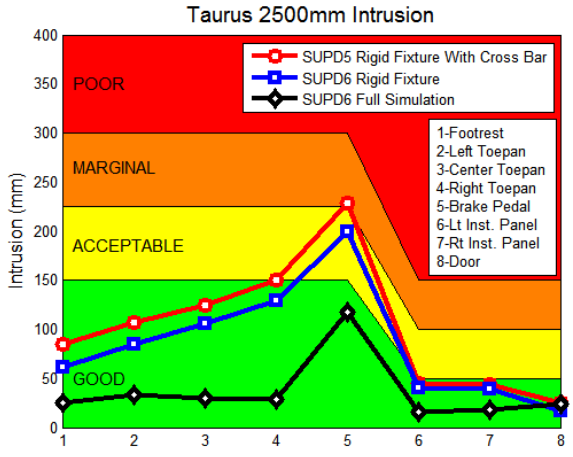

Figure 6.18 - SUPD Taurus 2500mm intrusion graph

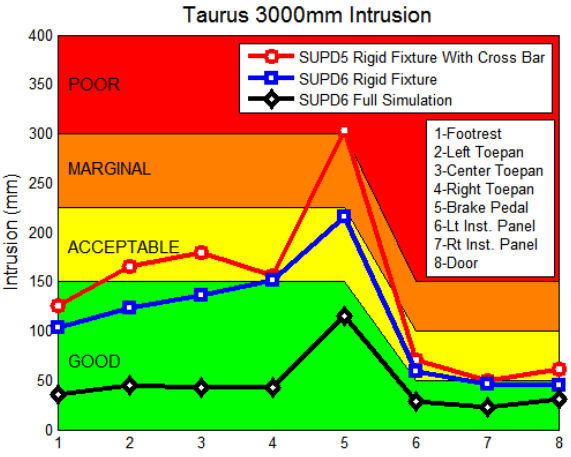

Figure 6.19 - SUPD Taurus 3000mm intrusion graph

The benefit of having an underride guard is clearly shown in Figure 6.20. Although it is observed that the impact force is greater when a guard is installed, the displacement and intrusion is greatly reduced in the passenger compartment.

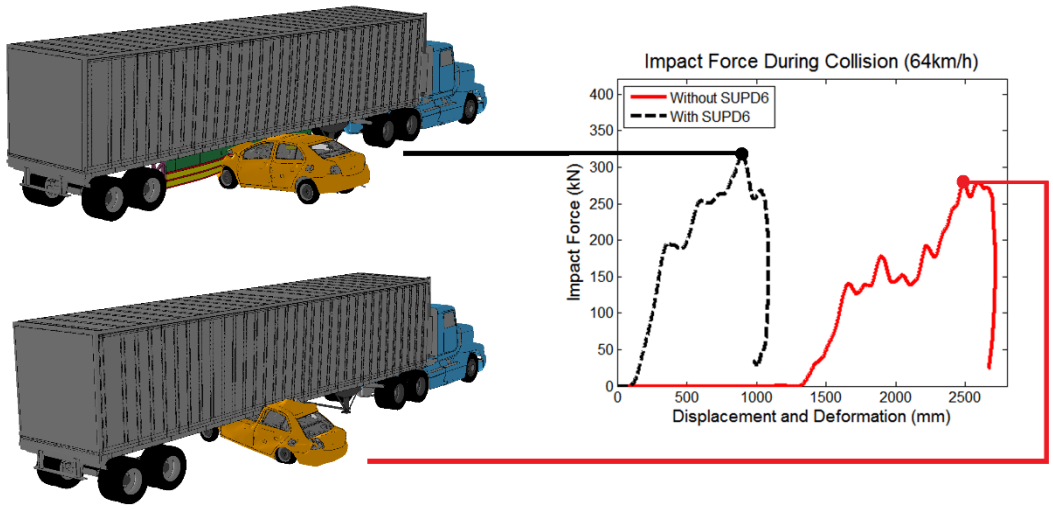

Figure 6.20 - Comparison of collision with and without SUPD6

6.2 STRAIGHT TRUCK SUPD-ST2

The new frontal impact area design of SUPD6 showed promising results which eliminated the need for a cross bar and added an aerodynamic advantage to the vehicle in question. Because of this, SUPD-ST2 was designed with the same idea in mind. The same brackets as SUPD-ST1 were utilized with the principle of three impact area bars with sheet metal placed between their gaps. On top of the impact area is a piece of plastic to finalize the aerodynamic shape of the device. Figure 6.21 shows the final design of SUPD-ST2. The weight to cover one side of the vehicle is 137.4kg which is 10.72kg less than SUPD-ST1.

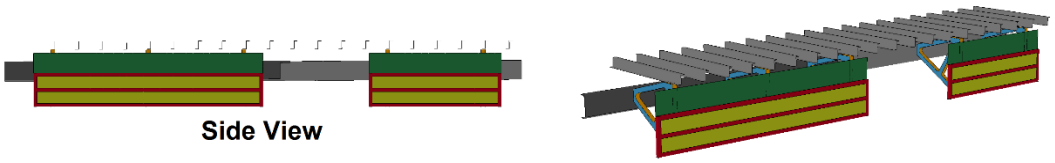

Figure 6.21 - Final SUPD-ST2 design

All of the offset test cases of this guard mounted on a rigid test fixture and straight truck can be seen in Figure 6.22 to Figure 6.28. As previously noted in the SUPD-ST1 section, when the offset reaches 1370mm, the deformation becomes larger and the impact force smaller due to the car reaching the end of the guard. The same is observed when looking at the 4200mm offset.

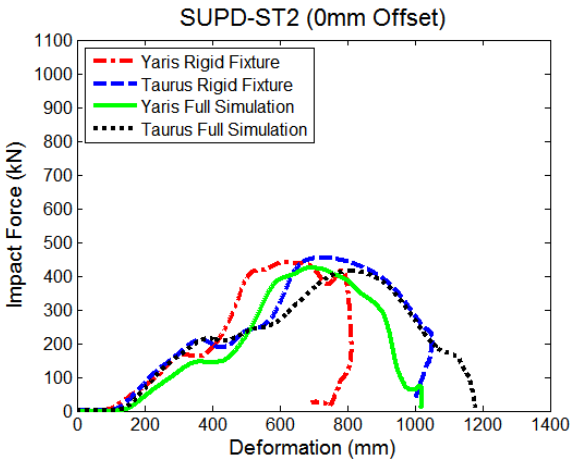

Figure 6.22 - SUPD-ST2 impact force graph at 0mm offset

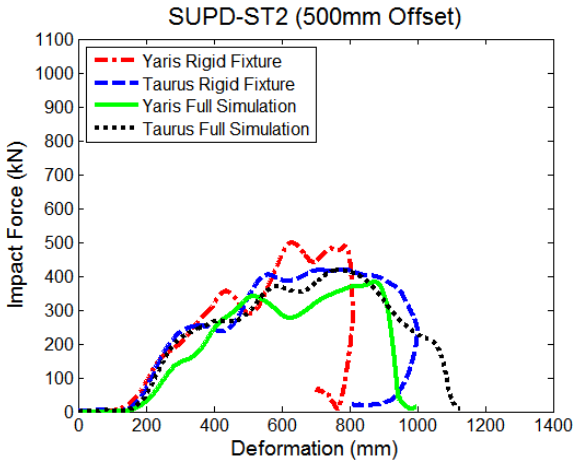

Figure 6.23 - SUPD-ST2 impact force graph at 500mm offset

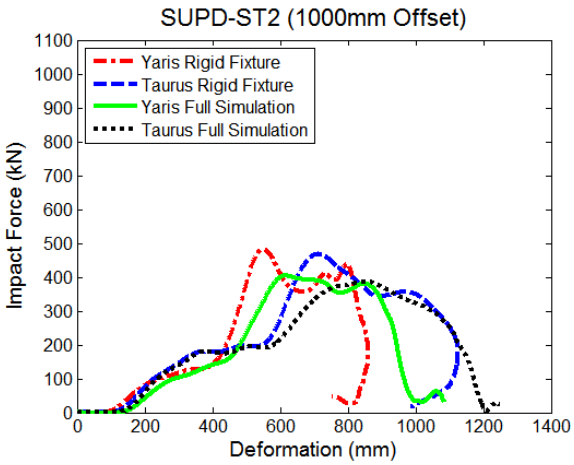

Figure 6.24 - SUPD-ST2 impact force graph at 1000mm offset

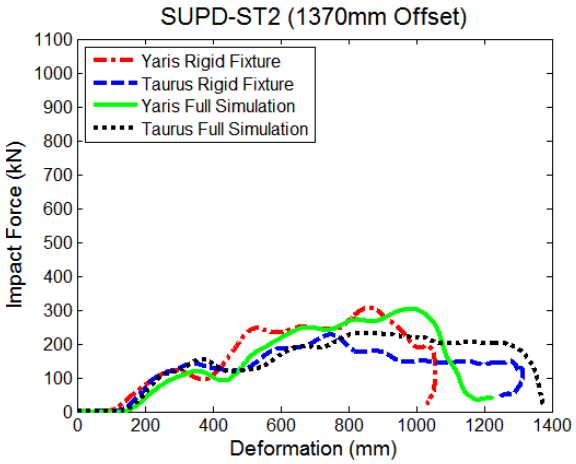

Figure 6.25 - SUPD-ST2 impact force graph at 1370mm offset

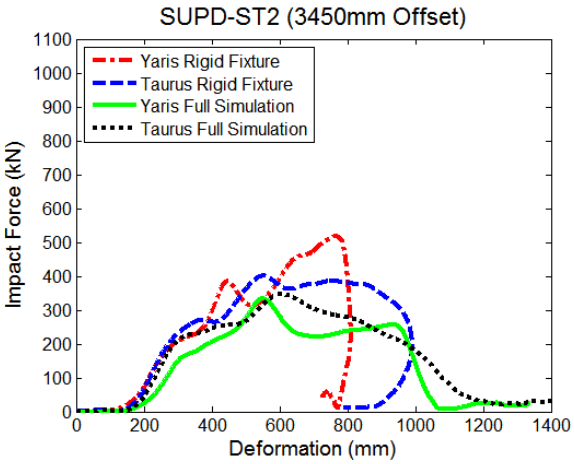

Figure 6.26 - SUPD-ST2 impact force graph at 3450mm offset

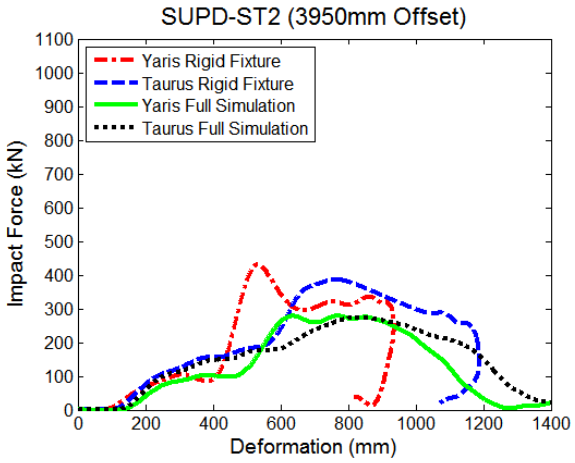

Figure 6.27 - SUPD-ST2 impact force graph at 3950mm offset

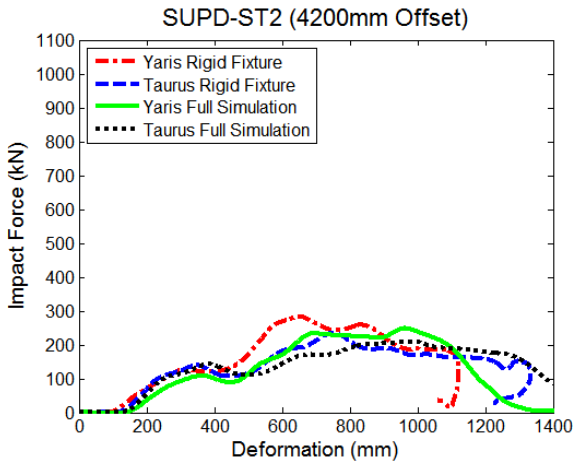

Figure 6.28 - SUPD-ST2 impact force graph at 4200mm offset

The overall deformation of the guard when mounted on the rigid test figure is seen in Figure 6.29. The values exceed the intended 100mm deformation in the 500, 1000, 3450 and 3950mm offsets. The data obtained in the 500 and 1000mm offsets are still feasible since the vehicle comes to a complete stop and the deformation is only exceeded by approximately 40mm. In the case of the rear guard at the 3450 and 3950mm cases, the values are around double the intended limit. The guard still brings the vehicles to a complete stop and stays significantly rigid throughout the process. Because of this, the values are still considered acceptable. To eliminate this, an additional cross bar may be added to increase the guard's rigidity.

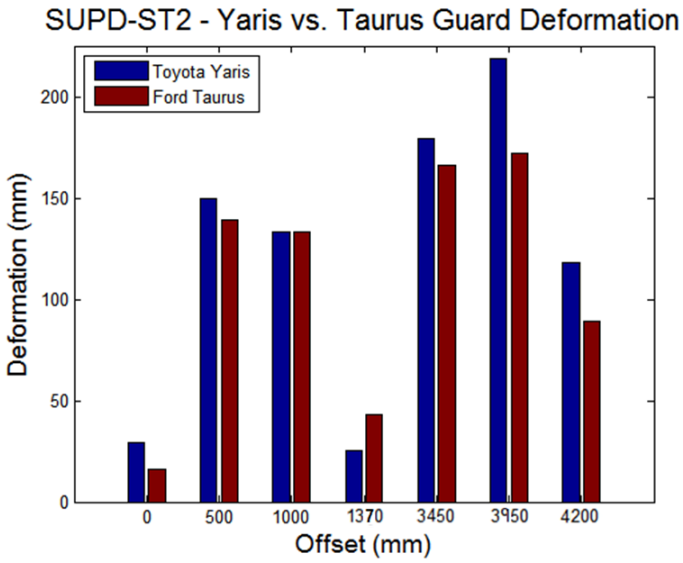

Figure 6.29 - SUPD-ST2 Yaris and Taurus guard deformation

The intrusion values for the 1370 and 4200mm offsets are shown for both the Yaris and Taurus in Figure 6.30 to Figure 6.33. The data of both guards mounted on the rigid test fixture is very similar. As concluded when investigating the SUPD6 intrusion numbers, the values are greatly reduced when the guard is mounted on the heavy vehicle.

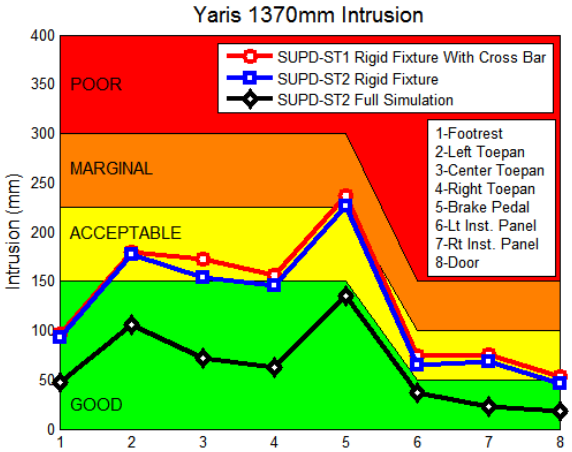

Figure 6.30 - SUPD-ST Yaris 1370mm intrusion graph

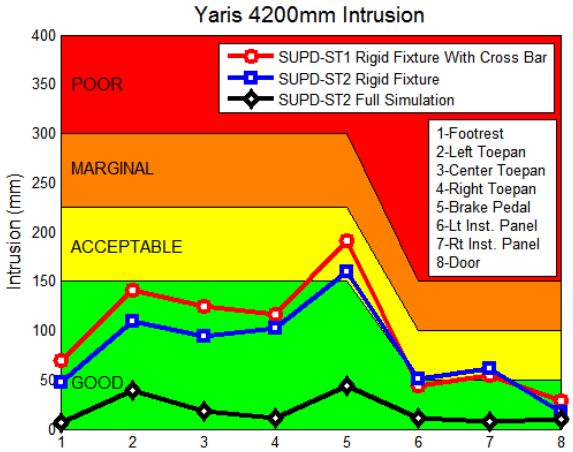

Figure 6.31 - SUPD-ST Yaris 4200mm intrusion graph

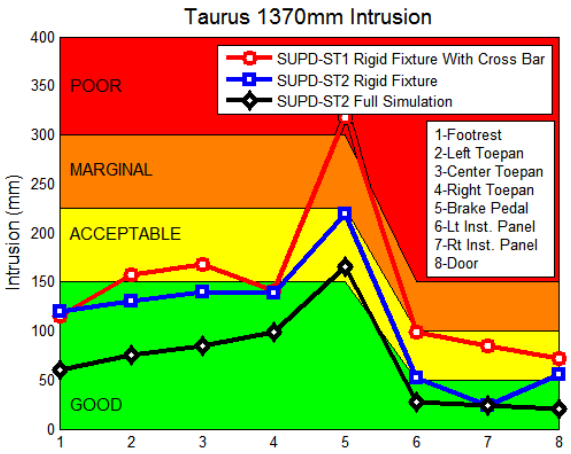

Figure 6.32 - SUPD-ST Taurus 1370mm intrusion graph

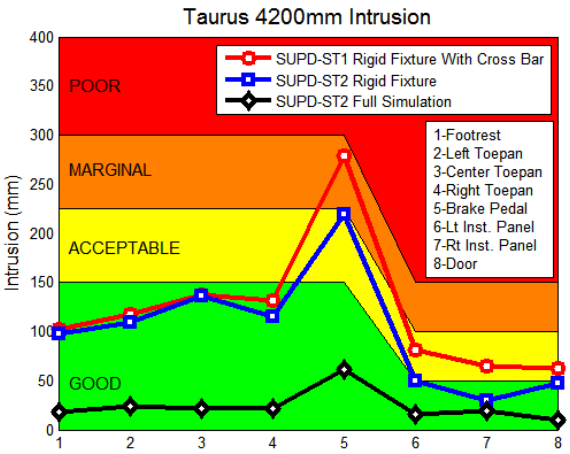

Figure 6.33 - SUPD-ST Taurus 4200mm intrusion graph

The benefits of having a straight truck with a side underride guard during a collision is shown in Figure 6.34

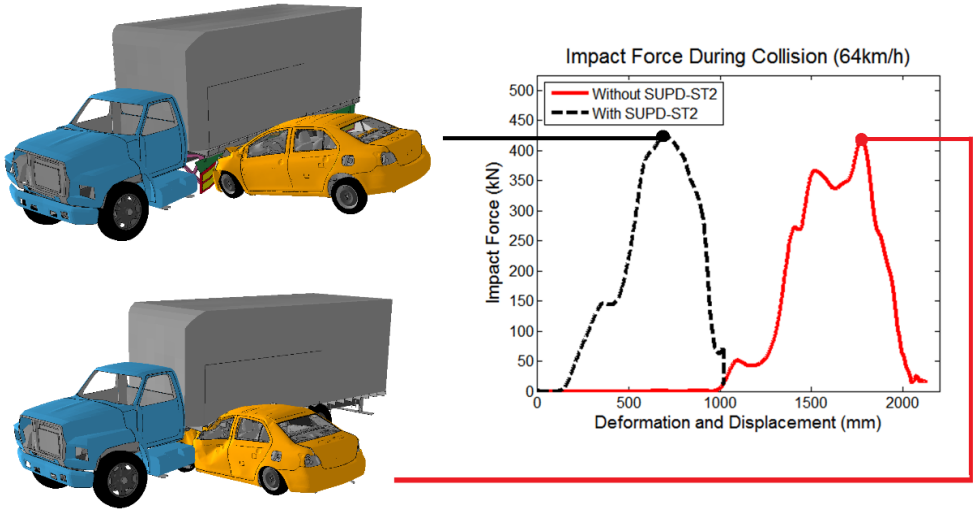

Figure 6.34 - Comparison of collision with and without SUPD-ST2

6.3 MOVING HEAVY VEHICLE

With SUPD6 and SUPD-ST2, an additional test was conducted. It involved crashing the Toyota Yaris traveling at 64km/h into the heavy vehicles traveling at 56km/h to investigate the properties of the guards in these cases. Figure 6.35 shows the Yaris colliding at the front, the center and the rear of SUPD6 mounted on the tractor-trailer. The impact force is plotted against the deformation and displacement since the vehicle

not only deforms but also has a yaw motion as it hits the trailer. In these tests, the rear of the guard yielded the greatest impact force. This occurs since the Yaris collides with the rear axle of the trailer. In all three tests, the guard remained rigid and proved to be effective at preventing the passenger vehicle from underriding.

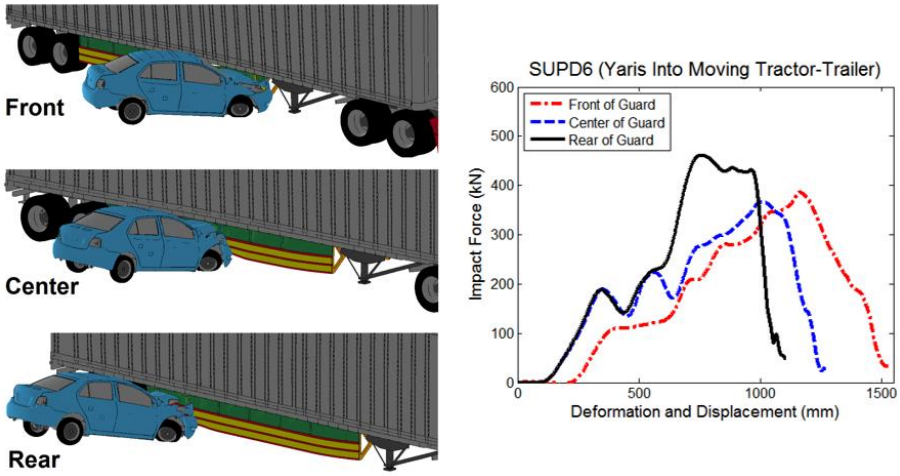

Figure 6.35 - Yaris (64km/h) into moving tractor-trailer (56km/h) with SUPD6

Three tests were also conducted with the straight truck and SUPD-ST2. The results are visually and graphically represented in Figure 6.36. The guard was feasible in these cases at preventing underride. The lowest impact force was seen in in the rear test since the vehicle would deflect off of the rear of the guard and vehicle.

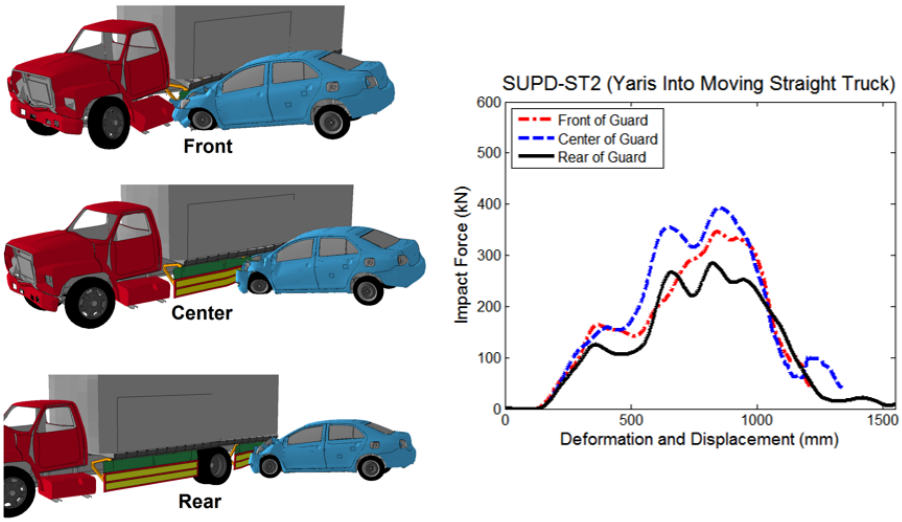

Figure 6.36 - Yaris (64km/h) into moving straight truck (56km/h) with SUPD-ST2

CHAPTER 7: CONCLUSIONS AND RECOMMENDATIONS

7.1 CONCLUSIONS

This research investigated passenger vehicles colliding with the sides of heavy vehicles. Due to the large and unprotected gap between the road and the bottom of the trailer or box, passenger vehicles can pass under the larger vehicles causing underride. Large deformation of the occupant compartment is observed and the collision often results in severe injury or death. To eliminate the underride effect, underride guards are created to remove the mismatch between the small vehicle's bumper and the ground clearance of the heavy vehicle.

Side underride statistics were investigated to determine the need for protection devices. From there, the existing front, side and rear device regulations were examined to determine the appropriate testing criterions for the side guards. The existing regulation for side guards in Europe was only for unprotected road users such as pedestrians and cyclists. As discovered, there was no testing measures to determine the effectiveness for side guards to prevent underride. A proposed regulation was therefore developed utilizing the principle of a large force application device from the Canadian rear underride guard regulation. After numerous tests, the final regulation was finalized and utilized for testing the effectiveness of SUPDs.

As shown in the literature review, there is a limited amount of existing side guard designs and they all lacked an appropriate testing method such as a regulation. Because of this, a design road map was effectively executed which used the proposed regulation along with topology and multi-objective optimization strategies. This would allow for the development and creation of the most lightweight, robust and feasible guards. Each step of the process was used to create SUPD5 for the tractor-trailer and SUPD-ST1 for the straight truck. Both final designs utilized a frontal impact area which resembled guard rails. The guards were then tested at each increment dynamically with the Toyota

Yaris and Ford Taurus. The results were then analysed and the guards proved to be feasible to prevent and stop underride from occurring.

By applying engineering intuition and analysing the aerodynamic advantage of trailer fairings, SUPD6 and SUPD-ST2 were created. The same brackets as the previous guards were used with a new impact area design. This incorporated using three cross bars with sheet metal placed between the gaps. A piece of plastic was added between the impact area and the bottom of the trailer or box of the straight truck to complete the aerodynamic shape. The regulation was also modified to accommodate the toe-in curve added to the front of the guard to deflect the air coming from the rear wheels. The final weight of SUPD6 was 198.9kg. Since a guard is needed on both sides of the trailer, the overall added weight to the vehicle is 397.8kg. When looking back at the referenced International Institute Highway Safety Status Report in the literature review, it was stated that side guards would affect the overall payload of the tractor-trailer and would effectively reduce the aerodynamics [22]. Both of these issues have been addressed by implementing the regulation to design the lightest possible guard while incorporating a fairing within a guard to reduce drag. SUPD-ST2 had a total weight of 134.7kg. To fully cover both side of the vehicle, the final added weight to the vehicle would be 269.4kg. The addition of the guards has shown that side underride can be eliminated. The data regarding injuries and fatalities in Chapter 1 can be dramatically reduced with the addition of these devices to heavy vehicles on the road.

7.2 RECOMMENDATIONS

Some weaknesses on the present work are that the tests are lacking physical validation at this point. Although validated vehicles where used during the dynamic simulations and that proper execution of the regulation was conducted, some physical validation may confirm the stated results. Physical tests can confirm the proposed testing method from the regulation along with showing that the applied load of 525kN with the force application devices is feasible.

The underride guard designs in this thesis showed very promising results when it came to stopping passenger vehicles from passing under the large vehicles The material used for the guards was the ASTM A653/A653M structural quality grade 80 steel which is the material used for the lateral cross I-beams of the trailer. Additional research can be conducted to determine an appropriate cost and manufacturing function to analyze different materials. Once completed, other materials may be utilized in the optimization procedures to further reduce the weight of the guards.

The mounting of the guards can also be investigated. SUPD6 and SUPD-ST2 were welded to the I-beam and Z-beams of the tractor-trailer and straight truck. An easier and more feasible mounting solution such as a bolt on application may be created.

The overall aerodynamic shape of the guard can be optimized to reduce drag while staying feasible as an underride guard. A cost analysis may also be developed to determine the advantages of the aerodynamics versus the added fuel consumption due to the weight of the devices.

This work may be of high importance to government agencies and the industry. The author has developed a proposed regulation for the testing of the devices which can be utilized if side guards are to be regulated in some countries. The work also showed possible guard designs that can be utilized on trailers and straight trucks of the same configuration. In addition to this, the design road map shown in Chapter 5 can be used to create the most lightweight designs while adhering to the regulation for other trailers or straight trucks in the industry.

REFERENCES

[1] Road Safety and Motor Vehicle Regulation Directorate, "Heavy Truck Casualty Collisions 2001 - 2005," April 2010. *Transport Canada*. [Online]. Available: http://www.tc.gc.ca/eng/roadsafety/tp-tp2436-rs201003-1042.htm. [Accessed 15 June 2013].

[2] P. Galipeau-Belair, M. El-Gindy, D. Critchley, S. Ramachandra and S. Ghantae, "A Review of Side Underride Statistics and Protection Device Literature and Designs," *Int. J. of Heavy Vehicle Systems,* vol. 20, no. 4, pp. 361-374, 2013. doi:10.1504/IJHVS.2013.056813

[3] Natural Resources Canada, "Canadian Vehicle Survey - 2009 Summary Report," 2009. [Online]. Available: http://oee.nrcan.gc.ca/publications/statistics/cvs09/. [Accessed 15 June 2013].

[4] National Highway Traffic Safety Administration, "Traffic Safety Facts - 2010 Data," U.S. Department of Transportation, 2012.

[5] J. Padmanaban, B. Martz and J. Salvage, "Evaluation of Light Vehicle Side Underride Collisions into Combination Trucks," *SAE Int. J. Commer. Veh,* vol. 1, no. 1, pp. 473-480, 2008.

[6] "Fatality Analysis Reporting System (FARS) Encyclopedia," 2013. [Online]. Available: http://www-fars.nhtsa.dot.gov/Main/index.aspx. [Accessed 15 June 2013].

[7] K. Allen, "The Effectiveness of Underride Guards for Heavy Trailers," National Highway Traffic Safety Administration (NHTSA), Washington, 2010.

[8] U.S. Department of Transportation, "Laboratory Test Procedure For FMVSS 223," National Highway Traffic Safety Administration (NHTSA), Washington, 1997.

[9] U.S. Department of Transportation, "Rear Impact Protection FMVSS 223," National Highway Traffic Safety Administration, Washington, 1997.

[10] Standards and Regulations Division, "Test Method 223 - Rear Impact Gaurd," Transport Canada Safety and Security - Road Safety, Ottawa, 2003.

[11] Economic Commission for Europe, "Addendum 92: Regulation No. 93," United Nations, Geneva, 1994.

[12] Economic Commission for Europe, "Addendum 72: Regulation No. 73," United Nations, Geneva, 2011.

[13] Economic Commission for Europe, "Addendum 57: Regulation No. 58," United Nations, Geneva, 2008.

[14] Canada Gazette Part II, "Regulations Amending the Motor Vehicle Safety Regulations - (Rear Impact Guards)," *Canada Gazette,* vol. 138, no. 20, pp. 1324-1442, 2004.

[15] J. Lambert and G. Rechnitzer, "Review of Truck Safety: Stage 1: Frontal, Side and Rear Underrun Protection," Monash University - Accident Research Centre, Monash, 2002.

[16] J. Patten and C. Tabra, "Side Guards for Trucks and Trailers Phase 1: Background Investigation," National Research Council Canada, Ottawa, 2010.

[17] P. Galipeau-Belair, M. El-Gindy, D. Critchley, S. Ramachandra and S. Ghantae, "Development of a regulation for testing the effectiveness of a rigid side underride protection device (SUPD)," *Int. J. of Crashworthiness,* 2013. doi:10.1080/13588265.2013.868083

[18] Australian Trucking Association, "Side Under Run Protection," Industry Technical Council Advisory Procedure, Forrest, 2012.

[19] V. K. K. Bodapati, "Evaluation of Energy Absorbing Pliers Underride Guard for Rear and Side of Large Truck," Graduate School of Wichita State University, Wichita, 2006.

[20] A. Aparicio, H. Puttenstein and F. Feist, "Demonstration of Truck Side Design Improvements," Adanved Protection Systems (APROSYS), 2009.

[21] A. Trego, B. Enz, D. Head and Y. Oshida, "A Scientific Approach to Tractor-Trailer Side Underride Anaylsis," *SAE Technical Paper - Advances in Vehicle Aggressivity and Compatibility, Side and Rear Impact and Rollover Protection,* no. 2003-01-0178, pp. 41-47, 2003.

[22] International Institue for Highway Safety, "Status Report - Not Good Enough," *Highway Loss Data Institute,* vol. 48, no. 2, pp. 1-8, 2013.

[23] M. L. Brumbelow, "Potential Benefits of Underride Guards in Large Truck Side

Crashes," *Traffic Injury Prevention,* vol. 13, no. 6, pp. 592-599, 2012.

[24] S. Kumar, B. Enz, P. Ponder and B. Anderson, "Biomechanical Analysis of Protective Countermeasures in Underride Motor Vehicle Accidents" Proceedings of the 46th Rocky Mountain Bio-engineering Biomedical Sciences Instrumentation Symposium in Milwaukee, Durham, NC, 2009.

[25] M. A. Roush, "Crash Attenuating Underride Guard - Patent No. US 7,780,244 B2," United States Patent, 2010.

[26] B. E. Enz, J. E. Tomassoni and A. Trego, "Vehicle Side Unde Ride Guard - Patent No. US 2008/0116702 A1," United States Patent, 2008.

[27] R. J. Giromini, L. W. Baker, R. P. Ehrlich and F. S. Smidler, "Side Underride Cable System for a Trailer - Patent N. US 8,162,384 B2," United States Patent, 2012.

[28] Freight Wing, "Trial Program on Aerodynamic Fairings," Transport Canada, 2011.

[29] J. Leuschen and K. R. Cooper, "Full-Scale Wind Tunnel Tests of Production and Prototype, Second-Generation Aerodynamic Drag-Reducing Devices for Tractor-Trailers," *SAE International,* no. 2006-01-3456, 2006.

[30] J. M. Ortega and K. Salari, "An Experimental Study of Drag Reduction Devices for a Trailer Underbody and Base," 34th AIAA Fluid Dynamics Conference and Exhibit, Portland, 2004.

[31] J. O. Hallquist, "LS-DYNA Theory Manual," Livermore Software Technology Corporation, California, 2006.

[32] Livermore Software Technology Corporation, "LS-DYNA Keyword User's Manual - Volume 1," Livermore Software Technology Corporation, Livermore, 2013.

[33] Livermore Software Technology Corporation, "LS-DYNA," 2011. [Online]. Available: http://www.lstc.com/products/ls-dyna. [Accessed 12 December 2013].

[34] Livermore Software Technology Corporation, "LS-PrePost," Livermore Software Technology Corporation, 2011. [Online]. Available: http://www.lstc.com/products/ls-prepost. [Accessed 12 December 2013].

[35] Livermore Software Technology Corporation, "LS-TaSC Topology and Shape Computations for LS-DYNA," Livermore Software Technology Corporation,

Livermore, 2011.

[36] N. Stander, W. Roux, A. Basudhar, T. Eggleston, T. Goel and K. Craig, "LS-Opt User's Manual - A Design Optimization and Probablistic Analysis Tool for the Engineering Analyst," Livermore Software Technology Corporation, Livermore, 2013.

[37] Amercian Association of State Highway and Transportation Officials, Manual for Assessing Safety Hardware, United States: Amercian Association of State Highway and Transportation Officials, 2009.

[38] M. Huang, Vehicle Crash Mechanics, Michigan: CRC Press, 2002.

[39] D. Marzougui, R. R. Samaha, C. Cui, C.-D. Kan and K. S. Opiela, "Extended Validation of the Finite Element Model for the 2010 Toyota Yaris Passenger Sedan," The National Crash Anaylsis Center, Ashburn, 2012.

[40] D. Marzougui, R. R. Samaha, C. Cui and C.-D. Kan, "Extended Validation of the Finite Element Model for the 2001 Ford Taurus Passenger Sedan," The National Crash Analysis Center, Ashburn, 2012.

[41] S. Simunovic and N. Zisi, "FEM Models for Semitrailer Trucks," National Transportation Research Center Inc., [Online]. Available: http://thyme.ornl.gov/FHWA/TractorTrailer/index.cgi?model=1&navv=0. [Accessed 1 June 2013].

[42] S. Simunovic and N. Zisi, "F800 Single Unit Truck FEM Model for Crash Simulations with LS-DYNA," National Transportation Research Center Inc., 30 November 2005. [Online]. Available: http://thyme.ornl.gov/fhwa/F800WebPage/description/description.html. [Accessed 1 June 2013].

[43] Insurance Institute for highway Safety, "Frontal Offset Crashworthiness Evaluation - Guidelines for Rating Structural Performance," IIHS, Arlington, 2002.

[44] I. I. f. H. Safety, "Moderate Overlap Frontal Crashworthiness Evaluation Crash Test Protocol (Version XIV)," IIHS, Arlington, 2012.

[45] Insurance Institute for Highway Safety, "2007 Toyota Yaris sedan," [Online]. Available: http://www.iihs.org/iihs/ratings/vehicle/v/toyota/yaris-sedan/2007?print. [Accessed 19 November 2013].

[46] Livermore Software Technology Corporation, "Download LSTC Dummy and Barrier Models for LS-DYNA," LSTC, 2011. [Online]. Available: http://www.lstc.com/download/dummy_and_barrier_models. [Accessed 19 November 2013].

[47] Insurance Institute for Highway Safety, "2001 Ford Taurus," IIHS, 2014. [Online]. Available: www.iihs.org/iihs/ratings/vehicle/v/ford/taurus/2001?print-view. [Accessed 19 November 2013].

[48] Service Ontario - e-Laws, "Ontario Regulation 413/05 - Vehicle Weights and Dimensions," 1 July 2012. [Online]. Available: http://www.e-laws.gov.on.ca/html/regs/english/elaws_regs_050413_e.htm. [Accessed 1 June 2013].

[49] Government of Canada - Justice Laws Website, "Railway-Highway Crossing at Grade Regulations (SOR/80-748)," 31 December 2012. [Online]. Available: http://laws-lois.justice.gc.ca/eng/regulations/SOR-80-748/page-3.html#h-7. [Accessed 1 June 2013].

[50] Transport Canada, "Draft Canadian Railway-Roadway Grade Crossings Standards (CRRGCS)," Transport Canada, Ottawa, 2012.

[51] J. E. Lloyd, "Vehicle Standard (Australian Design Rule 43/04 – Vehicle Configuration and Dimensions) 2006," Federal Register of Legislative Instruments F2006L01430 (Motor Vehicle Standards Act 1989), Australia, 2006.

[52] Transports' Friend, "Trailers," 2007. [Online]. Available: http://www.transportsfriend.org/road/trailer.html. [Accessed 1 June 2013].

[53] NZ Transport Agency, "Heavy Trailers and Combination Vehicles (full, semi, simple, pole, A- and B-train) (Factsheet 13c August 2011)," New Zealand Government, Wellington, 2011.

[54] Code of Federal Regulations, "40 CFR 600.315-82 Classes of Compatable Automobiles (47 FR 49814)," U.S. Governement Printing Office, Washington, 1996.

[55] U.S. Department of Energy (Energy Efficient & Renewable Energy), "Vehicle Weight Classes & Catagories," 30 December 2013. [Online]. Available: http://www.afdc.energy.gov/data/10380. [Accessed 10 January 2014].

[56] National Highway Traffic Safety Administration, "Query Vehicle Crash Test Database

on Select Test Parameters," NHTSA, [Online]. Available: http://www-nrd.nhtsa.dot.gov/database/VSR/veh/QueryTest.aspx. [Accessed 1 November 2013].

[57] H. J. Beerman, "Behaviour of Passenger Cars on Impact With Underride Guards," *Int. J. of Vehicle Design,* vol. 5, no. 1/2, pp. 86-103, 1984.

[58] N. W. Murray, "A Study of Car-Truck Impacts and the Feasibility of Fitting Energy-Absorbing Guards to Heavy Trucks," Road Traffic Authority, Melbourne, 1988.

[59] G. Rechnitzer, C. Powell and K. Seyer, "Performance Criteria, Design and Crash Tests of Effective Rear Underride Barriers for Heavy Vehicles," Proceedings of the 17th International Techincal Conference on Enhanced Safety of Vehicles, Amsterdam, Netherlands, 2001.

[60] American Society for Testing and Materials (ASTM), "Standard Specification for Steel Sheet, Zinc-Coated (Galvanized) or Zinc-Iron Alloy- Coated (Galvannealed) by the Hot-Dip Process (A653/A653M - 13)," ASTM International, West Conshohocken, PA, 2013.

[61] Kronos Energy Solution, "Trailer Fairings," Kronos, 2013. [Online]. Available: http://www.kronosenergysolutions.com/FleetFairings/skirt-side-fairings.html. [Accessed 12 October 2013].

[62] Aerofficient, "Side Fairing - Fixed: Toe-In or Gear Wrap," Aeroficient LLC, 2013. [Online]. Available: http://www.aerofficient.com/side-fairing-fixed-toe-in-or-gear-wrap.html. [Accessed 12 November 2013].

PUBLICATIONS

1. P. Galipeau-Belair, M. El-Gindy, D. Critchley, S. Ramachandra and S. Ghantae, "A Review of Side Underride Statistics and Protection Device Literature and Designs" *Int. J. of Heavy Vehicle Systems*, vol. 20, no. 4, pp. 361-374, 2013. DOI: 10.1504/IJHVS.2013.056813

2. P. Galipeau-Belair, M. El-Gindy, D. Critchley, S. Ramachandra and S. Ghantae, "Development of a regulation for testing the effectiveness of a rigid side underride protection device (SUPD)", International Journal of Crashworthiness, DOI: 10.1080/13588265.2013.868083.

3. P. Galipeau-Belair, M. El-Gindy, D. Critchley, S. Ramachandra and S. Ghantae, "Optimized Rigid Side Underride Protection Device Designs for Tractor-Trailers and Straight Trucks", *Accepted to SAE World Congress 2014 for publication and presentation*, 2014, 2014-01-0565

APPENDIX

Copyright Permission Letter

February 5th, 2014

International Journal of Crashworthiness

[Address of Publication] 4 PARK SQUARE
MILTON PARK, ABINGDON, OX14 4RN, UK.

I am preparing my Master of Applied Science thesis for submission to the Office of Graduate Studies at the University of Ontario Institute of Technology (UOIT) in Oshawa, Ontario, Canada. I am seeking your permission to include an original manuscript of the author's following paper as a chapter in the thesis:

"Development of a regulation for testing the effectiveness of a rigid side underride protection device (SUPD), P. Galipeau-Belair, M. El-Gindy, D. Critchley, S. Ramachandra and S. Ghantae, International Journal of Crashworthiness, DOI: 10.1080/13588265.2013.868083, 2013"

Canadian graduate theses are reproduced by the Library and Archives of Canada (formerly National Library of Canada) through a non-exclusive, world-wide license to reproduce, loan, distribute, or sell theses. I am also seeking your permission for the material described above to be reproduced and distributed by the LAC(NLC). Further details about the LAC(NLC) thesis program are available on the LAC(NLC) website (www.nlc-bnc.ca).

Full publication details and a copy of this permission letter will be included in the thesis.

Yours sincerely,

Patrick Galipeau-Belair

Permission is granted for:

a) the inclusion of the material described above in your thesis.

b) for the material described above to be included in the copy of your thesis that is sent to the Library and Archives of Canada (formerly National Library of Canada) for reproduction and distribution.

Name: FRANCESCA FARR Title: MANAGING EDITOR, TAYLOR + FRANCIS

Signature: _____ Date: 6/02/2014

Co-Authored Material Permission

February 5th, 2014

I am preparing my Master of Applied Science thesis for submission to the Office of Graduate Studies at the University of Ontario Institute of Technology (UOIT) in Oshawa, Ontario, Canada. I am seeking your permission to include your co-authored material of the original manuscript of the following paper as a chapter in the thesis:

"Development of a regulation for testing the effectiveness of a rigid side underride protection device (SUPD), P. Galipeau-Belair, M. El-Gindy, D. Critchley, S. Ramachandra and S. Ghantae, International Journal of Crashworthiness, DOI: 10.1080/13588265.2013.868083, 2013"

Name	Signature	Date
Dr. Moustafa El-Gindy		2/7/14
David Critchley		2/7/14
Sarathy Ramachandra	S. R. Partha Sarathy	2/7/14
Srikanth Ghantae		2/7/14

Yours sincerely,

Patrick Galipeau-Belair